SANDIA REPORT

SAND2012-8248
Unlimited Release
Printed March 2013

Probability of Loss of Assured Safety in Systems with Multiple Time-Dependent Failure Modes

Jon C. Helton, Martin Pilch, Cédric J. Sallaberry

Prepared by
Sandia National Laboratories
Albuquerque, New Mexico 87185 and Livermore, California 94550

Sandia National Laboratories is a multi-program laboratory managed and operated by Sandia Corporation,
a wholly owned subsidiary of Lockheed Martin Corporation, for the U.S. Department of Energy's
National Nuclear Security Administration under contract DE-AC04-94AL85000.

Sandia National Laboratories

Issued by Sandia National Laboratories, operated for the United States Department of Energy by Sandia Corporation.

Printed in the United States of America. This report has been reproduced directly from the best available copy.

Available to DOE and DOE contractors from
U.S. Department of Energy
Office of Scientific and Technical Information
P.O. Box 62
Oak Ridge, TN 37831

Telephone:	(865) 576-8401
Facsimile:	(865) 576-5728
E-Mail:	reports@adonis.osti.gov
Online ordering:	http://www.osti.gov/bridge

Available to the public from
U.S. Department of Commerce
National Technical Information Service
5285 Port Royal Rd.
Springfield, VA 22161

Telephone:	(800) 553-6847
Facsimile:	(703) 605-6900
E-Mail:	orders@ntis.fedworld.gov
Online order:	http://www.ntis.gov/help/ordermethods.asp?loc=7-4-0#online

SAND2012-8248
Unlimited Release
Printed September 2012

Probability of Loss of Assured Safety in Systems with Multiple Time-Dependent Failure Modes

J.C. Helton, M. Pilch, C.J. Sallaberry
Departments 1514 and 6224
Sandia National Laboratories
P.O. Box 5800
Albuquerque, New Mexico 87185-0748

Abstract

Weak link (WL)/strong link (SL) systems are important parts of the overall operational design of high-consequence systems. In such designs, the SL system is very robust and is intended to permit operation of the entire system under, and only under, intended conditions. In contrast, the WL system is intended to fail in a predictable and irreversible manner under accident conditions and render the entire system inoperable before an accidental operation of the SL system. The likelihood that the WL system will fail to deactivate the entire system before the SL system fails (i.e., degrades into a configuration that could allow an accidental operation of the entire system) is referred to as probability of loss of assured safety (PLOAS). Representations for PLOAS for situations in which both link physical properties and link failure properties are time-dependent are derived and numerically evaluated for a variety of WL/SL configurations, including PLOAS defined by (i) failure of all SLs before failure of any WL, (ii) failure of any SL before failure of any WL, (iii) failure of all SLs before failure of all WLs, and (iv) failure of any SL before failure of all WLs. The effects of aleatory uncertainty and epistemic uncertainty in the definition and numerical evaluation of PLOAS are considered.

Keywords: Aleatory uncertainty, Epistemic uncertainty, Probability of loss of assured safety, Strong link, Uncertainty analysis, Weak link

Acknowledgments

Work performed at Sandia National Laboratories (SNL), which is a multiprogram laboratory operated by Sandia Corporation, a Lockheed Martin Company, for the U.S. Department of Energy's National Nuclear Security Administration under Contract No. DE-AC04-94AL85000. Review provided by K.M. Groth at SNL. This presentation is an independent product of the authors and does not necessarily reflect views held by either SNL or the U.S. Department of Energy.

Contents

Figures

Tables

NOMENCLATURE

CCDF	Complementary Cumulative Distribution Function
CDF	Cumulative Distribution Function
LOAS	Loss of Assured Safety
PLOAS	Probability of Loss of Assured Safety
SL	Strong Link
WL	Weak Link

This page intentionally left blank.

1. Introduction

Weak link (WL)/strong link (SL) systems are important parts of the overall operational design of high-consequence systems [1-6]. In such designs, the SL system is very robust and is intended to permit operation of the entire system under, and only under, intended conditions (e.g., by transmitting a command to activate the system). In contrast, the WL system is intended to fail in a predictable and irreversible manner under accident conditions (e.g., in the event of a fire) and render the entire system inoperable before an accidental operation of the SL system. Possible configurations of a WL/SL system with one WL and one SL are illustrated in Fig. 1 of Ref. [7].

The likelihood that the WL system will fail to deactivate the entire system before the SL system fails (i.e., degrades into a configuration that could allow an accidental operation of the entire system) is referred to as probability of loss of assured safety (PLOAS). The descriptor loss of assured safety (LOAS) is used because failure of the WL system places the entire system in an inoperable configuration while failure of the SL system, although undesirable, does not necessarily result in an unintended operation of the entire system. Thus, safety is "assured" by failure of the WL system. In the context of accident conditions, the descriptor "failure of the WL system" is an oxymoron as such failure is actually a success in the sense that it results in a desired deactivation of the entire system.

Two previous publications [7; 8] develop time-dependent values $pF(t)$ for PLOAS for accidents involving fire for a variety of WL/SL configurations (Table 1). Further, two related publications [9; 10] develop verification test problems for the PLOAS representations in Refs. [7; 8]. The test problems involve assigning the same failure properties to all links, which results in (i) the same cumulative distribution function (CDF) for link failure time for all links and (ii) the indicated verification values shown in Table 1. The verification problems entail an exercising of all the conceptual development and numerical procedures underlying the PLOAS representations in Table 1 and yet have the simple numerical values for PLOAS shown in Table 1.

Table 1 Representation of Time-Dependent Values $pF_i(t)$, i = 1, 2, 3, 4, for PLOAS for W L/SL Systems with nWL WLs and nSL SLs and Associated Verifi cation Tests for Alternate Definitions of LOAS ([8], Table 10)

Case 1: Failure of all SLs before failure of any WL (Eqs. (2.1) and (2.5), Ref. [10])

$$pF_1(t) = \sum_{k=1}^{nSL}\left(\int_0^t \left\{\prod_{\substack{l=1\\ l\neq k}}^{nSL} CDF_{SL,l}(\tau)\right\}\left\{\prod_{j=1}^{nWL}\left[1 - CDF_{WL,j}(\tau)\right]\right\} \mathrm{d}CDF_{SL,k}(\tau)\right)$$

Verification test: $pF_1(\infty) = nWL!\,nSL!/(nWL + nSL)!$

Case 2: Failure of any SL before failure of any WL (Eqs. (3.1) and (3.4), Ref. [10])

$$pF_2(t) = \sum_{k=1}^{nSL}\left(\int_0^t \left\{\prod_{\substack{l=1\\ l\neq k}}^{nSL}\left[1 - CDF_{SL,l}(\tau)\right]\right\}\left\{\prod_{j=1}^{nWL}\left[1 - CDF_{WL,j}(\tau)\right]\right\} \mathrm{d}CDF_{SL,k}(\tau)\right)$$

Verification test: $pF_2(\infty) = nSL/(nWL + nSL)$

Case 3: Failure of all SLs before failure of all WLs (Eqs. (4.1) and (4.4), Ref. [10])

$$pF_3(t) = \sum_{k=1}^{nSL}\left(\int_0^t \left\{\prod_{\substack{l=1\\ l\neq k}}^{nSL} CDF_{SL,l}(\tau)\right\}\left\{1 - \prod_{j=1}^{nWL} CDF_{WL,j}(\tau)\right\} \mathrm{d}CDF_{SL,k}(\tau)\right)$$

Verification test: $pF_3(\infty) = nWL/(nWL + nSL)$

Case 4: Failure of any SL before failure of all WLs (Eqs. (5.1) and (5.4), Ref. [10])

$$pF_4(t) = \sum_{k=1}^{nSL}\left(\int_0^t \left\{\prod_{\substack{l=1\\ l\neq k}}^{nSL}\left[1 - CDF_{SL,l}(\tau)\right]\right\}\left\{1 - \prod_{j=1}^{nWL} CDF_{WL,j}(\tau)\right\} \mathrm{d}CDF_{SL,k}(\tau)\right)$$

Verification test: $pF_4(\infty) = 1 - \left[nWL!\,nSL!/(nWL + nSL)!\right]$

The PLOAS values developed in Refs. [7; 8] derive from aleatory uncertainty (i.e., random variability) [11-17] in the failure temperatures for the individual links. As illustrated in the notional example of Fig. 1, there is a distribution of possible failure values for the link under consideration, with link failure occurring when the temperature curve reaches a failure temperature. In turn, the distribution of failure temperatures leads to a distribution of failure times and a corresponding CDF for link failure time (i.e., $CDF(t)$ is the probability of link failure at or before time t). In the development of Ref. [7], a link is assumed to fail at the instant that its failure temperature is reached; Ref. [8] treats the more general situation in which there is a delay between when a link reaches its failure temperature and when the link actually fails. These differences affect the definitions of the CDFs for link failure time; however, once these CDFs are obtained, PLOAS can be determined as indicated in Table 1 for both definitions of link failure time.

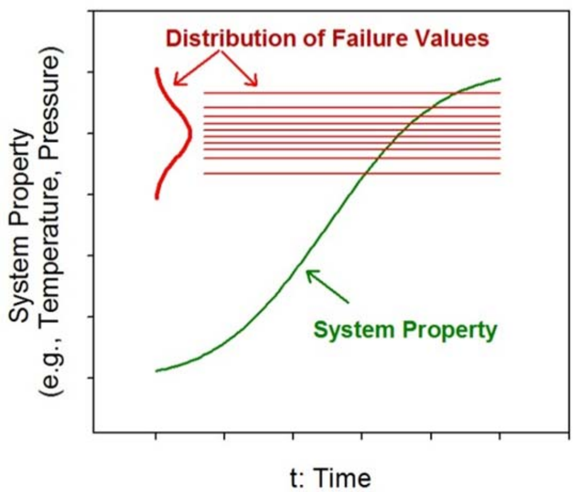

Fig. 1. Notional example of a time-dependent system property (e.g., temperature or pressure) and a corresponding distribution of failure values.

The developments in Refs. [7-10] always refer to the link properties under consideration as temperature. However, there is nothing in the development of the results in Table 1 that is specific to temperature. The results hold for any time-dependent property that has the potential to cause link failure. Further, different properties could be associated with the failure of different links. For example, some links might fail on the basis of temperature while other links fail on the basis of pressure or some other system property. Whatever the failure modes are for the individual links, PLOAS can be determined as indicated in Table 1 once the CDFs for failure time are determined.

The results contained in this presentation generalize the results in Ref. [7] in two ways. First, aleatory uncertainty is assumed to be present in the system properties (e.g., temperature, pressure, …) under consideration. Second, the failure values for a link are assumed to be time-dependent. These more general assumptions are illustrated in the notional example in Fig. 2.

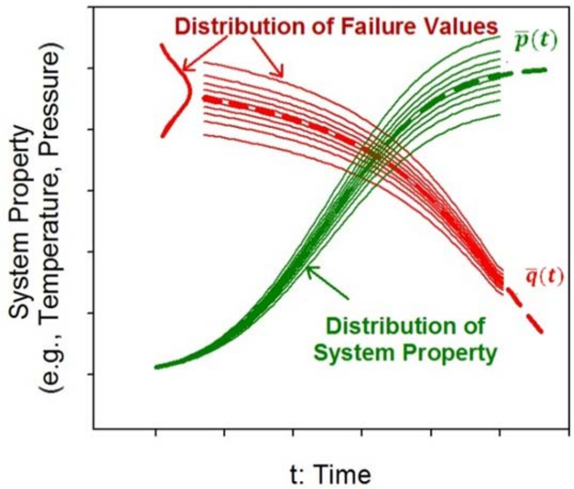

Fig. 2. Notional example of a distribution for a time-dependent system property (e.g., temperature or pressure) and a corresponding distribution for time-dependent failure values.

The following topics are considered in this presentation: (i) definition of failure time CDFs for single WLs or SLs (Sect. 2), (ii) evaluation of CDFs for known density functions (Sect. 3), (iii) evaluation of PLOAS with quadrature-based procedures (Sect. 4), (iv) evaluation of PLOAS with sampling-based (i.e., Monte Carlo) procedures (Sect. 5), (v) illustration of the verification tests for the PLOAS evaluations indicated in Table 1 (Sect. 6), (vi) alternative representations for PLOAS (Sect. 7), (viii) example system used to illustrate procedures for the evaluation of PLOAS (Sect. 8), (ix) example evaluations of PLOAS involving only aleatory uncertainty (Sect. 9), (x) example evaluations of PLOAS involving aleatory and epistemic uncertainty (Sect. 10), and (xi) example evaluations of PLOAS involving mixtures of aleatory and epistemic uncertainty (Sect. 11). The presentation then ends with a concluding discussion (Sect. 12).

2. Definition of Failure Time CDFs for Single WLs or SLs

The failure time CDF for a single WL or SL is based on the following assumed properties of that link for the time interval $t_{mn} \le t \le t_{mx}$:

$$\bar{p}(t) = \text{nondecreasing function defining nominal link property for } t_{mn} \le t \le t_{mx}, \tag{2.1}$$

$$\bar{q}(t) = \text{nonincreasing function defining nominal failure value for link property for } t_{mn} \le t \le t_{mx}, \tag{2.2}$$

$$d_\alpha(\alpha) = \text{density function for variable } \alpha \text{ used to characterize aleatory uncertainty in link property,} \tag{2.3}$$

$$d_\beta(\beta) = \text{density function for variable } \beta \text{ used to characterize aleatory uncertainty in link failure value,} \tag{2.4}$$

$$p(t \mid \alpha) = \alpha \bar{p}(t) = \text{link property for } t_{mn} \le t \le t_{mx} \text{ given } \alpha, \tag{2.5}$$

and

$$q(t \mid \beta) = \beta \bar{q}(t) = \text{link failure value for } t_{mn} \le t \le t_{mx} \text{ given } \beta. \tag{2.6}$$

Further, $d_\alpha(\alpha)$ and $d_\beta(\beta)$ are assumed to be defined on intervals $[\alpha_{mn}, \alpha_{mx}]$ and $[\beta_{mn}, \beta_{mx}]$ and to equal zero outside these intervals. Although this does not have to be the case, it is anticipated that α and β will be assigned distributions with a mode of 1.0 in most analyses so that $\bar{p}(t)$ and $\bar{q}(t)$ will be the modes (i.e., most likely values) for $p(t|\alpha)$ and $q(t|\beta)$.

The functions $p(t|\alpha)$ and $q(t|\beta)$ (i) define time-dependent values for a link property (e.g., temperature, pressure, …) and the failure values for that property (e.g., failure temperature, failure pressure, …) and (ii) have distributions that derive from the distributions for α and β characterized by the density functions $d_\alpha(\alpha)$ and $d_\beta(\beta)$. For given values for α and β, the link fails at the time t for which the equality

$$\beta \bar{q}(t) = q(t \mid \beta) = p(t \mid \alpha) = \alpha \bar{p}(t) \tag{2.7}$$

holds. In turn, the distributions for α and β result in a distribution of possible values for the failure time t that can be summarized by

$$CDF(t) = \text{probability that link failure occurs at or before time } t, \tag{2.8}$$

which is the CDF for link failure time. Two derivations and associated representations for $CDF(t)$ follow, with one representation involving Riemann integrals and the other representation involving Stieltjes integrals.

The derivation involving Riemann integrals is presented first. Because $p(t|\alpha)$ is nondecreasing and $q(t|\beta)$ is nonincreasing, link failure can occur at or before time t only if the inequality

$$\beta\bar{q}(t) = q(t \mid \beta) \le p(t \mid \alpha) = \alpha\,\bar{p}(t) \tag{2.9}$$

is satisfied (see Fig. 2), which in turn implies the inequality

$$\beta \le \alpha\,\bar{p}(t)/\bar{q}(t) = F(\alpha,t). \tag{2.10}$$

As a consequence,

$$CDF(t) \cong \sum_{i=1}^{n}\left[\int_{-\infty}^{F(\alpha_{i-1},t)} d_\beta(\beta)\,\mathrm{d}\beta\right]_1 \left[d_\alpha(\alpha_i)\Delta\alpha_i\right]_2, \tag{2.11}$$

where (i) $\alpha_{mn} = \alpha_0 < \alpha_1 < \cdots < \alpha_n = \alpha_{mx}$ is a subdivision of $[\alpha_{mn}, \alpha_{mx}]$, (ii) $[\sim]_1$ is the probability that β is less than or equal to $F(\alpha_{i-1},t)$, and (iii) $[\sim]_2$ is an approximation of the probability that α is in the interval $[\alpha_{i-1}, \alpha_i]$. In turn,

$$CDF(t) = \int_{\alpha_{mn}}^{\alpha_{mx}}\left[\int_{-\infty}^{F(\alpha,t)} d_\beta(\beta)\,\mathrm{d}\beta\right] d_\alpha(\alpha)\,\mathrm{d}\alpha \tag{2.12}$$

in the limit as $\Delta\alpha_i \to 0$, which is a representation of $CDF(t)$ with Riemann integrals.

The derivation involving Stieltjes integrals is now presented. This derivation is predicated on the assumption that it is possible to obtain the CDFs

$$\begin{aligned} CDF_p(p \mid t) &= \text{probability that link property is less than or equal to } p \text{ at time } t \\ &= \int_{-\infty}^{p} \tilde{d}_p(\tilde{p} \mid t)\,\mathrm{d}\tilde{p} \end{aligned} \tag{2.13}$$

and

$$\begin{aligned} CDF_q(q \mid t) &= \text{probability that link failure value is less than or equal to } q \text{ at time } t \\ &= \int_{-\infty}^{q} \tilde{d}_q(\tilde{q} \mid t)\,\mathrm{d}\tilde{q}, \end{aligned} \tag{2.14}$$

where $\tilde{d}_p(\tilde{p}\,|\,t)$ and $\tilde{d}_q(\tilde{q}\,|\,t)$ are the density functions for the possible values for the link property p and failure value q at time t. Given that $CDF_p(p\,|\,t)$ and $CDF_q(q\,|\,t)$ can be obtained, $CDF(t)$ can be approximated by

$$CDF(t) \cong \sum_{i=1}^{n} CDF_q(p_{i-1}\,|\,t)\left[CDF_p(p_i\,|\,t) - CDF_p(p_{i-1}\,|\,t)\right], \tag{2.15}$$

where (i) $[p_{mn}(t),\ p_{mx}(t)] = [\alpha_{mn}\bar{p}(t), \alpha_{mx}\bar{p}(t)]$, (ii) $p_{mn}(t) = p_0 < p_1 < \cdots < p_n = p_{mx}(t)$ is a subdivision of $[p_{mn}(t),\ p_{mx}(t)]$, (iii) $CDF_q(p_{i-1}\,|\,t)$ is the probability that failure value q is less than or equal to p_{i-1}, and (iv) [~] is the probability that property p is in the interval $[p_{i-1}, p_i]$. In turn,

$$CDF(t) = \int_{p_{mn}(t)}^{p_{mx}(t)} CDF_q(p\,|\,t)\,\mathrm{d}CDF_p(p\,|\,t) \tag{2.16}$$

in the limit as $\Delta p_i \to 0$, which is a representation of $CDF(t)$ with Stieltjes integrals.

The definitions of the density functions $\tilde{d}_p(\tilde{p}\,|\,t)$ and $\tilde{d}_q(\tilde{q}\,|\,t)$ in Eqs. (2.13) and (2.14) are now considered. The development of $\tilde{d}_p(\tilde{p}\,|\,t)$ and $\tilde{d}_q(\tilde{q}\,|\,t)$ involves a conversion from the distributions for α and β to the distributions for p and q at time t. If $y = f(\varepsilon)$ is a strictly monotonic function of a variable ε and ε has density function $d_\varepsilon(\varepsilon)$, then the density function $d_y(y)$ for y is given by ([18], Eq. (8.18))

$$d_y(y) = \left|\mathrm{d}f^{-1}(y)/\mathrm{d}y\right| d_\varepsilon\left[f^{-1}(y)\right]. \tag{2.17}$$

The values for p and q at time t are related to the values for α and β by

$$p = \alpha\bar{p}(t) = f_p(\alpha) \text{ and } \alpha = f_p^{-1}(p) = p/\bar{p}(t) \tag{2.18}$$

and

$$q = \beta\bar{q}(t) = f_q(\beta) \text{ and } \beta = f_q^{-1}(q) = q/\bar{q}(t). \tag{2.19}$$

Given the preceding relationships, application of the identity in Eq. (2.17) yields the density functions

$$\tilde{d}_p(\tilde{p}\,|\,t) = \left|\mathrm{d}f_p^{-1}(\tilde{p})/\mathrm{d}\tilde{p}\right| d_\alpha\left[f_p^{-1}(\tilde{p})\right] = \left[1/\bar{p}(t)\right] d_\alpha\left[\tilde{p}/\bar{p}(t)\right] \tag{2.20}$$

and

$$\tilde{d}_q\left(\tilde{q}\,|\,t\right)=\left|\mathrm{d}f_q^{-1}\left(\tilde{q}\right)/\mathrm{d}\tilde{q}\right|d_\beta\left[f_q^{-1}\left(\tilde{q}\right)\right]=\left[1/\bar{q}\left(t\right)\right]d_\beta\left[\tilde{q}/\bar{q}\left(t\right)\right] \tag{2.21}$$

in Eqs. (2.13) and (2.14).

In turn, substitution of the density functions in Eqs. (2.20) and (2.21) into the integrals defining $CDF_p(p\,|\,t)$ and $CDF_q(q\,|\,t)$ in Eqs. (2.13) and (2.14) produces

$$CDF_p\left(p\,|\,t\right)=\int_{-\infty}^{p}\left[1/\bar{p}\left(t\right)\right]d_\alpha\left[\tilde{p}/\bar{p}\left(t\right)\right]\mathrm{d}\tilde{p}=\int_{-\infty}^{p/\bar{p}(t)}d_\alpha\left(\alpha\right)\mathrm{d}\alpha \tag{2.22}$$

and

$$CDF_q\left(q\,|\,t\right)=\int_{-\infty}^{q}\left[1/\bar{q}\left(t\right)\right]d_\beta\left[\tilde{q}/\bar{q}\left(t\right)\right]\mathrm{d}\tilde{q}=\int_{-\infty}^{q/\bar{q}(t)}d_\beta\left(\beta\right)\mathrm{d}\beta, \tag{2.23}$$

where the change of variables formula

$$\int_a^b\left[\mathrm{d}f\left(x\right)/\mathrm{d}x\right]g\left[f\left(x\right)\right]\mathrm{d}x=\int_{f(a)}^{f(b)}g\left[f\right]\mathrm{d}f \tag{2.24}$$

is used to obtain the two final equalities.

The integrals defining $CDF(t)$ in Eqs. (2.12) and (2.16) are different in appearance but are numerically equivalent as indicated by the sequence of equalities in Table 2 that start with the Stieltjes integral in Eq. (2.16) and end with the Riemann integral in Eq. (2.12).

If there is no aleatory uncertainty associated with $\bar{p}(t)$, then $d_\alpha(\alpha)$ is the Dirac delta function $\delta(\alpha-1)$ corresponding to $\alpha = 1$ having probability one. In this case,

$$CDF\left(t\right)=\int_{-\infty}^{\bar{p}(t)/\bar{q}(t)}d_\beta\left(\beta\right)\mathrm{d}\beta. \tag{2.25}$$

Similarly, if there is no aleatory uncertainty associated with $\bar{q}(t)$, then $d_\beta(\beta)$ is the Dirac delta function $\delta(\beta-1)$ corresponding to $\beta = 1$ having probability one. In this case,

$$CDF\left(t\right)=\int_{\bar{q}(t)/\bar{p}(t)}^{\infty}d_\alpha\left(\alpha\right)\mathrm{d}\alpha. \tag{2.26}$$

The preceding representations for $CDF(t)$ follow by substituting the indicated density functions into the representation for $CDF(t)$ in Eq. (2.12). In both representations, $CDF(t) = 0$ if the range of integration is outside the range of nonzero values for the density function being integrated.

Table 2 Sequence of Equalities Starting with the Stieltjes Integral in Eq. (2.16) and Ending with the Riemann Integral in Eq. (2.12)

$$
\begin{aligned}
CDF(t) &\overset{1}{=} \int_{p_{mn}(t)}^{p_{mx}(t)} \left[\int_{-\infty}^{p} \mathrm{d}CDF_q(q \mid t) \right] \mathrm{d}CDF_p(p \mid t) \\
&\overset{2}{=} \int_{p_{mn}(t)}^{p_{mx}(t)} \left\{ \int_{-\infty}^{p} \left[\mathrm{d}CDF_q(q \mid t) / \mathrm{d}q \right] \mathrm{d}q \right\} \left\{ \mathrm{d}CDF_p(p \mid t) / \mathrm{d}p \right\} \mathrm{d}p \\
&\overset{3}{=} \int_{p_{mn}(t)}^{p_{mx}(t)} \left\{ \int_{-\infty}^{p} \left[1 / \overline{q}(t) \right] d_\beta \left[q / \overline{q}(t) \right] \mathrm{d}q \right\} \left\{ \left[1 / \overline{p}(t) \right] d_\alpha \left[p / \overline{p}(t) \right] \right\} \mathrm{d}p \\
&\overset{4}{=} \int_{p_{mn}(t)}^{p_{mx}(t)} \left\{ \int_{-\infty}^{p} \left[\mathrm{d}f_q^{-1}(q) / \mathrm{d}q \right] d_\beta \left[f_q^{-1}(q) \right] \mathrm{d}q \right\} \left\{ \left[\mathrm{d}f_p^{-1}(p) / \mathrm{d}p \right] d_\alpha \left[f_p^{-1}(p) \right] \right\} \mathrm{d}p \\
&\overset{5}{=} \int_{p_{mn}(t)}^{p_{mx}(t)} \left\{ \int_{f_q^{-1}(-\infty)}^{f_q^{-1}(p)} d_\beta(\beta) \mathrm{d}\beta \right\} \left\{ \left[\mathrm{d}f_p^{-1}(p) / \mathrm{d}p \right] d_\alpha \left[f_p^{-1}(p) \right] \right\} \mathrm{d}p \\
&\overset{6}{=} \int_{p_{mn}(t)}^{p_{mx}(t)} \left\{ \int_{-\infty}^{f_p[f_p^{-1}(p)]/\overline{q}(t)} d_\beta(\beta) \mathrm{d}\beta \right\} \left\{ \left[\mathrm{d}f_p^{-1}(p) / \mathrm{d}p \right] d_\alpha \left[f_p^{-1}(p) \right] \right\} \mathrm{d}p \\
&\overset{7}{=} \int_{f_p^{-1}[p_{mn}(t)]}^{f_p^{-1}[p_{mx}(t)]} \left\{ \int_{-\infty}^{f_p(\alpha)/\overline{q}(t)} d_\beta(\beta) \mathrm{d}\beta \right\} d_\alpha(\alpha) \mathrm{d}\alpha \\
&\overset{8}{=} \int_{\alpha_{mn}}^{\alpha_{mx}} \left[\int_{-\infty}^{F(\alpha,t)} d_\beta(\beta) \mathrm{d}\beta \right] d_\alpha(\alpha) \mathrm{d}\alpha,
\end{aligned}
$$

where (i) Equality 1 corresponds to the Stieltjes integral representation for $CDF(t)$ in Eq. (2.16), (ii) Equality 2 involves differentiation to convert Stieltjes integrals into Riemann integrals, (iii) Equality 3 results from performing the indicated differentiations for the CDFs defined in Eqs. (2.13) and (2.14) and then replacing the resultant density functions with their representations in Eqs. (2.20) and (2.21), (iv) Equality 4 involves a change in notation with the introduction of the functions $f_p^{-1}(p)$ and $f_q^{-1}(q)$ defined in Eqs. (2.18) and (2..19), (v) Equality 5 involves a change in the variable of integration based on the change of variables formula

$$\int_a^b \left[\mathrm{d}f(x) / \mathrm{d}x \right] g\left[f(x) \right] \mathrm{d}x = \int_{f(a)}^{f(b)} g(f) \mathrm{d}f,$$

(vi) Equality 6 involves a change in notation based on the relationship

$$f_q^{-1}(p) = p / \overline{q}(t) = f_p\left[f_p^{-1}(p) \right] / \overline{q}(t),$$

(vii) Equality 7 involves a change in the variable of integration based on the preceding change of variables formula, and (viii) Equation 8 involves the change of notation

$$f_p(\alpha) / \overline{q}(t) = \alpha \overline{p}(t) / \overline{q}(t) = F(\alpha, t)$$

and corresponds to the Riemann integral representation for $CDF(t)$ in Eq. (2.12).

This page intentionally left blank.

3. Evaluation of CDFs for Known Density functions

As indicated in Eq. (2.12), the function *CDF*(t) for cumulative link failure probability can be obtained from a Riemann integral involving the CDF for β. Similarly as shown in Eqs. (2.16), (2.22) and (2.23), *CDF*(t) can also be obtained from a Stieltjes integral involving the CDFs for α and β. Further, the special case representations for *CDF*(t) in Eqs. (2.25) and (2.26) are, in effect, CDFs for β and α, respectively. Thus, obtaining CDFs for α and β is a fundamental part of evaluating *CDF*(t). As shown in this section, CDFs for many known density functions can be easily constructed. In turn, these CDFs can be used in numerically efficient evaluations of the representations for *CDF*(t) in Eqs. (2.12), (2.16), (2.25) and (2.26).

As examples, normal, lognormal, uniform, loguniform and triangular distributions are considered. The density functions for these distributions are (i)

$$d_n(x) = \left(1/\sigma\sqrt{2\pi}\right)\exp\left[-(x-\mu)^2/2\sigma^2\right] \tag{3.1}$$

for x normal with mean μ and standard deviation σ, (ii)

$$d_{ln}(x) = \begin{cases} 0 & \text{for } x \le 0 \\ \left(1/x\sigma\sqrt{2\pi}\right)\exp\left[-(\ln x-\mu)^2/2\sigma^2\right] & \text{for } 0 < x \end{cases} \tag{3.2}$$

for x lognormal with $x > 0$, $E(\ln x) = \mu$, $V(\ln x) = \sigma^2$, and E and V used to represent expected value and variance, respectively, (iii)

$$d_u(x) = \begin{cases} 1/(b-a) & \text{for } a \le x \le b \\ 0 & \text{otherwise} \end{cases} \tag{3.3}$$

for x uniform on $[a, b]$ with $-\infty < a$ and $b < \infty$, (iv)

$$d_{lu}(x) = \begin{cases} 1/\left[x\ln(b/a)\right] & \text{for } a \le x \le b \\ 0 & \text{otherwise} \end{cases} \tag{3.4}$$

for x loguniform on $[a, b]$ with $0 < a$ and $b < \infty$, and (v)

$$d_t(x) = \begin{cases} (2x-2a)/(m-a)(b-a) & \text{for } a \le x \le m \\ (2b-2x)/(b-m)(b-a) & \text{for } m \le x \le b \\ 0 & \text{otherwise} \end{cases} \tag{3.5}$$

for x triangular on $[a, b]$ with $-\infty < a$ and $b < \infty$ with mode m.

In turn, the corresponding CDFs for normal, lognormal, uniform, loguniform and triangular distributions are

$$CDF_n(x) = \int_{-\infty}^{x} d_n(v)\,\mathrm{d}v = 1 - (1/2)\,erfc\left[(x-\mu)/\sigma\sqrt{2}\right], \tag{3.6}$$

$$CDF_{ln}(x) = \int_{-\infty}^{x} d_{ln}(v)\,\mathrm{d}v = \begin{cases} 0 & \text{for } x \le 0 \\ 1 - (1/2)\,erfc\left[(\ln x - \mu)/\sigma\sqrt{2}\right] & \text{orf0} < x, \end{cases} \tag{3.7}$$

$$CDF_u(x) = \int_{-\infty}^{x} d_u(v)\,\mathrm{d}v = \begin{cases} 0 & \text{for } x < a \\ (x-a)/(b-a) & \text{for } a \le x \le b \\ 1 & \text{for } b < x, \end{cases} \tag{3.8}$$

$$CDF_{lu}(x) = \int_{-\infty}^{x} d_{lu}(v)\,\mathrm{d}v = \begin{cases} 0 & \text{for } x < a \\ \ln(x/a)/\ln(b/a) & \text{for } a \le x \le b \\ 1 & \text{for } b < x, \end{cases} \tag{3.9}$$

and

$$CDF_t(x) = \int_{-\infty}^{x} d_t(v)\,\mathrm{d}v = \begin{cases} 0 & \text{for } x < a \\ (x-a)^2/(m-a)(b-a) & \text{for } a \le x \le m \\ 1-(b-x)^2/(b-m)(b-a) & \text{for } m \le x \le b \\ 1 & \text{for } b < x, \end{cases} \tag{3.10}$$

respectively, where

$$erfc(x) = \left(2/\sqrt{\pi}\right)\int_{x}^{\infty} \exp\left(-v^2\right)\mathrm{d}v \tag{3.11}$$

is the complementary error function. Similar expressions define complementary cumulative distribution functions (CCDFs) as a CCDF is simply one minus the corresponding CDF.

The CDFs and CCDFs for uniform, loguniform and triangular distributions are easy to evaluate and thus present no numerical challenges. The CDFs and CCDFs for normal and lognormal distributions are more complex to evaluate but, as the result of an algebraic approximation to the complementary error function, can be approximated in a computationally efficient manner. Specifically, $erfc(x)$ can be approximated by

$$
\begin{aligned}
erfc(x) \cong t\exp(-x^2 &- 1.26551223 + t(1.00002368 + t(0.37409196 + t(0.09678418 \\
&+t(-0.18628806 + t(0.27886807 + t(-1.13520398 + t(1.48851587 \\
&+t(-0.82215223 + t0.17087277)))))))))
\end{aligned}
\tag{3.12}
$$

for $x \geq 0$ and $t = 1/(1 + 0.5x)$ and by

$$erfc(x) = 2 - erfc(|x|) \tag{3.13}$$

for $x < 0$ ([19], p. 164). Although not aesthetically pleasing, the preceding approximation to $erfc(x)$ is easy to evaluate numerically.

Care must be used in the specification of distributions that have infinite tails (e.g., normal and lognormal distributions) as the infinite tails of such distributions typically correspond to variable values that are physically impossible. This may sound like a pedantic observation but the authors of this paper have seen serious errors introduced into important decision-supporting analyses by the use of distributions with infinite tails without the specification of truncation values for the tails.

As an example, the truncation of the normal and lognormal distributions introduced in Eqs. (3.1) and (3.2) is considered. If these distributions are truncated at lower and upper quantiles of q_{mn} and q_{mx}, respectively, then the density functions for the truncated distributions would be (i)

$$
d_{tn}(x) = \begin{cases} 0 & \text{for } x \leq x_{mn} \text{ and } x_{mx} \leq x \\ \dfrac{\left(1/\sigma\sqrt{2\pi}\right)\exp\left[-(x-\mu)^2/2\sigma^2\right]}{q_{mx}-q_{mn}} & \text{for } x_{mn} < x < x_{mx} \end{cases}
\tag{3.14}
$$

for the truncation of a normal distribution for x with mean μ and standard deviation σ, where $x_{mn} = \Phi_n^{-1}(q_{mn} \mid \mu, \sigma)$, $x_{mx} = \Phi_n^{-1}(q_{mx} \mid \mu, \sigma)$, and $\Phi_n^{-1}(q \mid \mu, \sigma)$ denotes the q-quantile value x_q of a normal distribution with mean μ and standard deviation σ, and (ii)

$$
d_{tln}(x) = \begin{cases} 0 & \text{for } x \leq x_{mn} \text{ and } x_{mx} \leq x \\ \dfrac{\left(1/x\sigma\sqrt{2\pi}\right)\exp\left[-(\ln x-\mu)^2/2\sigma^2\right]}{q_{mx}-q_{mn}} & \text{for } x_{mn} < x < x_{mx} \end{cases}
\tag{3.15}
$$

for the truncation of a lognormal distribution for x with $x > 0$, $E(\ln x) = \mu$, and $V(\ln x) = \sigma^2$, where $x_{mn} = \Phi_{ln}^{-1}(q_{mn} \mid \mu, \sigma)$, $x_{mx} = \Phi_{ln}^{-1}(q_{mx} \mid \mu, \sigma)$, and $\Phi_{ln}^{-1}(q \mid \mu, \sigma)$ denotes the q-quantile value x_q of a lognormal distribution with $E(\ln x) = \mu$ and $V(\ln x) = \sigma^2$.

In turn, the CDFs for truncated normal and lognormal distributions are

$$CDF_{tn}(x) = \int_{-\infty}^{x} d_{tn}(v)\,\mathrm{d}v$$
$$= \begin{cases} 0 & \text{for } x \le x_{mn} \\ \dfrac{1 - q_{mn} - (1/2)\,erfc\left[(x-\mu)/\sigma\sqrt{2}\right]}{q_{mx} - q_{mn}} & \text{for } x_{mn} < x < x_{mx} \\ 1 & \text{for } x_{mx} \le x \end{cases} \tag{3.16}$$

and

$$CDF_{tln}(x) = \int_{-\infty}^{x} d_{tln}(v)\,\mathrm{d}v$$
$$= \begin{cases} 0 & \text{for } x \le x_{mn} \\ \dfrac{1 - q_{mn} - (1/2)\,erfc\left[(\ln x-\mu)/\sigma\sqrt{2}\right]}{q_{mx} - q_{mn}} & \text{for } x_{mn} < x < x_{mx} \\ 1 & \text{for } x_{mx} \le x, \end{cases} \tag{3.17}$$

respectively. When q_{mn} and q_{mx} are related by $q_{mx} = 1 - q_{mn}$, the divisor $q_{mx} - q_{mn}$ in Eqs. (3.14)-(3.17) simplifies to $1 - 2q_{mn}$.

4. Evaluation of PLOAS with Quadrature-Based Procedures

Once $CDF(t)$ and $CCDF(t) = 1 - CDF(t)$ can be evaluated for individual links, the representations for PLOAS in Table 1 can be numerically evaluated. For example, the probability $pF_1(t)$ for the failure all SLs before the failure of any WL is defined as Case 1 in Table 1 and can be approximated by

$$
\begin{aligned}
pF_1(t) &\cong \sum_{k=1}^{nSL}\left(\sum_{i=1}^{n}\left\{\prod_{l=1,l\neq k}^{nSL} CDF_{SL,l}\left(t_{i-1}\right)\right\}\right. \\
&\quad \left.\times\left\{\prod_{j=1}^{nWL}\left[1-CDF_{WL,j}\left(t_i\right)\right]\right\}\left\{CDF_{SL,k}\left(t_i\right)-CDF_{SL,k}\left(t_{i-1}\right)\right\}\right) \\
&= \sum_{k=1}^{nSL}\left(\sum_{i=1}^{n}\left\{\prod_{l=1,l\neq k}^{nSL} CDF_{SL,l}\left(t_{i-1}\right)\right\}\right. \\
&\quad \left.\times\left\{\prod_{j=1}^{nWL}\left[CCDF_{WL,j}\left(t_i\right)\right]\right\}\left\{CDF_{SL,k}\left(t_i\right)-CDF_{SL,k}\left(t_{i-1}\right)\right\}\right)
\end{aligned}
\tag{4.1}
$$

for subdivisions $0 = t_0 < t_1 < \ldots < t_n = t$ of $[0, t]$. As shown below, similar approximations exist for the other three failure cases defined in Table 1. In the preceding approximation for $pF_1(t)$, left and right evaluations are indicated for SLs (i.e., $CDF_{SL,l}(t_{i-1})$ and $CCDF_{SL,l}(t_{i-1})$) and WLs (i.e., $CDF_{WL,j}(t_i)$ and $CCDF_{WL,j}(t_i)$), respectively, as the underlying assumption is that all SLs except for SL k have failed before time t_{i-1} and all WLs fail after time t_i. If the CDFs and CCDFs are continuous in time, this specification of evaluation times does not affect the limiting value for $pF_1(t)$ as Δt_i goes to zero.

Similarly, the representations $pF_2(t)$, $pF_3(t)$ and $pF_4(t)$ for PLOAS in Table 1 can be approximated by

$$
\begin{aligned}
pF_2(t) &\cong \sum_{k=1}^{nSL}\left(\sum_{i=1}^{n}\left\{\prod_{l=1,l\neq k}^{nSL}\left[1-CDF_{SL,l}\left(t_{i-1}\right)\right]\right\}\right.\\
&\qquad \left.\times\left\{\prod_{j=1}^{nWL}\left[1-CDF_{WL,j}\left(t_i\right)\right]\right\}\left\{CDF_{SL,k}\left(t_i\right)-CDF_{SL,k}\left(t_{i-1}\right)\right\}\right)\\
&= \sum_{k=1}^{nSL}\left(\sum_{i=1}^{n}\left\{\prod_{l=1,l\neq k}^{nSL}CCDF_{SL,l}\left(t_{i-1}\right)\right\}\right.\\
&\qquad \left.\times\left\{\prod_{j=1}^{nWL}CCDF_{WL,j}\left(t_i\right)\right\}\left\{CDF_{SL,k}\left(t_i\right)-CDF_{SL,k}\left(t_{i-1}\right)\right\}\right),
\end{aligned}
\tag{4.2}
$$

$$
\begin{aligned}
pF_3(t) &\cong \sum_{k=1}^{nSL}\left(\sum_{i=1}^{n}\left\{\prod_{l=1,l\neq k}^{nSL}CDF_{SL,l}\left(t_{i-1}\right)\right\}\right.\\
&\qquad \left.\times\left\{1-\prod_{j=1}^{nWL}CDF_{WL,j}\left(t_i\right)\right\}\left\{CDF_{SL,k}\left(t_i\right)-CDF_{SL,k}\left(t_{i-1}\right)\right\}\right)
\end{aligned}
\tag{4.3}
$$

and

$$
\begin{aligned}
pF_4(t) &\cong \sum_{k=1}^{nSL}\left(\sum_{i=1}^{n}\left\{\prod_{l=1,l\neq k}^{nSL}\left[1-CDF_{SL,l}\left(t_{i-1}\right)\right]\right\}\right.\\
&\qquad \left.\times\left\{1-\prod_{j=1}^{nWL}CDF_{WL,j}\left(t_i\right)\right\}\left\{CDF_{SL,k}\left(t_i\right)-CDF_{SL,k}\left(t_{i-1}\right)\right\}\right)\\
&= \sum_{k=1}^{nSL}\left(\sum_{i=1}^{n}\left\{\prod_{l=1,l\neq k}^{nSL}CCDF_{SL,l}\left(t_{i-1}\right)\right\}\right.\\
&\qquad \left.\times\left\{1-\prod_{j=1}^{nWL}CDF_{WL,j}\left(t_i\right)\right\}\left\{CDF_{SL,k}\left(t_i\right)-CDF_{SL,k}\left(t_{i-1}\right)\right\}\right)
\end{aligned}
\tag{4.4}
$$

for subdivisions $0 = t_0 < t_1 < \ldots < t_n = t$ of $[0, t]$.

5. Evaluation of PLOAS with Sampling-Based Procedures

Sampling-based (i.e., Monte Carlo) procedures can also be used to determine PLOAS. One approach is to use sampling-based procedures to estimate the expected values of functions $\delta_i(t\,|\,\mathbf{t})$, i = 1, 2, 3, 4, where

$$t = \text{ time at which PLOAS (i.e., } pF_i(t) \text{ in Table 1) is to be determined,} \tag{5.1}$$

$$tWL_j = \text{ time at which WL } j \text{ fails, } j = 1, 2, ..., nWL, \tag{5.2}$$

$$tSL_j = \text{ time at which SL } j \text{ fails, } j = 1, 2, ..., nSL, \tag{5.3}$$

$$\mathbf{t} = \left[tWL_1, tWL_2, ..., tWL_{nWL}, tSL_1, tSL_2, ..., tSL_{nSL}\right], \tag{5.4}$$

$$\delta_1(t\,|\,\mathbf{t}) = \begin{cases} 1 \text{ if } \max\{tSL_1, tSL_2, ..., tSL_{nSL}\} \le \min\{t, tWL_1, tWL_2, ..., tWL_{nSL}\} \\ 0 \text{ otherwise,} \end{cases} \tag{5.5}$$

$$\delta_2(t\,|\,\mathbf{t}) = \begin{cases} 1 \text{ if } \min\{tSL_1, tSL_2, ..., tSL_{nSL}\} \le \min\{t, tWL_1, tWL_2, ..., tWL_{nSL}\} \\ 0 \text{ otherwise,} \end{cases} \tag{5.6}$$

$$\delta_3(t\,|\,\mathbf{t}) = \begin{cases} 1 \text{ if } \max\{tSL_1, tSL_2, ..., tSL_{nSL}\} \le \min\{t, \max\{tWL_1, tWL_2, ..., tWL_{nSL}\}\} \\ 0 \text{ otherwise,} \end{cases} \tag{5.7}$$

and

$$\delta_4(t\,|\,\mathbf{t}) = \begin{cases} 1 \text{ if } \min\{tSL_1, tSL_2, ..., tSL_{nSL}\} \le \min\{t, \max\{tWL_1, tWL_2, ..., tWL_{nSL}\}\} \\ 0 \text{ otherwise.} \end{cases} \tag{5.8}$$

In words, $\delta_1(t\,|\,\mathbf{t}) = 1$ corresponds to all SLs failing before time t and also before any WL fails (i.e., Case 1 in Table 1); $\delta_2(t\,|\,\mathbf{t}) = 1$ corresponds to any SL failing before time t and also before any WL fails (i.e., Case 2 in Table 1); $\delta_3(t\,|\,\mathbf{t}) = 1$ corresponds to all SLs failing before time t and also before all WLs fail (i.e., Case 3 in Table 1); and $\delta_4(t\,|\,\mathbf{t}) = 1$ corresponds to any SL failing before time t and also before all WLs fail (i.e., Case 4 in Table 1). If a time interval $[t_{mn}, t_{mx}]$ is under consideration, the possible failure time t is assumed to be contained in $[t_{mn}, t_{mx}]$; further, if a link has not failed within $[t_{mn}, t_{mx}]$, its failure time is set to a value greater than t_{mx} for use with the indicator functions $\delta_i(t\,|\,\mathbf{t})$ defined in Eqs. (5.5)-(5.8).

When appropriately formulated, the expected value $E[\delta_i(t\,|\,\mathbf{t})]$, i = 1, 2, 3, 4, for $\delta_i(t\,|\,\mathbf{t})$ corresponds to the PLOAS value $pF_i(t)$ defined in Table 1. Two ways to defined the expected value $E[\delta_i(t\,|\,\mathbf{t})]$ for $pF_i(t)$ are illustrated in this section: (i) with use of the CDFs $CDF_{WL,j}(\tau)$, j = 1, 2, …, nWL, and $CDF_{SL,j}(\tau)$, j = 1, 2, …, nSL, for link failure times, and (ii) with use of the distributions for the variables $\alpha_{WL,j}, \beta_{WL,j}$, j = 1, 2, …, nWL, and $\alpha_{SL,j}, \beta_{SL,j}$, j = 1, 2, …, nSL, indicated in conjunction with Eqs. (2.1)-(2.6) that define properties and failure values for the individual links. In addition, approximations with both simple random sampling and importance sampling are described.

Approximation of $pF_i(t)$ with use of the CDFs $CDF_{WL,j}(\tau)$, j = 1, 2, … , nWL, and $CDF_{SL,j}(\tau)$, j = 1, 2, …, nSL, is considered first. In this approach, $pF_i(t)$ is approximated by

$$\begin{aligned} pF_i(t) &= \int_{I^{nL}} \delta_i\left[t\,|\,\mathbf{f}(\mathbf{r})\right]\prod_{k=1}^{nL} d_k\left(r_k\right)\prod_{k=1}^{nL} \mathrm{d}r_k \\ &= \int_{I^{nL}} \delta_i\left[t\,|\,\mathbf{f}(\mathbf{r})\right]\prod_{k=1}^{nL} \mathrm{d}r_k \\ &\cong \sum_{l=1}^{nR} \delta_i\left[t\,|\,\mathbf{f}(\mathbf{r}_l)\right]\Big/ nR \\ &= \sum_{l=1}^{nR} \delta_i\left\{t\,|\left[tWL_{1l}, tWL_{2l}, \dots, tWL_{nWL,l}, tSL_{1l}, tSL_{2l}, \dots, tSL_{nSL,l}\right]\right\}\Big/ nR, \end{aligned} \tag{5.9}$$

where (i) $nL = nWL + nSL$, (ii) $d_k(r_k) = 1$ is the density function for a variable r_k with a uniform distribution on [0, 1], (iii) $I^{nL} = [0,1]^{nL}$ (i.e., the unit cube of dimension nL), (iv) $\mathbf{r} = [r_1, r_2, \dots, r_{nL}] \in I^{nL}$, (v) the function $\mathbf{f}(\mathbf{r})$ is defined by

$$\begin{aligned} \mathbf{f}(\mathbf{r}) &= \Big[CDF_{WL,1}^{-1}(r_1), CDF_{WL,2}^{-1}(r_2), \dots, CDF_{WL,nWL}^{-1}(r_{nWL}), \\ &\qquad CDF_{SL,1}^{-1}(r_{nWL+1}), CDF_{SL,2}^{-1}(r_{nWL+2}), \dots, CDF_{SL,nSL}^{-1}(r_{nL})\Big] \\ &= \left[tWL_1, tWL_2, \dots, tWL_{nWL}, tSL_1, tSL_2, \dots, tSL_{nSL}\right] \end{aligned} \tag{5.10}$$

with $tWL_j = CDF_{WL,j}^{-1}(r_j)$ for j = 1, 2, …, nWL and $tSL_j = CDF_{SL,j}^{-1}(r_{nWL+j})$ for j = 1, 2, …, nSL, and (vi) $\mathbf{r}_l$, l = 1, 2, …, nR, is a random sample of size nR from a uniform distribution on I^{nL}. With respect to the approximation of $pF_i(t)$ in Eq. (5.9), the first equality defines $pF_i(t)$ as the expected value of $\delta_i[t\,|\,\mathbf{f}(\mathbf{r})]$; the second equality is a notational simplification based on the equalities $d_k(r_k) = 1$ for k = 1, 2, …, nL; the approximation at the third step is based on a random sample from the link failure times; and the final equality is a restatement of $\mathbf{f}(\mathbf{r})$ in terms of link failure times.

Importance sampling involves introducing selected distributions for the variables r_k, k = 1, 2, …, nL, in Eq. (5.9) that emphasize link failure times that are important in the determination of $pF_i(t)$. When this is done, the approximation to $pF_i(t)$ in Eq. (5.9) becomes

$$\begin{aligned} pF_i(t) &= \int_{I^{nL}} \left\{ \delta_i\left[t \mid \mathbf{f}(\mathbf{r})\right] \Big/ \prod_{k=1}^{nL} d_{I,k}\left(r_k\right) \right\} \prod_{k=1}^{nL} d_{I,k}\left(r_k\right) \prod_{k=1}^{nL} \mathrm{d}r_k \\ &\cong \sum_{l=1}^{nR} \left\{ \delta_i\left[t \mid \mathbf{f}\left(\mathbf{r}_l\right)\right] \Big/ \prod_{k=1}^{nL} d_{I,k}\left(r_{kl}\right) \right\} / nR \\ &= \sum_{l=1}^{nR} \frac{\delta_i\left\{t \mid \left[tWL_{1l}, tWL_{2l}, ..., tWL_{nWL,l}, tSL_{1l}, tSL_{2l}, ..., tSL_{nSL,l}\right]\right\}}{nR \prod_{k=1}^{nL} d_{I,k}\left(r_{kl}\right)}, \end{aligned} \tag{5.11}$$

where (i) the first equality derives from the introduction of the importance sampling distributions defined by the density functions $d_{I,k}(r_k)$, k = 1, 2, …, nL, into the representation for $pF_i(t)$ in Eq. (5.9), (ii) the following approximation involves a random sample $\mathbf{r}_l$, l = 1, 2, …, nR, from I^{nL} generated in consistency with the distributions defined by the density functions $d_{I,k}(r_k)$, and (iii) the final equality is a restatement of $\mathbf{f}(\mathbf{r})$ in terms of link failure times. In general, *a priori* knowledge with respect to the effects of the individual link failure times on $pF_i(t)$ is needed to define the density functions $d_{I,k}(r_k)$ in a manner that will enhance the convergence with increasing sample size of the approximation in Eq. (5.11) to $pF_i(t)$ over what would be obtained with simple random sampling as indicated in Eq. (5.9).

Approximation of $pF_i(t)$ with use of the distributions for the variables $\alpha_{WL,j}, \beta_{WL,j}$, j = 1, 2, …, nWL, and $\alpha_{SL,j}, \beta_{SL,j}$, j = 1, 2, …, nSL, indicated in conjunction with Eqs. (2.1)-(2.6) that define properties and failure values for the individual links is now considered. The approximation to $pF_i(t)$ in this case is similar to the approximation in Eq. (5.9) but with changed definitions for $\mathbf{r}$, $\mathbf{r}_l$, $\mathbf{f}(\mathbf{r})$ and $d_k(r_k)$. Specifically,

$$\begin{aligned} \mathbf{r} &= \left[r_1, r_2, ..., r_{2nL}\right] \text{ with } nL = nWL + nSL \\ &= \left[\alpha_{WL,1}, \alpha_{WL,2}, ..., \alpha_{WL,nWL}, \beta_{WL,1}, \beta_{WL,2}, ..., \beta_{WL,nWL}, \right. \\ &\qquad \left. \alpha_{SL,1}, \alpha_{SL,2}, ..., \alpha_{SL,nSL}, \beta_{SL,1}, \beta_{SL,2}, ..., \beta_{SL,nSL}\right], \end{aligned} \tag{5.12}$$

$$\mathbf{p}_{WL,j} = \left[\alpha_{WL,j}, \beta_{WL,j}\right] = \left[r_j, r_{nWL+j}\right], j = 1, 2, ..., nWL, \tag{5.13}$$

$$\mathbf{p}_{SL,j} = \left[\alpha_{SL,j}, \beta_{SL,j}\right] = \left[r_{2nWL+j}, r_{2nWL+nSL+j}\right], j = 1, 2, ..., nSL, \tag{5.14}$$

$$f_{WL,j}\left(\mathbf{p}_{WL,j}\right) = \text{ time at which WL } j \text{ fails with } \mathbf{p}_{WL,j} = \left[\alpha_{WL,j}, \beta_{WL,j}\right] \\ = tWL_j, \tag{5.15}$$

$$f_{SL,j}\left(\mathbf{p}_{SL,j}\right) = \text{ time at which SL } j \text{ fails with } \mathbf{p}_{SL,j} = \left[\alpha_{SL,j}, \beta_{SL,j}\right] \\ = tSL_j, \tag{5.16}$$

and

$$\begin{aligned} \mathbf{f}(\mathbf{r}) &= \Big[f_{WL,1}\left(\mathbf{p}_{WL,1}\right), f_{WL,2}\left(\mathbf{p}_{WL,2}\right), ..., f_{WL,nWL}\left(\mathbf{p}_{WL,nWL}\right) \\ &\qquad f_{SL,1}\left(\mathbf{p}_{SL,1}\right), f_{SL,2}\left(\mathbf{p}_{SL,2}\right), ..., f_{SL,nSL}\left(\mathbf{p}_{WL,nSL}\right) \Big] \\ &= \left[tWL_1, tWL_2, ..., tWL_{nWL}, tSL_1, tSL_2, ..., tSL_{nSL}\right]. \end{aligned} \tag{5.17}$$

In turn,

$$\begin{aligned} pF_i(t) &= \int_{\mathcal{S}} \delta_i\left[t \mid \mathbf{f}(\mathbf{r})\right] \prod_{k=1}^{2nL} d_k\left(r_k\right) \prod_{k=1}^{2nL} \mathrm{d}r_k \\ &\cong \sum_{l=1}^{nR} \delta_i\left[t \mid \mathbf{f}(\mathbf{r}_l)\right] \Big/ nR \\ &= \sum_{l=1}^{nR} \delta_i\left\{t \mid \left[tWL_{1l}, tWL_{2l}, ..., tWL_{nWL,l}, tSL_{1l}, tSL_{2l}, ..., tSL_{nSL,l}\right]\right\} \Big/ nR, \end{aligned} \tag{5.18}$$

where (i) $d_k(r_k)$ is the density function for r_k defined on the set $\mathcal{S}_k$ of possible values for r_k (i.e., for $\alpha_{WL,j}$, $\beta_{WL,j}$, $\alpha_{SL,j}$ or $\beta_{SL,j}$ as appropriate; see Eq. (5.12)), (ii) $\mathcal{S} = \mathcal{S}_1 \times \mathcal{S}_2 \times \cdots \times \mathcal{S}_{2nL}$, and (iii) $\mathbf{r}_l$, l = 1, 2, …, nR, is a random sample of size nR from $\mathcal{S}$ generated in consistency with the distributions defined by the density functions $d_k(r_k)$.

The approximation to $pF_i(t)$ in Eq. (5.18) based on sampling from the variables $\alpha_{WL,j}$, $\beta_{WL,j}$, $\alpha_{SL,j}$ and $\beta_{SL,j}$ can also be modified to include importance sampling. When this is done, the approximation to $pF_i(t)$ in Eq. (5.18) becomes

$$\begin{aligned} pF_i(t) &= \int_{\mathcal{S}} \left\{\delta_i\left[t \mid \mathbf{f}(\mathbf{r})\right] \prod_{k=1}^{2nL} d_k\left(r_k\right) \Big/ \prod_{k=1}^{2nL} d_{I,k}\left(r_k\right)\right\} \prod_{k=1}^{2nL} d_{I,k}\left(r_k\right) \prod_{k=1}^{2nL} \mathrm{d}r_k \\ &\cong \sum_{l=1}^{nR} \left\{\delta_i\left[t \mid \mathbf{f}(\mathbf{r}_l)\right] \prod_{k=1}^{2nL} d_k\left(r_{kl}\right) \Big/ \prod_{k=1}^{2nL} d_{I,k}\left(r_{kl}\right)\right\} \Big/ nR \\ &= \sum_{l=1}^{nR} \frac{\delta_i\left\{t \mid \left[tWL_{1l}, tWL_{2l}, ..., tWL_{nWL,l}, tSL_{1l}, tSL_{2l}, ..., tSL_{nSL,l}\right]\right\} \prod_{k=1}^{2nL} d_k\left(r_{kl}\right)}{nR \prod_{k=1}^{2nL} d_{I,k}\left(r_{kl}\right)}, \end{aligned} \tag{5.19}$$

where (i) the first equality derives from the introduction of the importance sampling distributions defined by the density functions $d_{I,k}(r_k)$, $k = 1, 2, \ldots, 2nL$, into the representation for $pF_i(t)$ in Eq.(5.18), (ii) the following approximation involves a random sample $\mathbf{r}_l$, $l = 1, 2, \ldots, nR$, from $\mathcal{S}$ generated in consistency with the distributions defined by the density functions $d_{I,k}(r_k)$, and (iii) the final equality is a restatement of $\mathbf{f}(\mathbf{r})$ in terms of link failure times.

In addition to sample size effects, the accuracy of the methods defined in Eqs. (5.18) and (5.19) is also dependent on the accuracy with which the link failure times tWL_j and tSL_j in Eqs. (5.15) and (5.16) are determined.

In general, the quadrature-based procedures for the evaluation $pF_i(t)$ described in Sect. 4 will be more computationally efficient than the sampling-based procedures described in this section. It is anticipated that the primary use of the sampling-based procedures will be in the verification of the correctness of the implementation of quadrature-based procedures for the evaluation of $pF_i(t)$. The sampling-based procedures are effective verification tools because their implementation is, to a great extent, independent of the implementation of the quadrature-based procedures. This is especially true for the procedures described in Eqs. (5.18) and (5.19) based on sampling the variables $\alpha_{WL,j}$, $\beta_{WL,j}$, $j = 1, 2, \ldots, nWL$, and $\alpha_{SL,j}$, $\beta_{SL,j}$ $j = 1, 2, \ldots, nSL$. The procedures described in Eqs. (5.9) and (5.11) are somewhat less effective as verification tools because of the use of the same CDFs (i.e., $CDF_{WL,j}(\tau)$, $j = 1, 2, \ldots, nWL$, and $CDF_{SL,j}(\tau)$, $j = 1, 2, \ldots, nSL$) for link failure times as used in the quadrature procedures.

A way to potentially enhance the efficiency of the sampling techniques described in this section is to perform the calculations indicated in Eqs. (5.9), (5.11), (5.18) and (5.19) in two steps. In the first step, sets

$$\mathcal{WL}_j = \left\{tWL_{jl} : l = 1,2,\ldots,nR1\right\},\ j = 1,2,\ldots,nWL \tag{5.20}$$

and

$$\mathcal{SL}_j = \left\{tSL_{jl} : l = 1,2,\ldots,nR1\right\},\ j = 1,2,\ldots,nSL \tag{5.21}$$

of link failure times are generated with the sampling method used in conjunction with the procedure in Eq. (5.9), (5.11), (5.18) or (5.19). As a result of the use of different sampling methods, the failure times for the individual links in Eqs. (5.20) and (5.21) have weights (i.e., probabilities) defined by (i)

$$wL_{kl} = 1/nR1 = \begin{cases} wWL_{jl} \text{ for } j{=}k = 1,2,\ldots,nWL \\ wSL_{jl} \text{ for } j = k - nWL \text{ with } k = nWL+1, nWL+2,\ldots, nL = nWL + nSL \end{cases} \tag{5.22}$$

for the simple random sampling used in conjunction with Eqs. (5.9) and (5.18), (ii)

$$
\begin{aligned}
wL_{kl} &= 1/\left[nR1 d_{I,k}\left(r_{kl}\right)\right], k = 1,2,....,nL = nWL + nSL \\
&= \begin{cases} wWL_{jl} \text{ for } j = k = 1,2,....,nWL \\ wSL_{jl} \text{ for } j = k - nWL \text{ with } k = nWL+1, nWL+2,....,nL \end{cases}
\end{aligned} \tag{5.23}
$$

for the importance sampling used in conjunction with Eq. (5.11), and (iii)

$$
wL_{kl} = \begin{cases} wWL_{jl} \text{ for } j = k = 1,2,....,nWL \\ wSL_{jl} \text{ for } j = k - nWL \text{ with } k = nWL+1, nWL+2,....,nL = nWL + nSL \end{cases} \tag{5.24}
$$

with

$$
wWL_{jl} = \left[\frac{d_j\left(r_{jl}\right) d_{nWL+j}\left(r_{nWL+j,l}\right)}{d_{I,j}\left(r_{jl}\right) d_{I,nWL+j}\left(r_{nWL+j,l}\right)}\right] \Big/ nR1 \tag{5.25}
$$

and

$$
wSL_{jl} = \left[\frac{d_{2nWL+j}\left(r_{2nWL+j,l}\right) d_{2nWL+nSL+j}\left(r_{2nWL+nSL+j,l}\right)}{d_{I,2nWL+j}\left(r_{2nWL+j,l}\right) d_{I,2nWL+nSL+j}\left(r_{2nWL+nSL+j,l}\right)}\right] \Big/ nR1 \tag{5.26}
$$

for the importance sampling used in conjunction with Eq. (5.19). The subscripting in Eqs. (5.25) and (5.26) matches the order in which the α's and β's appear in the vector $\mathbf{r}$ in Eq. (5.12).

In the second step, the sets $\mathcal{WL}_j$ and $\mathcal{SL}_j$ defined in Eqs. (5.20) and (5.21) and the associated weights indicated in Eqs. (5.22)-(5.26) are used to construct an approximation to $pF_i(t)$. One possibility is to approximate $pF_i(t)$ with an exhaustive combination of all the times contained in $\mathcal{WL}_j$ and $\mathcal{SL}_j$, which produces the approximation

$$
pF_i(t) \cong \sum_{\mathbf{l}=[l_1,l_2,...,l_{nL}]\in\mathcal{S}} \delta_i\left(\mathbf{t_l}\right) \prod_{k=1}^{nL} wL_{kl_k}, \tag{5.27}
$$

where

$$
\mathcal{S}_k = \{1,2,...,nR1\} \text{ for } k = 1,2,...,nL,
$$

$$
\mathcal{S} = \mathcal{S}_1 \times \mathcal{S}_2 \times \cdots \times \mathcal{S}_{nL} = \{\mathbf{l} = [l_1,l_2,...,l_{nL}] : l_k \in \mathcal{S}_k \text{ for } k = 1,2,...,nL\},
$$

and

$$\mathbf{t_l} = \left[tWL_{1l_1}, tWL_{2l_2}, ..., tWL_{nWL,l_{nWL}}, tSL_{1,l_{nWL+1}}, tSL_{2,l_{nWL+2}}, ..., tSL_{nSL,nL} \right].$$

This approach has the advantage that it uses all the information generated in the first sampling but can computationally demanding if $nR1$ and nL are large as the number of terms in the summation in Eq. (5.27) is $nR1^{nL}$.

An alternate approach is to use simple random sampling from the sets $\mathcal{WL}_j$ and $\mathcal{SL}_j$ in conjunction with the associated weights indicated in Eqs. (5.22)-(5.26)In this approach, the weights indicated in Eqs. (5.22)-(5.26)are used as the probabilities for the individual elements of $\mathcal{WL}_j$ and $\mathcal{SL}_j$ to generate a random sample of the form

$$\mathbf{t}_l = \left[tWL_{1l}, tWL_{2l}, ..., tWL_{nWL,l}, tSL_{1l}, tSL_{2l}, ..., tSL_{nSL,l} \right], l = 1, 2, ..., nR2, \tag{5.28}$$

from the sets $\mathcal{WL}_j$ and $\mathcal{SL}_j$. Once generated, these samples can be used as shown in Eq. (5.9) with $nR = nR2$ to estimate the PLOAS value $pF_i(t)$. In general, the sample size $nR2$ would be larger than the sample size $nR1$ used to generate $\mathcal{WL}_j$ and $\mathcal{SL}_j$ but smaller than $nR1^{nL}$.

If some of the weights in Eqs. (5.22)-(5.26) are very small, the random sampling approach indicated in the preceding paragraph could require a very large sample size to obtain an adequate approximation to $pF_i(t)$. In this situation, it could be advantageous to use importance sampling from the times contained in $\mathcal{WL}_j$ and $\mathcal{SL}_j$. With this approach, probabilities

$$\mathbf{pWL}_j = \left[pL_{j1}, pL_{j2}, ..., pL_{j,nR1} \right], j = 1, 2, ..., nWL, \tag{5.29}$$

and

$$\mathbf{pSL}_j = \left[pL_{nWL+j,1}, pSL_{nWL+j,2}, ..., pSL_{nWL+j,nR1} \right], j = 1, 2, ..., nSL, \tag{5.30}$$

are assigned to the times in $\mathcal{WL}_j$ and $\mathcal{SL}_j$, where pL_{jl} and $pL_{nWL+j,l}$ are the probabilities assigned to element l of $\mathcal{WL}_j$ and $\mathcal{SL}_j$, respectively, for use in importance sampling. Once assigned, the probabilities in Eqs. (5.29) and (5.30) can be used to generate a sample of size $nR2$ of the form shown in Eq. (5.28) from the times in $\mathcal{WL}_j$ and $\mathcal{SL}_j$, which corresponds to generating a subset $\mathcal{S}_I$ of size $nR2$ from the set $\mathcal{S}$ defined in conjunction with Eq. (5.27). In turn,

$$
\begin{aligned}
pF_i(t) &\cong \sum_{\mathbf{l}=[l_1,l_2,\ldots,l_{nL}]\in\mathcal{S}} \delta_i(\mathbf{t_l})\prod\nolimits_{k=1}^{nL} wL_{kl_k} \\
&= \sum_{\mathbf{l}=[l_1,l_2,\ldots,l_{nL}]\in\mathcal{S}} \left[\delta_i(\mathbf{t_l})\prod\nolimits_{k=1}^{nL} wL_{kl_k} \Big/ \prod\nolimits_{k=1}^{nL} pL_{kl_k}\right]\prod\nolimits_{k=1}^{nL} pL_{kl_k} \\
&\cong \sum_{\mathbf{l}=[l_1,l_2,\ldots,l_{nL}]\in\mathcal{S}_I} \frac{\delta_i\left\{t \mid \left[tWL_{1l}, tWL_{2l}, \ldots, tWL_{nWL,l}, tSL_{1l}, tSL_{2l}, \ldots, tSL_{nSL,l}\right]\right\}\prod\nolimits_{k=1}^{nL} wL_{kl_k}}{nR2\prod\nolimits_{k=1}^{nL} pL_{kl_k}},
\end{aligned}
\tag{5.31}
$$

where (i) the initial approximation is the same as shown in Eq. (5.27) for all possible combinations of WL and SL failure times, (ii) the following equality introduces the link probabilities used in importance sampling, and (iii) the final approximation results from the importance sample from the link failure times in $\mathcal{WL}_j$ and $\mathcal{SL}_j$.

The sets $\mathcal{WL}_j$ and $\mathcal{SL}_j$ are indicated as all being of the same size (i.e., $nR1$) in Eqs. (5.20) and (5.21). However, this is not necessary as the relations in Eqs. (5.27)-(5.31) remain valid with only minor notational changes if $\mathcal{WL}_j$ and $\mathcal{SL}_j$ do not have equal numbers of elements.

The advantage of this two-step approach is that the sample size $nR1$ used to generate the sets in Eqs. (5.20) and (5.21) can be much smaller than the sample size $nR2$ required to generate the sample in Eq. (5.28) used to estimate $pF_i(t)$. This has the potential to result in significant computational efficiency. It also provides an efficient basis for a bootstrap procedure to place confidence intervals around estimates for $pF_i(t)$. However, this approach to estimating $pF_i(t)$ does require that the failure time distributions for the individual links be independent, which is also the assumption under which the representations for PLOAS in Table 1 were developed.

6. Illustration of Verification Test Problems

Quadrature and sampling-based procedures to determine PLOAS for the four WL/SL configurations described in Table 1 are developed in Sects. 2-5. Also contained in Table 1 are verification test problems for the determination of PLOAS for the four WL/SL configurations. These verification problems involve the assignment of the same properties to all links, with the result that PLOAS has a simple algebraic form for each WL/SL configuration that is a function of the numbers *nWL* and *nSL* of WLs and SLs.

As an illustration, an application of the verification problems in Table 1 to the procedures developed in Sects. 2-5 is presented. Specifically, WLs and SLs with identical properties are considered (Fig. 3), and PLOAS is determined with the CPLOAS_2 program [20] for each of the WL/SL configurations in Table 1 and several different combinations of WLs and SLs (Table 3). The similarity of the corresponding results in Table 3 to both each other and the known solutions to the verification test problems provides a strong indication, but not an absolute proof, that the conceptual development and computational implementation of the PLOAS determinations described in Sects. 2-5 are correct.

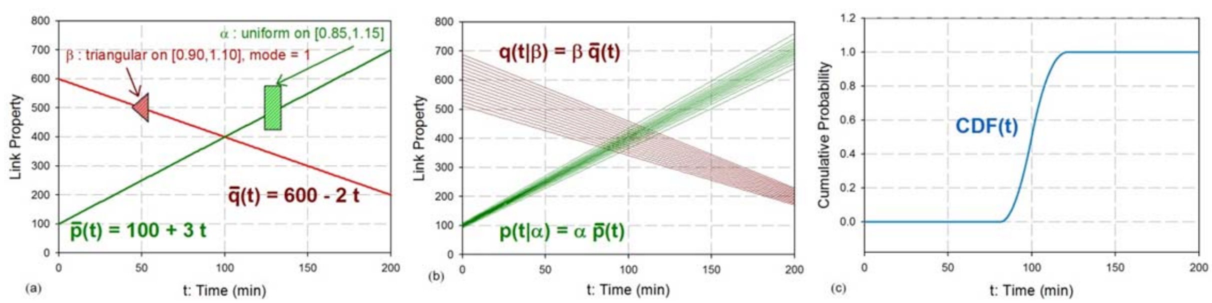

Fig. 3. Link properties for illustration of verification tests: (a) base physical property $\overline{p}(t)$, base failure property $\overline{q}(t)$, and distributions for aleatory variables α and β, (b) physical properties $p(t|\alpha) = \alpha\,\overline{p}(t)$ and failure properties $q(t|\beta) = \beta\,\overline{q}(t)$ generated with random samples of size 100 from the distributions for α and β, and (c) cumulative distribution $CDF(t)$ for link failure time.

Table 3 Verification of PLOAS Calculations for WL/SL Configurations in Table 1 with Link Properties Defined in Fig. 3 Assigned to All Links

	Verification[a]	Quadrature 1[b]	Quadrature 2[c]	Sampling 1[d]	Importance 1[e]	Sampling 2[f]	Importance 2[g]
Case 1: Failure of all SLs before failure of any WL; Verification test: $pF_1(\infty) = nWL!nSL!/(nWL+nSL)!$							
$nWL = nSL = 2$:	$1/6 \cong 0.1667$	0.1618 (-2.9%)[h]	0.1662 (-0.3%)	0.1663 (-0.2%)	0.1668 (0.1%)	0.1672 (0.3%)	0.1684 (1.0%)
$nWL = 3$, $nSL = 5$:	$1/56 \cong 0.0179$	0.0167 (-6.5%)	0.0177 (-0.9%)	0.0181 (1.4%)	0.0178 (-0.3%)	0.0183 (2.5%)	0.0177 (-0.9%)
$nWL = 5$, $nSL = 3$:	$1/56 \cong 0.0179$	0.0167 (-6.5%)	0.0177 (-0.9%)	0.0179 (0.2%)	0.0179 (0.2%)	0.0180 (0.7%)	0.0180 (0.7%)
Case 2: Failure of any SL before failure of any WL; Verification test: $pF_2(\infty) = nSL/(nWL+nSL)$							
$nWL = nSL = 2$:	$1/2 = 0.50$	0.4977 (-0.5%)	0.4998 (0.0%)	0.5035 (0.7%)	0.4982 (-1.4%)	0.5054 (1.1%)	0.5000 (0.0%)
$nWL = 3$, $nSL = 5$:	$5/8=0.625$	0.6269 (0.3%)	0.6252 (0.0%)	0.6305 (0.9%)	0.6381 (2.1%)	0.6324 (1.2%)	0.6051 (-3.2%)
$nWL = 5$, $nSL = 3$:	$3/8=0.375$	0.3714 (-1.0%)	0.3746 (-0.1%)	0.3769 (0.5%)	0.3702 (-1.3%)	0.3788 (1.0%)	0.3533 (-5.8%)
Case 3: Failure of all SLs before failure of all WLs; Verification test: $pF_3(\infty) = nWL/(nWL+nSL)$							
$nWL = nSL = 2$:	$1/2 = 0.50$	0.4909 (-1.8%)	0.4991 (-0.2%)	0.5030 (0.6%)	0.5010 (0.2%)	0.5056 (1.1%)	0.4925 (-1.5%)
$nWL = 3$, $nSL = 5$:	$3/8=0.375$	0.3622 (-3.4%)	0.3737 (-0.3%)	0.3767 (0.5%)	0.3723 (-0.7%)	0.3787 (1.0%)	0.3800 (1.3%)
$nWL = 5$, $nSL = 3$:	$5/8=0.625$	0.6116 (-2.1%)	0.6237 (-0.2%)	0.6295 (0.7%)	0.6282 (0.5%)	0.6319 (1.1%)	0.5940 (-5.0%)
Case 4: Failure of any SL before failure of all WLs; Verification test: $pF_4(\infty) = 1 - [nWL!nSL!/(nWL+nSL)!]$							
$nWL = nSL = 2$:	$5/6 \cong 0.8333$	0.8356 (0.3%)	0.8336 (0.0%)	0.8414 (1.0%)	0.8265 (-0.8%)	0.8426 (1.1%)	0.8284 (-0.6%)
$nWL = 3$, $nSL = 5$:	$55/56 \cong 0.982$	0.9974 (1.6%)	0.9837 (0.2%)	0.9915 (1.0%)	1.0170 (3.5%)	0.9917 (1.0%)	0.9627 (-2.0%)
$nWL = 5$, $nSL = 3$:	$55/56 \cong 0.982$	0.9919 (1.0%)	0.9831 (0.1%)	0.9917 (1.0%)	0.9704 (-1.2%)	0.9920 (1.0%)	1.0130 (3.1%)

[a]Verification ~ Verification test values.

[b]Quadrature 1 ~ PLOAS values obtained with quadrature procedures in Eqs. (4.1)-(4.4) for Cases 1, 2, 3 and 4, respectively, and a subdivision size of $n = 10^3$.

[c]Quadrature 2 ~ PLOAS values obtained with quadrature procedures in Eqs. (4.1)-(4.4) for Cases 1, 2, 3 and 4, respectively, and a subdivision size of $n = 10^4$.

[d]Sampling 1 ~ PLOAS values obtained with random sampling procedure in Eq. (5.9) and a sample size of $nR = 10^6$. [e]Importance 1 ~ PLOAS values obtained with importance sampling procedure in Eq. (5.11), density functions $d_{I,k}(r_k)$, $k = 1,2,\ldots, nL = nWL + nSL$, for sampling link failure times right triangular on [0, 1] for WLs and left triangular on [0, 1] for SLs, and a sample size of $nR = 10^6$.

[f]Sampling 2 ~ PLOAS values obtained with random sampling procedure in Eq. (5.18), a sample size of $nR = 10^6$, and time steps of size 0.1 min in determining the link failure times defined in Eqs. (5.15) and (5.16). [g]Importance 2 ~ PLOAS values obtained with importance sampling procedure in Eq. (5.19), density functions $d_{I,k}(r_k)$, $k = 1,2,\ldots, 2nL = 2(nWL + nSL)$, right triangular for sampling WL β's and SL α's from their assigned ranges and left triangular for sampling WL α's and SL β's from their assigned ranges, a sample size of $nR = 10^6$, and time steps of size 0.1 min in determining the link failure times defined in Eqs. (5.15) and (5.16).

[h]Percent difference of calculated value from verification value.

Two of the test results for Case 4 in Table 3 are slightly larger than 1.0. This is due to sampling variability around a PLOAS value of 0.982 that is very close to 1.0. Both of the values that exceed 1.0 occur for importance sampling. With the weighting for importance sampling in use, early WL and SL failure times are under and over represented, respectively, in the initial sampling of link failure times. Although this overweighting is corrected for, it probably enhances variability in estimates for very large PLOAS values (i.e., values close to 1.0). In general, the weights chosen for importance sampling must be chosen for the specific problem under consideration as a poor choice of weights can impede rather enhance the convergence of the sampling process. If desired, a bootstrap procedure can be used to place confidence intervals around PLOAS values obtained with sampling-based methods.

As part of the verification process for the CPLOAS_2 program [20], a number of additional verification problems of type illustrated in this section were performed with a variety of (i) assumed link properties $\bar{p}(t)$ and $\bar{q}(t)$, and (ii) aleatory distributions for α and β. The verification test problems in Table 1 are particularly effective because, although they possess simple closed solutions, their implementation within the CPLOAS_2 program entails a full exercising of the conceptual development and computational implementation of the PLOAS determinations described in Sects. 2-5.

This page intentionally left blank.

7. Alternative Representations for PLOAS

The representations $pF_1(t)$ and $pF_3(t)$ for PLOAS in Table 1 involve the failure of all SLs before the failure of any WL and the failure of all SLs before the failure of all WLs, respectively. These representations explicitly incorporate the CDFs $CDF_{SL,k}(\tau)$, k = 1, 2, …, nSL, for the failure of the individual SLs. An alternative representation is to precalculate the CDF $CDF_{SL}(\tau)$ for the failure of all SLs by time τ. Specifically, $CDF_{SL}(\tau)$ is defined by

$$CDF_{SL}(\tau) = \prod_{k=1}^{nSL} CDF_{SL,k}(\tau) \tag{7.1}$$

provided the failures of the individual SLs are independent. In turn, this leads to the representations

$$pF_1(t) = \int_0^t \left\{ \prod_{j=1}^{nWL} \left[1 - CDF_{WL,j}(\tau)\right] \right\} \mathrm{d}CDF_{SL}(\tau) \tag{7.2}$$

and

$$pF_3(t) = \int_0^t \left\{ 1 - \prod_{j=1}^{nWL} CDF_{WL,j}(\tau) \right\} \mathrm{d}CDF_{SL}(\tau) \tag{7.3}$$

for $pF_1(t)$ and $pF_3(t)$.

The preceding representations for $pF_1(t)$ and $pF_3(t)$ do not look like the representations in Table 1. However, as indicated in Table 4, it is straight forward to demonstrate the equivalence of the two representations for $pF_1(t)$ and $pF_3(t)$ with use of the equality

$$\prod_{k=1}^{n} a_k - \prod_{k=1}^{n} b_k = \sum_{k=1}^{n} \left(\prod_{l=1}^{k-1} b_l \right) (a_k - b_k) \left(\prod_{l=k+1}^{n} a_l \right) \tag{7.4}$$

For (i) sequences $a_1, a_2, ..., a_n$ and $b_1, b_2, ..., b_n$ of real numbers and (ii) the notational convention that

$$\prod_{l=1}^{0} b_l = \prod_{l=n+1}^{n} a_l = 1.$$

As CDFs are functions of bounded variation, the final expression in Table 4 is valid as long as the CDFs involved are continuous functions. If the CDFs are not continuous, then subdivision-refinement type integrals with appropriate left-right integrand evaluations must be used to appropriately incorporate the effects of discontinuous CDFs (i.e., CDFs that have nonzero jumps in cumulative probability).

Table 4 Relationships Establishing Equality of Representations for $pF_1(t)$ in Table 1 and Eq. (7.2)

$$
\begin{aligned}
pF_1(t) &= \int_0^t \left\{ \prod_{j=1}^{nWL} \left[1 - CDF_{WL,j}(\tau)\right] \right\} \mathrm{d}CDF_{SL}(\tau) \\
&\cong \sum_{i=1}^{N} \left\{ \prod_{j=1}^{nWL} \left[1 - CDF_{WL,j}(\tau_i)\right] \right\} \left\{ CDF_{SL}(\tau_i) - CDF_{SL}(\tau_{i-1}) \right\} \\
&= \sum_{i=1}^{N} \left\{ \prod_{j=1}^{nWL} \left[1 - CDF_{WL,j}(\tau_i)\right] \right\} \left\{ \prod_{k=1}^{nSL} CDF_{SL,k}(\tau_i) - \prod_{k=1}^{nSL} CDF_{SL,k}(\tau_{i-1}) \right\} \\
&= \sum_{i=1}^{N} \left\{ \prod_{j=1}^{nWL} \left[1 - CDF_{WL,j}(\tau_i)\right] \right\} \left\{ \sum_{k=1}^{nSL} \left[\prod_{l=1}^{k-1} CDF_{SL,l}(\tau_i) \right] \left[CDF_{SL,k}(\tau_i) - CDF_{SL,k}(\tau_{i-1}) \right] \left[\prod_{l=k+1}^{nSL} CDF_{SL,l}(\tau_{i-1}) \right] \right\} \\
&= \sum_{k=1}^{nSL} \sum_{i=1}^{N} \left\{ \prod_{\substack{l=1 \\ l \neq k}}^{nSL} CDF_{SL,l}(\tau_i) \right\} \left\{ \prod_{j=1}^{nWL} \left[1 - CDF_{WL,j}(\tau_i)\right] \right\} \left\{ CDF_{SL,k}(\tau_i) - CDF_{SL,k}(\tau_{i-1}) \right\} \\
&\cong \sum_{k=1}^{nSL} \left(\int_0^t \left\{ \prod_{\substack{l=1 \\ l \neq k}}^{nSL} CDF_{SL,l}(\tau) \right\} \left\{ \prod_{j=1}^{nWL} \left[1 - CDF_{WL,j}(\tau)\right] \right\} \mathrm{d}CDF_{SL,k}(\tau) \right),
\end{aligned}
$$

where $0 = t_1 < t_2 < \cdots < t_N = t$ and the final expression results in the limit as Δt_i goes to zero.

In like manner, a pattern of relationships similar to that used in Table 4 also connects the two representations for $pF_3(t)$ and establishes the following sequence of equalities

$$
\begin{aligned}
CDF_{SL}(t) &= \prod_{k=1}^{nSL} CDF_{SL,k}(t) \\
&= \int_0^t \mathrm{d}CDF_{SL}(\tau) \\
&= \int_0^t \mathrm{d}\left[\prod_{k=1}^{nSL} CDF_{SL,k}(\tau)\right] \\
&= \sum_{k=1}^{nSL}\left(\int_0^t \left\{\prod_{\substack{l=1 \\ l\neq k}}^{nSL} CDF_{SL,l}(\tau)\right\} \mathrm{d}CDF_{SL,k}(\tau)\right)
\end{aligned}
\tag{7.5}
$$

connecting several different representations for $CDF_{SL}(t)$.

Given that $CDF_{SL}(t)$ can be de termined, it is easy to m ake the m istake of ass uming that $pF_1(t)$ and $pF_3(t)$ can be defined by

$$
\widehat{pF_1}(t) = \left\{\prod_{j=1}^{nWL}\left[1 - CDF_{WL,j}(t)\right]\right\} CDF_{SL}(t) \tag{7.6}
$$

and

$$
\widehat{pF_3}(t) = \left\{1 - \prod_{j=1}^{nWL} CDF_{WL,j}(t)\right\} CDF_{SL}(t). \tag{7.7}
$$

However, as a consequence of the inequalities

$$
\prod_{j=1}^{nWL}\left[1 - CDF_{WL,j}(\tau)\right] \geq \prod_{j=1}^{nWL}\left[1 - CDF_{WL,j}(t)\right] \tag{7.8}
$$

and

$$
1 - \prod_{j=1}^{nWL} CDF_{WL,j}(\tau) \geq 1 - \prod_{j=1}^{nWL} CDF_{WL,j}(t) \tag{7.9}
$$

for $0 \leq \tau \leq t$, $\widehat{pF_1}(t)$ and $\widehat{pF_3}(t)$ underestimate $pF_1(t)$ and $pF_3(t)$. Specifically,

$$
\begin{aligned}
pF_1(t) &= \int_0^t \left\{ \prod_{j=1}^{nWL} \left[1 - CDF_{WL,j}(\tau) \right] \right\} \mathrm{d}CDF_{SL}(\tau) \\
&\geq \int_0^t \left\{ \prod_{j=1}^{nWL} \left[1 - CDF_{WL,j}(t) \right] \right\} \mathrm{d}CDF_{SL}(\tau) \\
&= \left\{ \prod_{j=1}^{nWL} \left[1 - CDF_{WL,j}(t) \right] \right\} \int_0^t \mathrm{d}CDF_{SL}(\tau) \\
&= \left\{ \prod_{j=1}^{nWL} \left[1 - CDF_{WL,j}(t) \right] \right\} CDF_{SL}(t) \\
&= \widehat{pF_1}(t),
\end{aligned}
\tag{7.10}
$$

and the inequality $pF_3(t) \geq \widehat{pF_3}(t)$ follows in a similar manner.

Analogously to the representation for $CDF_{SL}(\tau)$ in Eq. (7.1), the CDF $CDF_{WL}(\tau)$ for the failure of all WLs by time τ is defined by

$$
CDF_{WL}(\tau) = \prod_{j=1}^{nWL} CDF_{WL,j}(\tau) \tag{7.11}
$$

provided the failures of the individual WLs are independent. If desired, $CDF_{SL}(\tau)$ can be precalculated and used instead of the product in Eq. (7.11) in the representations $pF_3(t)$ and $pF_4(t)$ for PLOAS in Table 1.

8. Example System

A multicompartment system in a fire is now defined for use in illustrating the procedures described in Sects. 2-5 (Fig. 4). Specifically, the 16 compartments that comprise the system are shown in Fig. 4, and the system of differential equations defining time-dependent temperature for the individual compartments is shown in Table 5. As indicated, the pressure $P_9(t)$ in compartment 9 is assumed to be a function of the temperatures in compartments 7, 8, 9 and 10. Values for the coefficients appearing in the system of equations in Table 5 were chosen to produce interesting results for the purpose of demonstration, and the resulting analyses are not intended to be representative of any specific system of interest to Sandia.

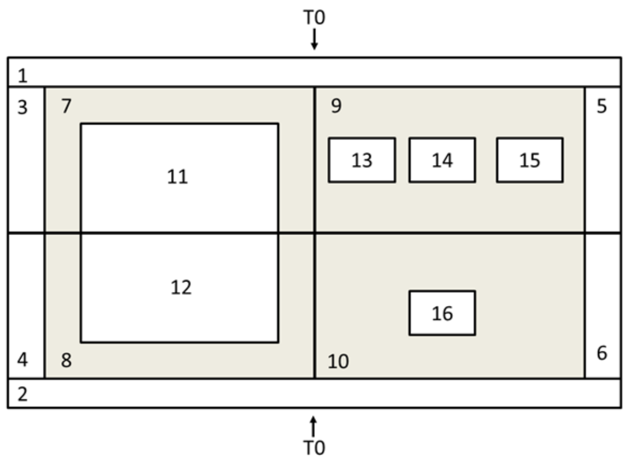

Fig. 4. Multicompartment system in a fire.

A more compact representation of the system of differential equations in Table 5 is given by

$$\begin{aligned} c_j \mathrm{d}T_j/\mathrm{d}t &= r_{0j}\left(T_0^4 - T_j^4\right) + \sum_{k \in \mathcal{S}_j} r_{jk}\left(T_k - T_j\right),\ j = 1, 2, \\ c_j \mathrm{d}T_j/\mathrm{d}t &= \sum_{k \in \mathcal{S}_j} r_{jk}\left(T_k - T_j\right),\ j = 3, 4, \ldots, 16, \end{aligned} \tag{8.1}$$

with (i) the sets $\mathcal{S}_1, \mathcal{S}_2, \ldots, \mathcal{S}_{16}$ defined by

$\mathcal{S}_1 = \{3, 5, 7, 9\}$, $\mathcal{S}_2 = \{4, 6, 8, 10\}$, $\mathcal{S}_3 = \{1, 4, 7\}$, $\mathcal{S}_4 = \{2, 3, 8\}$, $\mathcal{S}_5 = \{1, 6, 9\}$,
$\mathcal{S}_6 = \{2, 5, 10\}$, $\mathcal{S}_7 = \{1, 3, 8, 9, 11\}$, $\mathcal{S}_8 = \{2, 4, 7, 10, 12\}$, $\mathcal{S}_9 = \{1, 5, 7, 10, 13, 14, 15\}$,
$\mathcal{S}_{10} = \{2, 6, 8, 9, 16\}$, $\mathcal{S}_{11} = \{7, 12\}$, $\mathcal{S}_{12} = \{8, 11\}$, $\mathcal{S}_{13} = \{9\}$, $\mathcal{S}_{14} = \{9\}$, $\mathcal{S}_{15} = \{9\}$,
$\mathcal{S}_{16} = \{10\}$,

and (ii) the rates related by $r_{jk} = r_{kj}$ when both rates appear.

Table 5 System of Differential Equations Defining Time-Dependent Temperature for the Individual Compartments Shown in the Multicompartment System in Fig. 4

$$dT_1/dt = \left[r_{10}\left(T_0^4 - T_1^4\right) + r_{13}\left(T_3 - T_1\right) + r_{15}\left(T_5 - T_1\right) + r_{17}\left(T_7 - T_1\right) + r_{19}\left(T_9 - T_1\right) \right] / c_1$$
$$= \left[(1.41\text{E}-8)\left(800^4 - T_1^4\right) + 3.91\left(T_3 - T_1\right) + 3.91\left(T_5 - T_1\right) + 3.06\left(T_7 - T_1\right) + 3.06\left(T_9 - T_1\right) \right] / 1.28\text{E}4$$

$$dT_2/dt = \left[r_{20}\left(T_0^4 - T_2^4\right) + r_{24}\left(T_4 - T_2\right) + r_{26}\left(T_6 - T_2\right) + r_{28}\left(T_8 - T_2\right) + r_{2,10}\left(T_{10} - T_2\right) \right] / c_2$$
$$= \left[(1.41\text{E}-8)\left(800^4 - T_2^4\right) + 3.91\left(T_4 - T_2\right) + 3.91\left(T_6 - T_2\right) + 3.06\left(T_8 - T_2\right) + 3.06\left(T_{10} - T_2\right) \right] / 1.28\text{E}4$$

$$dT_3/dt = \left[r_{31}\left(T_1 - T_3\right) + r_{34}\left(T_4 - T_3\right) + r_{37}\left(T_7 - T_3\right) \right] / c_3$$
$$= \left[3.91\left(T_1 - T_3\right) + 2.42\left(T_4 - T_3\right) + 0.855\left(T_7 - T_3\right) \right] / 8.79\text{E}2$$

$$dT_4/dt = \left[r_{42}\left(T_2 - T_4\right) + r_{43}\left(T_3 - T_4\right) + r_{48}\left(T_8 - T_4\right) \right] / c_4$$
$$= \left[3.91\left(T_2 - T_4\right) + 2.42\left(T_3 - T_4\right) + 0.855\left(T_8 - T_4\right) \right] / 8.79\text{E}2$$

$$dT_5/dt = \left[r_{51}\left(T_1 - T_5\right) + r_{56}\left(T_6 - T_5\right) + r_{59}\left(T_9 - T_5\right) \right] / c_5$$
$$= \left[3.91\left(T_1 - T_5\right) + 2.42\left(T_6 - T_5\right) + (1.43\text{E}-2)\left(T_9 - T_5\right) \right] / 8.79\text{E}2$$

$$dT_6/dt = \left[r_{62}\left(T_2 - T_6\right) + r_{65}\left(T_5 - T_6\right) + r_{6,10}\left(T_{10} - T_6\right) \right] / c_6$$
$$= \left[3.91\left(T_2 - T_6\right) + 2.42\left(T_5 - T_6\right) + (1.43\text{E}-2)\left(T_{10} - T_6\right) \right] / 8.79\text{E}2$$

$$dT_7/dt = \left[r_{71}\left(T_1 - T_7\right) + r_{73}\left(T_3 - T_7\right) + r_{78}\left(T_8 - T_7\right) + r_{79}\left(T_9 - T_7\right) + r_{7,11}\left(T_{11} - T_7\right) \right] / c_7$$
$$= \left[3.06\left(T_1 - T_7\right) + 0.855\left(T_3 - T_7\right) + (2.00\text{E}-3)\left(T_8 - T_7\right) + 0.140\left(T_9 - T_7\right) + 26.0\left(T_{11} - T_7\right) \right] / 6.54\text{E}3$$

$$dT_8/dt = \left[r_{82}\left(T_2 - T_8\right) + r_{84}\left(T_4 - T_8\right) + r_{87}\left(T_7 - T_8\right) + r_{8,10}\left(T_{10} - T_8\right) + r_{8,12}\left(T_{12} - T_8\right) \right] / c_8$$
$$= \left[3.06\left(T_2 - T_8\right) + 0.855\left(T_4 - T_8\right) + (2.00\text{E}-3)\left(T_7 - T_8\right) + 0.140\left(T_{10} - T_8\right) + 26.0\left(T_{12} - T_8\right) \right] / 6.54\text{E}3$$

$$dT_9/dt = \left[r_{91}\left(T_1 - T_9\right) + r_{95}\left(T_5 - T_9\right) + r_{97}\left(T_7 - T_9\right) + r_{9,10}\left(T_{10} - T_9\right) + r_{9,13}\left(T_{13} - T_9\right) + r_{9,14}\left(T_{14} - T_9\right) + r_{9,15}\left(T_{15} - T_9\right) \right] / c_9$$
$$= \left[3.06\left(T_1 - T_9\right) + (1.43\text{E}-2)\left(T_5 - T_9\right) + 0.140\left(T_7 - T_9\right) + 0.06\left(T_{10} - T_9\right) + 0.575\left(T_{13} - T_9\right) + 0.230\left(T_{14} - T_9\right) \right.$$
$$\left. + 5.12\left(T_{15} - T_9\right) \right] / 1.64\text{E}4$$

$$dT_{10}/dt = \left[r_{10,2}\left(T_2 - T_{10}\right) + r_{10,6}\left(T_6 - T_{10}\right) + r_{10,8}\left(T_8 - T_{10}\right) + r_{10,9}\left(T_9 - T_{10}\right) + r_{10,16}\left(T_{16} - T_{10}\right) \right] / c_{10}$$
$$= \left[3.06\left(T_2 - T_{10}\right) + (1.43\text{E}-2)\left(T_6 - T_{10}\right) + 0.140\left(T_8 - T_{10}\right) + 0.06\left(T_9 - T_{10}\right) + 1.41\left(T_{16} - T_{10}\right) \right] / 1.64\text{E}4$$

$$dT_{11}/dt = \left[r_{11,7}\left(T_7 - T_{11}\right) + r_{11,12}\left(T_{12} - T_{11}\right) \right] / c_{11} = \left[26.0\left(T_7 - T_{11}\right) + 0.448\left(T_{12} - T_{11}\right) \right] / 8.91\text{E}2$$

$$dT_{12}/dt = \left[r_{12,8}\left(T_8 - T_{12}\right) + r_{12,11}\left(T_{11} - T_{12}\right) \right] / c_{12} = \left[26.0\left(T_8 - T_{12}\right) + 0.448\left(T_{11} - T_{12}\right) \right] / 8.91\text{E}2$$

$$dT_{13}/dt = r_{13,9}\left(T_9 - T_{13}\right) / c_{13} = 0.575\left(T_9 - T_{13}\right) / 5.10\text{E}2$$

$$dT_{14}/dt = r_{14,9}\left(T_9 - T_{14}\right) / c_{14} = 0.230\left(T_9 - T_{14}\right) / 5.10\text{E}2$$

$$dT_{15}/dt = r_{15,9}\left(T_9 - T_{15}\right) / c_{15} = 5.12\left(T_9 - T_{15}\right) / 9.99\text{E}2$$

$$dT_{16}/dt = r_{16,10}\left(T_{10} - T_{16}\right) / c_{16} = 1.41\left(T_{10} - T_{16}\right) / 1.98\text{E}3$$

$$P_9 = c\left\{ \left[\left(T_7 + T_8 + T_9 + T_{10}\right)/4 \right] - T_0 \right\} = 2.7\left\{ \left[\left(T_7 + T_8 + T_9 + T_{10}\right)/4 \right] - 800 \right\}$$

$$T_i(0) = 288 \text{ K for } i = 1, 2, \ldots, 16$$

For purposes of illustration, components associated with compartments 1, 5, 13 and 14 are treated as SLs in the sense that the failure of these components is involved in LOAS. Specifically, single SLs are associated with compartments 1, 13 and 14, and two SLs are associated with compartment 5. For notational purposes, the SLs associated with compartments 1, 13 and 14 are designated SL 1, SL 4 and SL 5, respectively, and the SLs associated with compartment 5 are designated SL 2 and SL 3. Further, components associated with compartments 11 and 16 are treated as WLs in the sense that their failure disables the system and thus prevents LOAS. For notational purposes, the WLs associated with compartments 11 and 16 are designated WL 1 and WL 2.

The failure of SLs 1, 2 and 3 is assumed to be pressure based. Specifically, each link fails when the pressure $P_9(t)$ in compartment 9 as defined in Table 5 reaches its failure pressure. In turn, failure pressure is a function of link temperature. In the context of the notation introduced in Sect. 3, the base link properties are

$$\bar{p}_{SL,1}(t) = \bar{p}_{SL,2}(t) = \bar{p}_{SL,3}(t) = P_9(t), \tag{8.2}$$

and the base link failure properties are

$$\bar{q}_{SL,1}(t) = f_{SL,1}\left[T_1(t)\right], \bar{q}_{SL,2}(t) = f_{SL,2}\left[T_5(t)\right], \bar{q}_{SL,3}(t) = f_{SL,3}\left[T_5(t)\right] \tag{8.3}$$

for the functions $f_{SL,i}(T), i = 1,2,3,$ in Fig. 5.

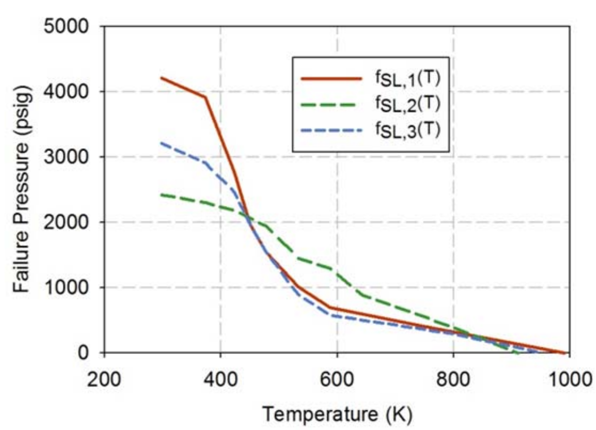

Fig. 5. Failure pressures as functions $f_{SL,1}(T)$, $f_{SL,2}(T)$ and $f_{SL,3}(T)$ of temperature T for SLs 1, 2 and 3, respectively.

The failure of SLs 4 and 5 is assumed to be temperature based. Specifically, these links fail when the temperature in their corresponding compartments (i.e., compartments 13 and 14) reaches a specified failure temperature. In the context of the notation introduced in Sect. 3, the base link properties are

$$\bar{p}_{SL,4}(t) = T_{13}(t), \bar{p}_{SL,5}(t) = T_{14}(t), \tag{8.4}$$

and the base link failure properties are

$$\bar{q}_{SL,4}(t) = 623 \text{ K}, \bar{q}_{SL,5}(t) = 673 \text{ K}. \tag{8.5}$$

Similarly, the failure of WLs 1 and 2 is assumed to be temperature based with base link properties and base link failure properties defined by

$$\bar{p}_{WL,1}(t) = T_{11}(t), \bar{p}_{WL,2}(t) = T_{16}(t) \tag{8.6}$$

and

$$\bar{q}_{WL,1}(t) = 600 \text{ K}, \bar{q}_{WL,2}(t) = 550 \text{ K}, \tag{8.7}$$

respectively.

For purposes of illustration, five failure patterns leading to LOAS will be considered (Table 6). Two variants on the treatment of uncertainty are illustrated for the indicated failure patterns: (i) only aleatory uncertainty present (Sect. 9), and (ii) both aleatory and epistemic uncertainty present (Sect. 10).

Table 6 Example Failure Patterns Leading to LOAS Used for Illustration

Failure Pattern 1: LOAS occurs if SL 1, SL 2 or SL 3 fails before WL 1 fails.

Failure Pattern 2: LOAS occurs if SL 4 and SL 5 both fail before WL 2 fails.

Failure Pattern 3: LOAS occurs if (i) SL 1, SL 2 or SL 3 fails before WL 1 fails or (ii) SL 4 and SL 5 both fail before WL 2 fails.

Failure Pattern 4: LOAS occurs if SL 4 and SL 5 both fail before WL 1 or WL 2 fails.

Failure Pattern 5: LOAS occurs if (i) SL 1, SL 2 or SL 3 fails before WL 1 fails or (ii) SL 4 and SL 5 both fail before WL 1 or WL 2 fails.

9. Examples Involving Only Aleatory Uncertainty

For the case of only aleatory uncertainty, aleatory variables $\alpha_{SL,i}, i = 1,2,3,4,5,$ $\beta_{SL,i}, i = 1,2,3,4,5,$ $\alpha_{WL,i}, i = 1,2,$ and $\beta_{WL,i}, i = 1,2,$ are defined such that

$$p_{SL,i}\left(t \mid \alpha_{SL,i}\right) = \alpha_{SL,i}\,\bar{p}_{SL,i}\left(t\right), i = 1,2,3,4,5, \tag{9.1}$$

$$q_{SL,i}\left(t \mid \beta_{SL,i}\right) = \beta_{SL,i}\,\bar{q}_{SL,i}\left(t\right), i = 1,2,3,4,5, \tag{9.2}$$

$$p_{WL,i}\left(t \mid \alpha_{WL,i}\right) = \alpha_{WL,i}\,\bar{p}_{WL,i}\left(t\right), i = 1,2, \tag{9.3}$$

and

$$q_{WL,i}\left(t \mid \beta_{WL,i}\right) = \beta_{WL,i}\,\bar{q}_{WL,i}\left(t\right), i = 1,2. \tag{9.4}$$

The distributions associated with the variables $\alpha_{SL,i}, i = 1,2,3,4,5,$ $\beta_{SL,i}, i = 1,2,3,4,5,$ $\alpha_{WL,i}, i = 1,2,$ and $\beta_{WL,i}, i = 1,2,$ are defined in Table 7.

Table 7 Summary of WL-SL Properties and Defining Distributions for the Aleatory Variables $\alpha_{SL,i}, i = 1,2,3,4,5,$ $\beta_{SL,i}, i = 1,2,3,4,5,$ $\alpha_{WL,i}, i = 1,2,$ and $\beta_{WL,i}, i = 1,2$

WL 1: Associated with Compartment 11 in Fig. 4. Link failure based on temperature, with (i) base temperature $\bar{p}_{WL,1}(t)$ defined by function $T_{11}(t)$ in Table 5 with aleatory variable $\alpha_{WL,1}$ assigned a truncated normal distribution with $\mu = 1.0$, $\sigma = 0.1$ and $q = 0.01$, and (ii) base failure temperature $\bar{q}_{WL,1}(t) = 600$ K with aleatory variable $\beta_{WL,1}$ assigned a triangular distribution on [0.91, 1.09] with mode 1.0.

WL 2: Associated with Compartment 16 in Fig. 4. Link failure based on temperature, with (i) base temperature $\bar{p}_{WL,2}(t)$ defined by function $T_{16}(t)$ in Table 5 with aleatory variable $\alpha_{WL,2}$ assigned a truncated normal distribution with $\mu = 1.0$, $\sigma = 0.1$ and $q = 0.01$, and (ii) base failure temperature $\bar{q}_{WL,2}(t) = 550$ K with aleatory variable $\beta_{WL,2}$ assigned a triangular distribution on [0.9, 1.1] with mode 1.0.

SL 1: Associated with Compartment 1 in Fig. 4. Link failure based on pressure, with (i) temperature defined by function $T_1(t)$ in Table 5, (ii) base pressure $\bar{p}_{SL,1}(t)$ defined by function $P_9(t)$ in Table 5 with aleatory variable $\alpha_{SL,1}$ assigned a truncated normal distribution with $\mu = 1.0$, $\sigma = 0.1$ and $q = 0.01$, and (iii) base failure pressure $\bar{q}_{SL,1}(t)$ defined by $f_{SL,1}[T_1(t)]$ for function $f_{SL,1}(T)$ defined in Fig. 5 with aleatory variable $\beta_{SL,1}$ assigned a truncated normal distribution with $\mu = 1.0$, $\sigma = 0.1$ and $q = 0.01$.

SL 2: Associated with Compartment 5 in Fig. 4. Link failure based on pressure, with (i) temperature defined by function $T_5(t)$ in Table 5, (ii) base pressure $\bar{p}_{SL,2}(t)$ defined by function $P_9(t)$ in Table 5 with aleatory variable $\alpha_{SL,2}$ assigned a truncated normal distribution with $\mu = 1.0$, $\sigma = 0.1$ and $q = 0.01$, and (iii) base failure pressure $\bar{q}_{SL,2}(t)$ defined by $f_{SL,2}[T_5(t)]$ for function $f_{SL,2}(T)$ defined in Fig. 5 with aleatory variable $\beta_{SL,2}$ assigned a truncated normal distribution with $\mu = 1.0$, $\sigma = 0.1$ and $q = 0.01$.

SL 3: Associated with Compartment 5 in Fig. 4. Link failure based on pressure, with (i) temperature defined by function $T_5(t)$ in Table 4, (ii) base pressure $\bar{p}_{SL,3}(t)$ defined by function $P_9(t)$ in Table 5 with aleatory variable $\alpha_{SL,3}$ assigned a truncated normal distribution with $\mu = 1.0$, $\sigma = 0.1$ and $q = 0.01$, and (iii) base failure pressure $\bar{q}_{SL,3}(t)$ defined by $f_{SL,3}[T_5(t)]$ for function $f_{SL,3}(T)$ defined in Fig. 5 with aleatory variable $\beta_{SL,3}$ assigned a truncated normal distribution with $\mu = 1.0$, $\sigma = 0.1$ and $q = 0.01$.

SL 4: Associated with Compartment 13 in Fig. 4. Link failure based on temperature, with (i) base temperature $\bar{p}_{SL,4}(t)$ defined by function $T_{13}(t)$ in Table 5 with aleatory variable $\alpha_{SL,4}$ assigned a truncated normal distribution with $\mu = 1.0$, $\sigma = 0.1$ and $q = 0.01$, and (ii) base failure temperature $\bar{q}_{SL,4}(t) = 623$ K with aleatory variable $\beta_{SL,4}$ assigned a triangular distribution on [0.85, 1.15] with mode 1.0.

SL 5: Associated with Compartment 14 in Fig. 4. Link failure based on temperature, with (i) base temperature $\bar{p}_{SL,5}(t)$ defined by function $T_{14}(t)$ in Table 5 with aleatory variable $\alpha_{SL,5}$ assigned a truncated normal distribution with $\mu = 1.0$, $\sigma = 0.1$ and $q = 0.01$, and (ii) base failure temperature $\bar{q}_{SL,5}(t) = 673$ K with aleatory variable $\beta_{SL,5}$ assigned a triangular distribution on [0.85, 1.15] with mode 1.0.

Note: Indicated 14 distributions for aleatory variables are assumed to be independent.

9.1 Failure Pattern 1: Only Aleatory Uncertainty

For Failure Pattern 1, LOAS occurs if SL 1, SL 2 or SL 3 fails before WL 1. As described in Sect. 8, failure of the indicated SLs depends on the system pressures

$$p_{SL,i}\left(t \mid \alpha_{SL,i}\right) = \alpha_{SL,i}\bar{p}_{SL,i}\left(t\right) = \alpha_{SL,i}P_9\left(t\right), i = 1,2,3, \tag{9.5}$$

and the corresponding failure pressures

$$\begin{aligned} q_{SL,i}\left(t \mid \beta_{SL,i}\right) &= \beta_{SL,i}\bar{q}_{SL,i}\left(t\right), i = 1,2,3 \\ &= \begin{cases} \beta_{SL,i}\, f_{SL,i}\left[T_1\left(t\right)\right], i = 1 \\ \beta_{SL,i}\, f_{SL,i}\left[T_5\left(t\right)\right], i = 2,3. \end{cases} \end{aligned} \tag{9.6}$$

Specifically, SL i, i = 1, 2, 3, fails at the time t for which the equality

$$p_{SL,i}\left(t \mid \alpha_{SL,i}\right) = q_{SL,i}\left(t \mid \beta_{SL,i}\right) \tag{9.7}$$

is satisfied. Similarly, failure of WL 1 depends on system temperatures and failure temperatures defined by

$$p_{WL,1}\left(t \mid \alpha_{WL,1}\right) = \alpha_{WL,1}\bar{p}_{WL,1}\left(t\right) = \alpha_{WL,1}T_{11}\left(t\right) \tag{9.8}$$

and

$$q_{WL,1}\left(t \mid \beta_{WL,1}\right) = \beta_{WL,1}\bar{q}_{WL,1}\left(t\right) = \beta_{WL,1}\left(600\text{ K}\right), \tag{9.9}$$

respectively, with failure occurring at the time t for which the equality

$$p_{WL,1}\left(t \mid \alpha_{WL,1}\right) = q_{WL,1}\left(t \mid \beta_{WL,1}\right) \tag{9.10}$$

is satisfied. The system and failure properties appearing in Eqs. (9.5) - (9.10) are illustrated in Fig. 6.

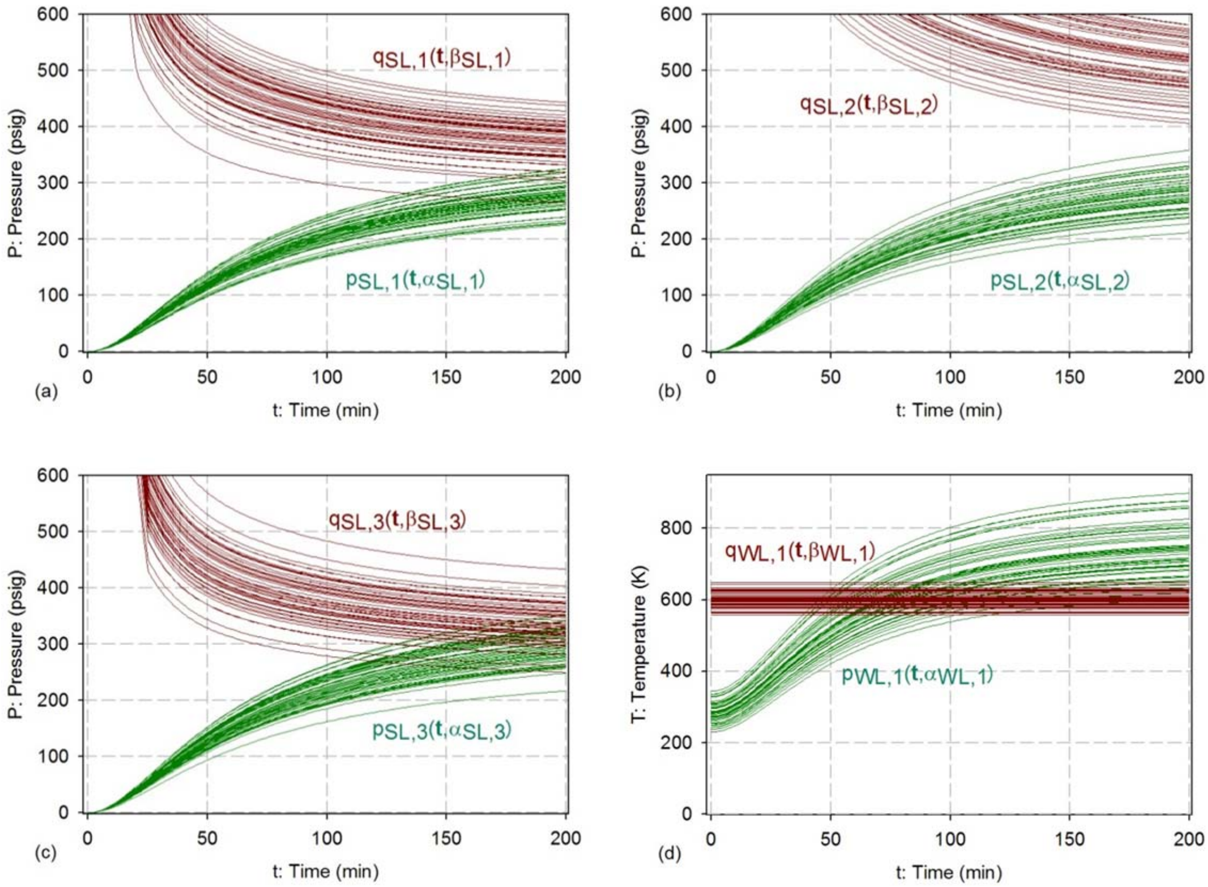

Fig. 6. System and failure properties for SL 1, SL 2, SL 3 and WL 1 generated with random samples of size 100 from the defining aleatory variables: (a) $p_{SL,1}(t \mid \alpha_{SL,1})$ and $q_{SL,1}(t \mid \beta_{SL,1})$ for SL 1, (b) $p_{SL,2}(t \mid \alpha_{SL,2})$ and $q_{SL,2}(t \mid \beta_{SL,2})$ for SL 2, (c) $p_{SL,3}(t \mid \alpha_{SL,3})$ and $q_{SL,3}(t \mid \beta_{SL,3})$ for SL 3, and (d) $p_{WL,1}(t \mid \alpha_{WL,1})$ and $q_{WL,1}(t \mid \beta_{WL,1})$ for WL 1.

For each link, the corresponding CDF for failure time can be calculated as shown in Eq. (2.12). This results in the failure time CDFs $CDF_{SL,1}(t)$, $CDF_{SL,2}(t)$, $CDF_{SL,3}(t)$ and $CDF_{WL,1}(t)$ for SL 1, SL 2, SL 3 and WL 1, respectively (Fig. 7). The failure pattern under consideration corresponds to Case 2 in Table 1 with $nSL = 3$ and $nWL = 1$. The resultant time-dependent probability $pP_1(t)$ of LOAS calculated with the quadrature procedure indicated in Eq. (4.2) is also shown in Fig. 7.

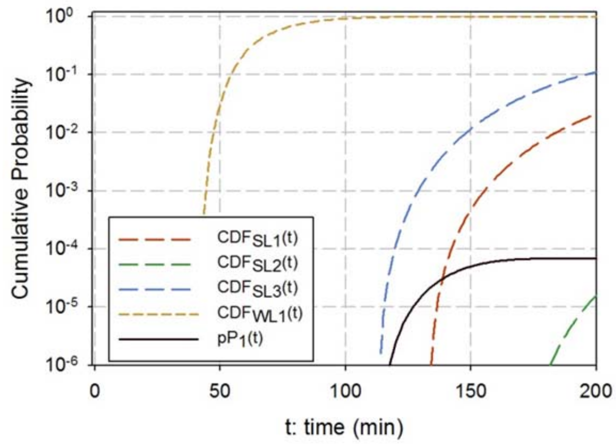

Fig. 7. Failure time CDFs for Failure Pattern 1 with only aleatory uncertainty: (i) $CDF_{SL,1}(t)$, $CDF_{SL,2}(t)$, $CDF_{SL,3}(t)$ and $CDF_{WL,1}(t)$ for SL 1, SL 2, SL 3 and WL 1, respectively, and (ii) $pP_1(t)$ for system.

As a verification test, $pP_1(t)$ can also be estimated with a Monte Carlo procedure. As an example, the following values for $pP_1(200)$ were obtained with quadrature and Monte Carlo procedures:

$$pP_1(200) \cong \begin{cases} 6.88\times 10^{-5} & \text{(with quadrature formula in Eq. (4.2))} \\ 6.60\times 10^{-5} & \text{(with Monte Carlo procedure in Eq. (5.9))} \\ 7.40\times 10^{-5} & \text{(with Monte Carlo procedure in Eq. (5.18)).} \end{cases} \tag{9.11}$$

For the quadrature procedure, a subdivision

$$i(200 \text{ min}/n), i = 0, 1, \ldots, n = 10^4, \tag{9.12}$$

of [0, 200 min] is used to define the time steps in Eq. (4.2). For the Monte Carlo procedures, the indicator function $\delta_i(t|\mathbf{t})$ in Eqs. (5.9) and (5.18) corresponds to the function $\delta_2(t|\mathbf{t})$ in Eq. (5.6) with $\mathbf{t} = \mathbf{t}_2$ defined by

$$\mathbf{t}_2 = [tWL_1, tSL_1, tSL_2, tSL_3]; \tag{9.13}$$

a sample size of $nR = 10^6$ for possible values for $\mathbf{t}_2$ is used for both approximations; and time steps of size 0.1 min are used to determine the link failure times defined in Eqs. (5.15) and (5.16) for use in Eq. (5.18). The similarity of the results obtained with the quadrature procedure and with the Monte Carlo procedures helps provide a verification that $pP_1(t)$ is derived and numerically evaluated correctly.

One caveat is in order. The defining relationships for LOAS in Table 1 are predicated on the assumption that the failure times for the individual links are independent. As a consequence, the values for the aleatory variables in Table 7 cannot be correlated. As an example in the context of the example of this section, $\alpha_{SL,1}$, $\alpha_{SL,2}$ and $\alpha_{SL,3}$ cannot be correlated.

9.2 Failure Pattern 2: Only Aleatory Uncertainty

For Failure Pattern 2, LOAS occurs if SL 4 and SL 5 both fail before WL 2 fails. As described in Sect. 8, failure of SL 4, SL 5 and WL 2 depends on system temperatures

$$p_{SL,i}\left(t \mid \alpha_{SL,i}\right) = \alpha_{SL,i}\,\bar{p}_{SL,i}\left(t\right) = \begin{cases} \alpha_{SL,4}T_{13}\left(t\right), i = 4 \\ \alpha_{SL,5}T_{14}\left(t\right), i = 5 \end{cases} \tag{9.14}$$

$$p_{WL,2}\left(t \mid \alpha_{WL,2}\right) = \alpha_{WL,2}\,\bar{p}_{WL,2}\left(t\right) = \alpha_{WL,2}T_{16}\left(t\right) \tag{9.15}$$

and failure temperatures

$$q_{SL,i}\left(t \mid \beta_{SL,i}\right) = \beta_{SL,i}\bar{q}_{SL,i}\left(t\right) = \begin{cases} \beta_{SL,4}\left(623\text{ K}\right), i = 4 \\ \beta_{SL,5}\left(673\text{ K}\right), i = 5 \end{cases} \tag{9.16}$$

$$q_{WL,2}\left(t \mid \beta_{WL,2}\right) = \beta_{WL,2}\bar{q}_{WL,2}\left(t\right) = \beta_{WL,2}\left(550\text{ K}\right). \tag{9.17}$$

Specifically, the equalities

$$p_{SL,i}\left(t \mid \alpha_{SL,i}\right) = q_{SL,i}\left(t \mid \beta_{SL,i}\right), i = 4, 5, \tag{9.18}$$

and

$$p_{WL,2}\left(t \mid \alpha_{WL,2}\right) = q_{WL,2}\left(t \mid \beta_{WL,2}\right) \tag{9.19}$$

define the failure times for SL 4, SL 5 and WL 2, respectively. The system and failure properties appearing in Eqs. (9.14) - (9.17) are illustrated in Fig. 8.

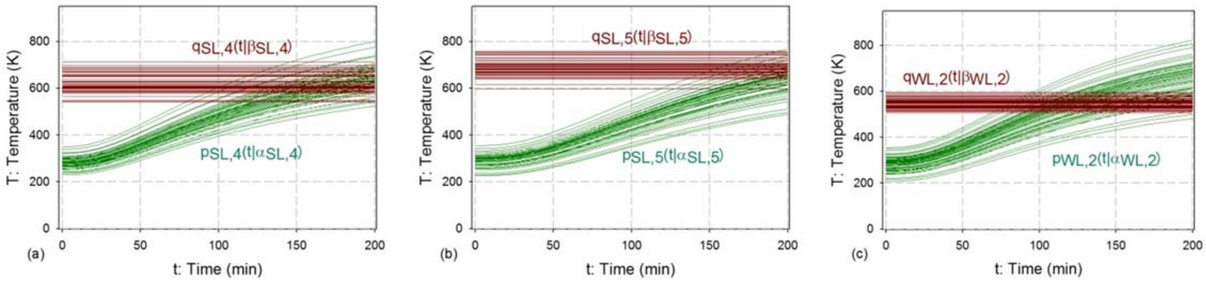

Fig. 8. System and failure properties for SL 4, SL 5 and WL 2 generated with random samples of size 100 from the defining aleatory variables: (a) $p_{SL,4}(t \mid \alpha_{SL,4})$ and $q_{SL,4}(t \mid \beta_{SL,4})$ for SL 4, (b) $p_{SL,5}(t \mid \alpha_{SL,5})$ and $q_{SL,5}(t \mid \beta_{SL,5})$ for SL 5, and (c) $p_{WL,2}(t \mid \alpha_{WL,2})$ and $q_{WL,2}(t \mid \beta_{WL,2})$ for WL 2.

For each link, the corresponding CDF for failure time can be calculated as shown in Eq. (2.12). This results in the failure time CDFs $CDF_{SL,4}(t)$, $CDF_{SL,5}(t)$ and $CDF_{WL,2}(t)$ for SL 4, SL 5 and WL 2, respectively (Fig. 9a). The failure pattern under consideration corresponds to Case 1 in Table 1 with $nSL = 2$ and $nWL = 1$. The resultant time-dependent probability $pP_2(t)$ of LOAS calculated with the quadrature procedure indicated in Eq. (4.1) is also shown in Fig. 9a.

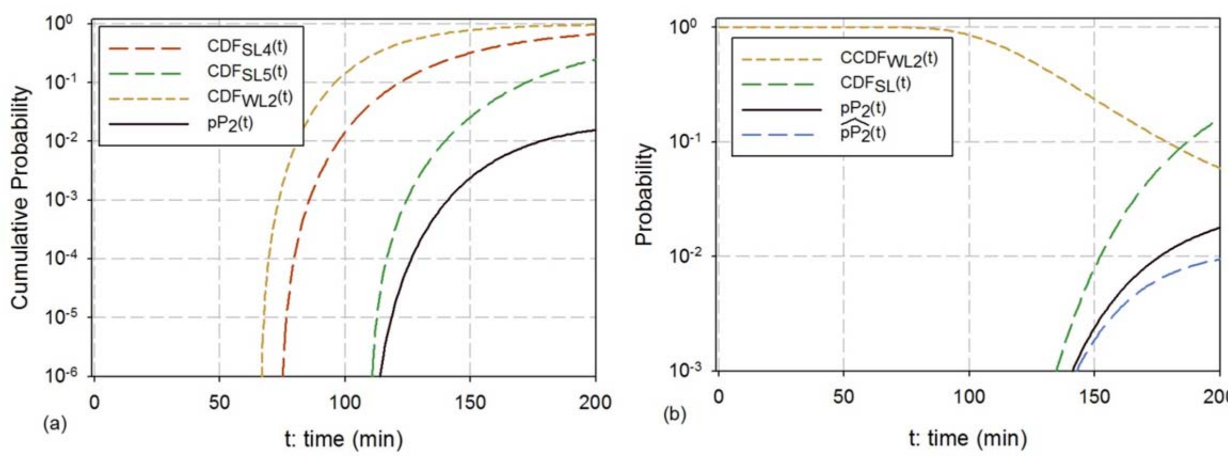

Fig. 9. Failure time CDFs for Failure Pattern 2 with only aleatory uncertainty: (a) $CDF_{SL,4}(t)$, $CDF_{SL,5}(t)$ and $CDF_{WL,2}(t)$ for SL 4, SL 5 and WL 2, respectively, and $pP_2(t)$ for system, and (b) $CDF_{SL}(t)$ for SLs 4 and 5, $CCDF_{WL,2}(t) = 1 - CDF_{WL,2}(t)$ for WL 2, and $pP_2(t)$ and $\widehat{pP_2}(t)$ for system.

As discussed in Sect. 7, PLOAS for Cases 1 and 3 in Table 1 can also be obtained by initially calculating the CDF $CDF_{SL}(\tau)$ for the failure of all SLs by time τ as shown in Eq. (7.1) and then determining $pP_1(t)$ and $pP_3(t)$ as shown in Eqs. (7.2) and (7.3). For Failure Pattern 2, the representation for $pF_1(t)$ in Eq. (7.2) simplifies to

$$pP_2(t) = \int_0^t \left[1 - CDF_{WL,2}(\tau)\right] \mathrm{d}CDF_{SL}(\tau) = \int_0^t CCDF_{WL,2}(\tau) \mathrm{d}CDF_{SL}(\tau). \qquad (9.20)$$

The values for $CDF_{SL}(\tau)$ and $pP_2(t)$ for Failure Pattern 2 are shown in Fig. 9b. As should be the case, the values for $pP_2(t)$ in Fig. 9a obtained as indicated in Table 1 for $pF_1(t)$ and in Fig. 9b obtained as indicated in Eq. (9.20) are the same.

As also discussed in Sect. 7, the values of the WL failure time CCDFs $CCDF_{WL,j}(t) = 1 - CDF_{WL,j}(t)$ and the SL failure time CDF $CDF_{SL}(t)$ cannot be directly multiplied to obtain $pF_1(t)$. Specifically, $\widehat{pF_1}(t)$ calculated as indicated in Eq. (7.6) is not the same as $pF_1(t)$ calculated with the numerically equivalent representations in Table 1 and Eq. (7.2). For Failure Pattern 2, the representation for $\widehat{pF_1}(t)$ in Eq. (7.6) simplifies to

$$\widehat{pP_2}(t) = \left[1 - CDF_{WL,2}(t)\right] CDF_{SL}(t) = CCDF_{WL,2}(t) CDF_{SL}(t). \qquad (9.21)$$

The resultant value for $\widehat{pP_2}(t)$ is also shown in Fig. 9b and is not the same as $pP_2(t)$. The extent of the difference between $pF_1(t)$ and $\widehat{pF_1}(t)$ for Case 1 in Table 1 depends on the properties of the failure CDFs for the WLs and SLs for the analysis under consideration. The same is also true for $pF_3(t)$ and $\widehat{pF_3}(t)$ for Case 3 in Table 1.

As a verification test, $pP_2(t)$ can also be estimated with a Monte Carlo procedure. As an example, the following values for $pP_2(200)$ were obtained with quadrature and Monte Carlo procedures:

$$pP_2(200) \cong \begin{cases} 1.56 \times 10^{-2} & \text{(with quadrature formula in Eq. (4.1))} \\ 1.60 \times 10^{-2} & \text{(with Monte Carlo procedure in Eq. (5.9))} \\ 1.59 \times 10^{-2} & \text{(with Monte Carlo procedure in Eq. (5.18)).} \end{cases} \qquad (9.22)$$

For the quadrature procedure, the subdivision of [0, 200 min] in Eq. (9.12) with $n = 10^4$ is used to define the time steps in Eq. (4.1). For the Monte Carlo procedures, the indicator function $\delta_i(t|\mathbf{t})$ in Eqs. (5.9) and (5.18) corresponds to the function $\delta_1(t|\mathbf{t})$ in Eq. (5.5) with $\mathbf{t} = \mathbf{t}_1$ defined by

$$\mathbf{t}_1 = \left[tWL_2, tSL_4, tSL_5\right]; \qquad (9.23)$$

a sample size of $nR = 10^6$ for possible values for $\mathbf{t}_1$ is used for both approximations; and time steps of size 0.1 min are used to determine the link failure times defined in Eqs. (5.15) and (5.16) for use in Eq. (5.18). As for the results in Eq. (9.11), the similarity of the results obtained with the quadrature procedure and with the Monte Carlo procedures helps provide a verification that $pP_2(t)$ is derived and numerically evaluated correctly.

9.3 Failure Pattern 3: Only Aleatory Uncertainty

For Failure Pattern 3, LOAS occurs if (i) SL 1, SL 2 or SL 3 fails before WL 1 (i.e., Failure Pattern 1) or (ii) SL 4 and SL 5 both fail before WL 2 (i.e., Failure Pattern 2). The distributions $pP_1(t)$ and $pP_2(t)$ for the times at which LOAS occurs for the WL/SL systems indicated in (i) and (ii) are derived in Sects. 9.1 and 9.2. Because there are no correlations between the aleatory variables involved in the definition of $pP_1(t)$ and the aleatory variables involved in the definition of $pP_2(t)$, the distributions defined by $pP_1(t)$ and $pP_2(t)$ are independent. As a consequence, the time-dependent probability $pP_3(t)$ of LOAS for Failure Pattern 3 is given by

$$\begin{aligned} pP_3(t) &= 1 - \prod_{i=1}^{2}\left[1 - pP_i(t)\right] \\ &= pP_1(t) + pP_2(t) - pP_1(t)\,pP_2(t) \end{aligned} \tag{9.24}$$

as illustrated in Fig. 10. From a numerical perspective, the second expression for $pP_3(t)$ in Eq. (9.24) is preferable as it avoids the potential numerical problems that can arise from subtractions involving two similar sized numbers.

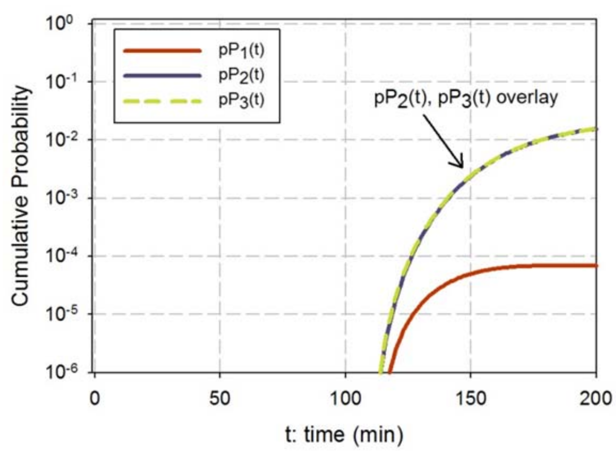

Fig. 10. Time-dependent probabilities $pP_1(t)$, $pP_2(t)$ and $pP_3(t)$ for LOAS for Failure Patterns 1, 2 and 3, respectively, with only aleatory uncertainty.

9.4 Failure Pattern 4: Only Aleatory Uncertainty

For Failure Pattern 4, LOAS occurs if SL 4 and SL 5 both fail before either WL 1 or WL 2 fails. The properties of the indicated links and the associated CDFs $CDF_{SL,4}(t)$, $CDF_{SL,5}(t)$, $CDF_{WL,1}(t)$ and $CDF_{WL,2}(t)$ for link failure time are discussed in Sects. 9.1 and 9.2. The failure pattern under consideration corresponds to Case 1 in Table 1 with $nSL = nWL = 2$. The resultant time-dependent probability $pP_4(t)$ of LOAS calculated with the quadrature procedure indicated in Eq. (4.1) is shown in Fig. 11.

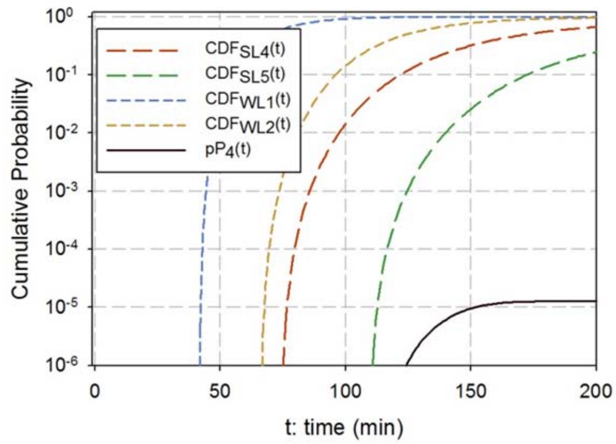

Fig. 11. Failure time CDFs for Failure Pattern 4 with only aleatory uncertainty: (i) $CDF_{SL,4}(t)$, $CDF_{SL,5}(t)$, $CDF_{WL,1}(t)$ and $CDF_{WL,2}(t)$ for SL 4, SL 5, WL 1 and WL 2, respectively, and (ii) $pP_4(t)$ for system.

As a verification test, $pF_4(t)$ can also be estimated with a Monte Carlo procedure. As an example, the following values for $pF_4(200)$ were obtained with quadrature and Monte Carlo procedures:

$$pP_4(200) \cong \begin{cases} 1.27\times10^{-5} & \text{(with quadrature formula in Eq. (4.1))} \\ 1.60\times10^{-5} & \text{(with Monte Carlo procedure in Eq. (5.9))} \\ 1.00\times10^{-5} & \text{(with Monte Carlo procedure in Eq. (5.18)).} \end{cases} \tag{9.25}$$

For the quadrature procedure, the subdivision of [0, 200 min] in Eq. (9.12) with $n = 10^4$ is used to define the time steps in Eq. (4.1). For the Monte Carlo procedures, the indicator function $\delta_i(t|\mathbf{t})$ in Eqs. (5.9) and (5.18) corresponds to the function $\delta_1(t|\mathbf{t})$ in Eq. (5.5) with $\mathbf{t} = \mathbf{t}_1$ defined by

$$\mathbf{t}_1 = \left[tWL_1, tWL_2, tSL_4, tSL_5\right]; \tag{9.26}$$

a sample size of $nR = 10^6$ for possible values for $\mathbf{t}_1$ is used for both approximations; and time steps of size 0.1 min are used to determine the link failure times defined in Eqs. (5.15) and (5.16) for use in Eq. (5.18). As for the results in Eqs. (9.11) and (9.22), the similarity of the results obtained with the quadrature and Monte Carlo procedures helps provide a verification that $pP_4(t)$ is derived and numerically evaluated correctly.

9.5 Failure Pattern 5: Only Aleatory Uncertainty

For Failure Pattern 5, LOAS occurs if (i) SL 1, SL 2 or SL 3 fails before WL 1 fails (i.e., Failure Pattern 1) or (ii) SL 4 and SL 5 both fail before WL 1 or WL 2 fails (i.e., Failure Pattern 4). The properties of the indicated links and the associated CDFs $CDF_{SL,i}(t)$, i = 1, 2, 3, 4, 5, and $CDF_{WL,i}(t)$, i = 1, 2, for link failure time are discussed in Sects. 9.1 and 9.2. Further, the time-dependent probabilities $pP_1(t)$ and $pP_4(t)$ for LOAS for the failure patterns indicated in (i) and (ii) are obtained in Sects. 9.1 and 9.4, respectively. However, the probability distributions for the time at which LOAS occurs defined by $pP_1(t)$ and $pP_4(t)$ are not independent as the distribution defined by $CDF_{WL,1}(t)$ is involved in the definition of both $pP_1(t)$ and $pP_4(t)$. As a result, the relationship in Eq. (9.24) is not appropriate for the determination of the time-dependent probability $pF_5(t)$ for LOAS for Failure Pattern 5.

Although none of the WL/SL failure patterns leading to LOAS in Table 1 correspond to Failure Pattern 5, it is possible to derive a representation for $pP_5(t)$ that is similar in concept to the representations $pF_i(t)$ in Table 1. The starting point in this derivation is the relationship

$$pP_5(t+\Delta t) - pP_5(t) \cong p\left[\mathcal{W}_1(t)\right]\sum_{i=1}^{5} p\left[\mathcal{S}_i(t,t+\Delta t) \mid \mathcal{W}_1(t)\right], \tag{9.27}$$

where

$\mathcal{W}_1(t) =$ event WL 1 has not failed by time t,

$\mathcal{S}_i(t,t+\Delta t) =$ event LOAS occurs in time interval $[t, t+\Delta t]$ due to failure of SL i,

and $p(\sim)$ designates probability. In turn,

$$p\left[\mathcal{W}_1(t)\right] = 1 - CDF_{WL,1}(t), \tag{9.28}$$

where $1 - CDF_{WL,1}(t)$ is the probability that WL 1 has not failed prior to time t;

$$p\left[\mathcal{S}_i\left(t,t+\Delta t\right)\mid \mathcal{W}_1\left(t\right)\right]=\left\{\prod_{j=1,\, j\neq i}^{3}\left[1-CDF_{SL,\,j}\left(t\right)\right]\right\}_1\left\{1-pP_2\left(t\right)\right\}_2 \times\left\{CDF_{SL,i}\left(t+\Delta t\right)-CDF_{SL,i}\left(t\right)\right\}_3, \tag{9.29}$$

for i = 1, 2, 3, where $\{\sim\}_1$ is the probability that SLs j , j = 1, 2, 3 with $j \neq i$, have not failed prior to time t, $\{\sim\}_2$ is the probability that SLs 4 and 5 have not failed before the failure of WL 2 prior to time t (see Sect. 5.2), and $\{\sim\}_3$ is the probability that SL i fails between times t and $t + \Delta t$;

$$p\left[\mathcal{S}_4\left(t,t+\Delta t\right)\mid \mathcal{W}_1\left(t\right)\right]=CDF_{SL,5}\left(t\right)\left\{1-CDF_{WL,2}\left(t\right)\right\}_1\left\{\prod_{j=1}^{3}\left[1-CDF_{SL,\,j}\left(t\right)\right]\right\}_2 \times\left\{CDF_{SL,4}\left(t+\Delta t\right)-CDF_{SL,4}\left(t\right)\right\}_3, \tag{9.30}$$

where $CDF_{SL,5}(t)$ is the probability that SL 5 has f ailed prior to time t, $\{\sim\}_1$ is the probability that WL 2 has not failed prior to time t, $\{\sim\}_2$ is the probability that SLs 1, 2 and 3 have not faile d prior to time t, and $\{\sim\}_3$ is the probability that SL 4 fails between times t and $t + \Delta t$; and

$$p\left[\mathcal{S}_5\left(t,t+\Delta t\right)\mid \mathcal{W}_1\left(t\right)\right]=CDF_{SL,4}\left(t\right)\left\{1-CDF_{WL,2}\left(t\right)\right\}_1\left\{\prod_{j=1}^{3}\left[1-CDF_{SL,\,j}\left(t\right)\right]\right\}_2 \times\left\{CDF_{SL,5}\left(t+\Delta t\right)-CDF_{SL,5}\left(t\right)\right\}_3, \tag{9.31}$$

where $CDF_{SL,4}(t)$ is the probability that SL 4 has f ailed prior to time t, $\{\sim\}_1$ is the probability that WL 2 has not failed prior to time t, $\{\sim\}_2$ is the probability that SLs 1, 2 and 3 have not faile d prior to time t, and $\{\sim\}_3$ is the probability that SL 5 fails between times t and $t + \Delta t$.

Combining the relationships in Eqs. (9.27) - (9.31) produces

$$
\begin{aligned}
pP_5(t+\Delta t) - pP_5(t) \cong \big(1 - CDF_{WL,1}(t)\big) \\
\times \Bigg(\sum_{i=1}^{3} \left\{ \prod_{j=1,\, j\neq i}^{3} \left[1 - CDF_{SL,j}(t)\right] \right\} \left\{1 - pP_2(t)\right\} \Delta CDF_{SL,i}(t) \\
+ CDF_{SL,5}(t)\left\{1 - CDF_{WL,2}(t)\right\} \left\{ \prod_{j=1}^{3} \left[1 - CDF_{SL,j}(t)\right] \right\} \Delta CDF_{SL,4}(t) \\
+ CDF_{SL,4}(t)\left\{1 - CDF_{WL,2}(t)\right\} \left\{ \prod_{j=1}^{3} \left[1 - CDF_{SL,j}(t)\right] \right\} \Delta CDF_{SL,5}(t) \Bigg)
\end{aligned}
\tag{9.32}
$$

with

$$
\Delta CDF_{SL,i}(t) = CDF_{SL,i}(t+\Delta t) - CDF_{SL,i}(t).
$$

In turn, if $0 = t_0 < t_1 < \cdots < t_n = t$ is a subdivision of [0, t] and $pP_5(0) = 0$ as should be the case, then

$$
\begin{aligned}
pP_5(t) &\cong \sum_{k=0}^{n-1} pP_5(t_k + \Delta t_k) - pP_5(t_k) \\
&= \sum_{k=0}^{n-1} \big(1 - CDF_{WL,1}(t_k)\big) \Bigg(\sum_{i=1}^{3} \left\{ \prod_{j=1,\, j\neq i}^{3} \left[1 - CDF_{SL,j}(t_k)\right] \right\} \left\{1 - pP_2(t_k)\right\} \Delta CDF_{SL,i}(t_k) \\
&\quad + CDF_{SL,5}(t_k)\left\{1 - CDF_{WL,2}(t_k)\right\} \left\{ \prod_{j=1}^{3} \left[1 - CDF_{SL,j}(t_k)\right] \right\} \Delta CDF_{SL,4}(t_k) \\
&\quad + CDF_{SL,4}(t_k)\left\{1 - CDF_{WL,2}(t_k)\right\} \left\{ \prod_{j=1}^{3} \left[1 - CDF_{SL,j}(t_k)\right] \right\} \Delta CDF_{SL,5}(t_k) \Bigg).
\end{aligned}
\tag{9.33}
$$

Finally, the representation

$$
\begin{aligned}
pP_5(t) = \int_0^t \big(1 - CDF_{WL,1}(\tau)\big) \Bigg(\sum_{i=1}^{3} \left\{ \prod_{j=1,\, j\neq i}^{3} \left[1 - CDF_{SL,j}(\tau)\right] \right\} \left\{1 - pP_2(\tau)\right\} \mathrm{d}CDF_{SL,i}(\tau) \\
+ CDF_{SL,5}(\tau)\left\{1 - CDF_{WL,2}(\tau)\right\} \left\{ \prod_{j=1}^{3} \left[1 - CDF_{SL,j}(\tau)\right] \right\} \mathrm{d}CDF_{SL,4}(\tau) \\
+ CDF_{SL,4}(\tau)\left\{1 - CDF_{WL,2}(\tau)\right\} \left\{ \prod_{j=1}^{3} \left[1 - CDF_{SL,j}(\tau)\right] \right\} \mathrm{d}CDF_{SL,5}(\tau) \Bigg)
\end{aligned}
\tag{9.34}
$$

for $pP_5(t)$ as a Stieltjes integral involving five differentials (i.e., $\mathrm{d}CDF_{SL,i}(t)$, i = 1, 2, 3, 4, 5) is obtained as $\Delta t_k \to 0$. Equivalently, $pP_5(t)$ could also be expressed as a sum of five Stieltjes integrals each involving a single differential. In computational practice, it is more efficient to approximate $pF_5(t)$ with the sum in Eq. (9.33) than to approximate five individual Stieltjes integrals and then sum the results of these approximations. The result of approximating $pP_5(t)$ with the sum in Eq. (9.33) is shown in Fig. 12.

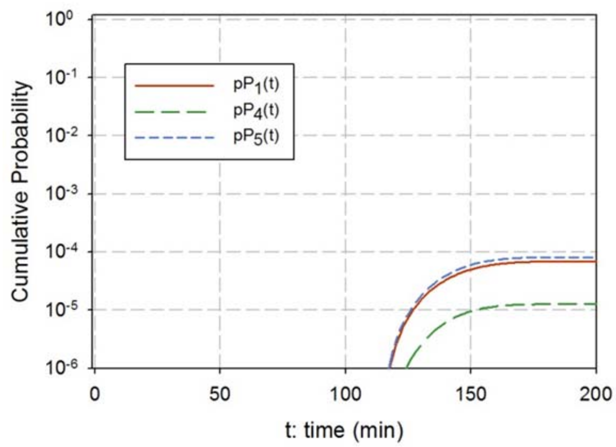

Fig. 12. Time-dependent probabilities $pP_1(t)$, $pP_4(t)$ and $pP_5(t)$ for LOAS for Failure Patterns 1, 4 and 5, respectively, with only aleatory uncertainty.

As a verification test, $pP_5(t)$ can also be estimated with a Monte Carlo procedure. As an example, the following values for $pP_5(t)$ were obtained with quadrature and Monte Carlo procedures:

$$pP_5(t) \cong \begin{cases} 8.18\times 10^{-5} & \text{(with quadrature formula in Eq. (7.31))} \\ 8.20\times 10^{-5} & \text{(with Monte Carlo procedure in Eq. (5.9))} \\ 7.80\times 10^{-5} & \text{(with Monte Carlo procedure in Eq. (5.18)).} \end{cases} \tag{9.35}$$

For the quadrature procedure, the subdivision of [0, 200 min] in Eq. (9.12) with $n = 10^4$ is used to define the time steps in Eq. (9.33). For the Monte Carlo procedures, the indicator function $\delta_i(t|\mathbf{t})$ in Eqs. (5.9) and (5.18) corresponds to the function $\delta_5(t|\mathbf{t}_5)$ defined by

$$\delta_5(t\,|\,\mathbf{t}_5) = \begin{cases} 1 \text{ if } \delta_1(t\,|\,\mathbf{t}_1) = 1 \text{ or } \delta_2(t\,|\,\mathbf{t}_2) = 1 \\ 0 \text{ otherwise} \end{cases} \tag{9.36}$$

with $\delta_1(t|\mathbf{t}_1)$, $\delta_2(t|\mathbf{t}_2)$, $\mathbf{t}_1$ and $\mathbf{t}_2$ defined in Eqs. (5.5), (5.6), (9.26) and (9.13), respectively, and

$$\mathbf{t}_5 = [tWL_1, tWL_2, tSL_1, tSL_2, tSL_3, tSL_4, tSL_5]; \tag{9.37}$$

a sample size of $nR = 10^6$ for possible values for $\mathbf{t}_5$ is used for both approximations; and time steps of size 0.1 min are used to determine the link failure times defined in Eqs. (5.15) and (5.16) for use in Eq. (5.18). As for the results in Eqs. (9.11), (9.22) and (9.25), the similarity of the results obtained with the quadrature and Monte Carlo procedures helps provide a verification that $pP_5(t)$ is derived and numerically evaluated correctly.

The representation for PLOAS in Eq. (9.34) is not based on any of the WL/SL failure patterns in Table 1. Thus, none of the test problems in Table 1 apply to this representation for PLOAS. However, procedures analogous to those used in Ref. [10] to obtain the test problems in Table 1 can be used to obtain a test problem for the representation for PLOAS in Eq. (9.34). Specifically, this involves assigning the same failure properties to all links. When this is done, all links have identical, but independent, distributions of failure times. These distributions can be represented by a function p, where (i) $p(\tau)$ is the probability that a link has failed by time τ, (ii) $p(0) = 0$, and (iii) $p(\infty) = 1$. Specifically, $p(\tau)$ corresponds to the CDF for failure time for each link. Or, put another way, the CDFs for SL and WL failure time are assumed to be defined by

$$p_{SL,i}(\tau) = p_{WL,j}(\tau) = p(\tau) \tag{9.38}$$

for $i = 1, 2, 3, 4, 5$ and $j = 1, 2$.

Substitution of the CDF representations in Eq. (9.38) into the representation for PLOAS in Eq. (9.34) produces

$$\begin{aligned} pP_5(t) = \int_0^t \left(1 - p_{WL,1}(\tau)\right) &\left(\sum_{i=1}^{3} \left\{ \prod_{j=1,\, j\neq i}^{3} \left[1 - p_{SL,j}(\tau)\right] \right\} \left\{1 - pP_2(\tau)\right\} \mathrm{d}p_{SL,i}(\tau) \right. \\ &+ p_{SL,5}(\tau)\left\{1 - p_{WL,2}(\tau)\right\} \left\{ \prod_{j=1}^{3} \left[1 - p_{SL,j}(\tau)\right] \right\} \mathrm{d}p_{SL,4}(\tau) \\ &\left. + p_{SL,4}(\tau)\left\{1 - p_{WL,2}(\tau)\right\} \left\{ \prod_{j=1}^{3} \left[1 - p_{SL,j}(\tau)\right] \right\} \mathrm{d}p_{SL,5}(\tau) \right) \\ = \int_0^t \left(3\left[1 - p(\tau)\right]^3 \left[1 - pP_2(\tau)\right] + 2p(\tau)\left[1 - p(\tau)\right]^5 \right) &\left(\mathrm{d}p(\tau)/\mathrm{d}\tau\right)\mathrm{d}\tau, \end{aligned} \tag{9.39}$$

where the second equality follows from the equalities in Eq. (9.38) and the differential relationship $\mathrm{d}p(\tau) = (\mathrm{d}p(\tau)/\mathrm{d}\tau)\mathrm{d}\tau$. Further, $pP_2(\tau)$ is given by

$$
\begin{aligned}
pP_2(\tau) &= \sum_{i=4}^{5} \int_0^{\tau} p_{SL,i}(\alpha)\left[1 - p_{WL,2}(\alpha)\right] \mathrm{d}p_{SL,i}(\alpha) \\
&= 2\int_0^{\tau} p(\alpha)\left[1 - p(\alpha)\right]\left[\mathrm{d}p(\alpha)/\mathrm{d}\alpha\right]\mathrm{d}\alpha \\
&= 2\int_0^{p(\tau)} p(1-p)\mathrm{d}p \\
&= p^2(\tau) - (2/3)p^3(\tau),
\end{aligned}
\tag{9.40}
$$

where (i) the first equality follows from the first failure pattern in Table 1 with $nSL = 2$ and $nWL = 1$ and (ii) the third equality follows from a change of variables (see Eq. (2.24)).

Combining the relationships in Eqs. (9.39) and (9.40) results in the following representation for $pP_5(t)$:

$$
\begin{aligned}
pP_5(t) &= \int_0^{t}\left(3\left[1 - p(\tau)\right]^3\left[1 - p^2(\tau) + (2/3)p^3(\tau)\right] + 2p(\tau)\left[1 - p(\tau)\right]^5\right)\left(\mathrm{d}p(\tau)/\mathrm{d}\tau\right)\mathrm{d}\tau \\
&= \int_0^{p(t)}\left(3\left[1 - p\right]^3\left[1 - p^2 + (2/3)p^3\right] + 2p\left[1 - p\right]^5\right)\mathrm{d}p,
\end{aligned}
\tag{9.41}
$$

where the second equality follows from a change of variables as indicated in Eq. (2.24). In turn,

$$
\begin{aligned}
pP_5(\infty) &= \int_0^{1}\left(3\left[1 - p\right]^3\left[1 - p^2 + (2/3)p^3\right] + 2p\left[1 - p\right]^5\right)\mathrm{d}p \\
&= 16/21,
\end{aligned}
\tag{9.42}
$$

where the final verification result

$$
pP_5(\infty) = 16/21 \cong 0.7619 \tag{9.43}
$$

follows by standard integration procedures.

As a test, Failure Pattern 5 was analyzed with all links assigned the properties indicated in Fig. 3. The result of this calculation with the CPLOAS_2 program was $pP_5(\infty) = 0.7609$, which is in good agreement with the verification value in Eq. (9.43).

10. Examples Involving Aleatory and Epistemic Uncertainty

For the case of both aleatory and epistemic uncertainty, the boundary value temperature T_0 and the coefficients c, c_i and r_{jk} in Table 5 are assumed to be uncertain in an epistemic sense (i.e., these quantities have fixed but poorly known values). For purposes of illustration, each of these quantities is assumed to have a uniform distribution on the interval $[0.9\bar{v}, 1.1\bar{v}]$, where $\bar{v}$ is the base value given in Table 5. The preceding assignments result in 26 epistemically uncertain analysis inputs (i.e., T_0, c, 9 unique values for the c_i, and 15 unique values for the r_{jk}) as summarized in Table 8.

Table 8 Defining Distributions for Epistemic Uncertainty

Variables T_0, c, c_i, r_{jk} with uniform distributions on $[0.9\,\bar{v}, 1.1\,\bar{v}]$:

T_0: $\bar{v}$ = 800 K

c: $\bar{v}$ = 2.7; $c_1 = c_2$: $\bar{v}$ = 1.28E4; $c_3 = c_4$: $\bar{v}$ = 8.79E2; $c_5 = c_6$: $\bar{v}$ = 8.79E2; $c_7 = c_8$: $\bar{v}$ = 6.54E3; $c_9 = c_{10}$: $\bar{v}$ = 1.64E4; $c_{11} = c_{12}$: $\bar{v}$ = 8.91E2; $c_{13} = c_{14}$: $\bar{v}$ = 5.10E2; c_{15}: $\bar{v}$ = 9.99E2; c_{16}: $\bar{v}$ = 1.98E3

$r_{10} = r_{20}$: $\bar{v}$ =1.41E–8; $r_{13} = r_{31} = r_{15} = r_{51} = r_{24} = r_{42} = r_{26} = r_{62}$: $\bar{v}$ = 3.91; $r_{17} = r_{71} = r_{19} = r_{91} = r_{28} = r_{82} = r_{2,10} = r_{10,2}$: $\bar{v}$ = 3.06; $r_{34} = r_{43} = r_{56} = r_{65}$: $\bar{v}$ = 2.42; $r_{37} = r_{73} = r_{48} = r_{84}$: $\bar{v}$ = 0.855; $r_{59} = r_{95} = r_{6,10} = r_{10,6}$: $\bar{v}$ = 1.43E–2; $r_{78} = r_{87}$: $\bar{v}$ = 2.00E–3; $r_{79} = r_{97} = r_{8,10} = r_{10,8}$: $\bar{v}$ = 0.140; $r_{7,11} = r_{11,7} = r_{8,12} = r_{12,8}$: $\bar{v}$ = 26.0; $r_{9,10} = r_{10,9}$: $\bar{v}$ = 0.06; $r_{9,13} = r_{13,9}$: $\bar{v}$ = 0.575; $r_{9,14} = r_{14,9}$: $\bar{v}$ = 0.230; $r_{9,15} = r_{15,9}$: $\bar{v}$ = 5.12; $r_{10,16} = r_{16,10}$: $\bar{v}$ = 1.41; $r_{11,12} = r_{12,11}$: $\bar{v}$ = 0.448

Variables defining standard deviations of normal distributions with $\mu = 1.0$ and $q = 0.01$ characterizing aleatory uncertainty:

SAWL1, standard deviation of $\alpha_{WL,1}$: uniform on 0.1[0.5, 1.5] = [0.05, 0.15]
SAWL2, standard deviation of $\alpha_{WL,2}$: uniform on 0.1[0.5, 1.5] = [0.05, 0.15]
SASL1, standard deviation of $\alpha_{SL,1}$: uniform on 0.1[0.5, 1.5] = [0.05, 0.15]
SASL2, standard deviation of $\alpha_{SL,2}$: uniform on 0.1[0.5, 1.5] = [0.05, 0.15]
SASL3, standard deviation of $\alpha_{SL,3}$: uniform on 0.1[0.5, 1.5] = [0.05, 0.15]
SASL4, standard deviation of $\alpha_{SL,4}$: uniform on 0.1[0.5, 1.5] = [0.05, 0.15]
SASL5, standard deviation of $\alpha_{SL,5}$: uniform on 0.1[0.5, 1.5] = [0.05, 0.15]
SBSL1, standard deviation of $\beta_{SL,1}$: uniform on 0.1[0.5, 1.5] = [0.05, 0.15]
SBSL2, standard deviation of $\beta_{SL,2}$: uniform on 0.1[0.5, 1.5] = [0.05, 0.15]
SBSL3, standard deviation of $\beta_{SL,3}$: uniform on 0.1[0.5, 1.5] = [0.05, 0.15]

Variables defining modes of triangular distributions characterizing aleatory uncertainty:

MBWL1, mode of distribution for of $\beta_{WL,1}$ on [0.91, 1.09]: uniform on [0.91, 1.09]
MBWL2, mode of distribution for of $\beta_{WL,2}$ on [0.9, 1.1]: uniform on [0.9, 1.1]
MBSL4, mode of distribution for of $\beta_{SL,4}$ on [0.85, 1.15]: uniform on [0.85, 1.15]
MBSL5, mode of distribution for of $\beta_{SL,5}$ on [0.85, 1.15]: uniform on [0.85, 1.15]

Further, additional uncertain variables related to the characterization of aleatory uncertainty are also included in the analysis. For each specified normal distribution for aleatory uncertainty and associated assigned value of σ for standard deviation (see Table 7), an epistemically uncertain variable s with a uniform distribution on [0.5 σ, 1.5 σ] is defined such that s is the standard deviation for the corresponding aleatory variable α. This introduces 10 epistemically uncertain variables into the analysis. For each specified triangular distribution and associated assigned interval [a, b] for aleatory uncertainty (see Table 7), an epistemically uncertain variable m with a uniform distribution on [a, b] is defined such that m is the mode for the distribution of the corresponding aleatory variable α on [a, b]. This introduces 4 epistemically uncertain variables into the analysis. The preceding assignments result in 14 epistemically uncertain analysis inputs (i.e., 10 standard deviations for normal distributions and 4 modes for triangular distributions) as summarized in Table 8. In effect, the uncertain standard deviations correspond to uncertainty in the spread of a distribution characterizing aleatory uncertainty, and the uncertain modes correspond to uncertainty in where the values of a distribution characterizing aleatory uncertainty are concentrated.

The preceding assignments result in a vector

$$\mathbf{e} = \left[e_1, e_2, \cdots, e_{nE}\right] \tag{10.1}$$

of $nE = 40$ epistemically uncertain analysis inputs as summarized in Table 8. For the examples of this section, epistemic uncertainty is propagated with a Latin hypercube sample [21; 22]

$$\mathbf{e}_k = \left[e_{k1}, e_{k2}, \cdots, e_{k,nE}\right], k = 1, 2, \cdots, nLHS, \tag{10.2}$$

of size $nLHS = 100$ from the $nE = 40$ epistemically uncertain quantities indicated in conjunction with Eq. (10.1). Further, the Iman/Conover restricted pairing technique was used to assure that the correlations within the sample between individual variables are close to zero [23; 24].

As a result of the epistemically uncertain values assigned to T_0, c, c_i and r_{jk}, the base physical properties $\overline{p}_{WL,i}(t), i = 1, 2,$ and $\overline{p}_{SL,i}(t), i = 1, 2, ..., 5,$ and base failure properties $\overline{q}_{SL,i}(t), i = 1, 2, 3,$ are epistemically uncertain. Specifically,

$$\overline{p}_{WL,1}(t \mid \mathbf{e}_k) = T_{11}(t \mid \mathbf{e}_k), \overline{p}_{WL,2}(t \mid \mathbf{e}_k) = T_{16}(t \mid \mathbf{e}_k), \tag{10.3}$$

$$\overline{p}_{SL,i}(t \mid \mathbf{e}_k) = P_9(t \mid \mathbf{e}_k), i = 1, 2, 3, \tag{10.4}$$

$$\overline{p}_{SL,4}(t \mid \mathbf{e}_k) = T_{13}(t \mid \mathbf{e}_k), \overline{p}_{SL,5}(t \mid \mathbf{e}_k) = T_{14}(t \mid \mathbf{e}_k), \tag{10.5}$$

and

$$\bar{q}_{SL,i}(t\,|\,\mathbf{e}_k) = \begin{cases} f_{SL,i}\left[T_1(t\,|\,\mathbf{e}_k)\right], i = 1 \\ f_{SL,i}\left[T_5(t\,|\,\mathbf{e}_k)\right], i = 2,3. \end{cases} \tag{10.6}$$

In contrast, the base failure values

$$\bar{q}_{WL,1}(t) = 600 \text{ K}, \bar{q}_{WL,2}(t) = 550 \text{ K}, \bar{q}_{SL,4}(t) = 623 \text{ K}, \bar{q}_{SL,5}(t) = 673 \text{ K} \tag{10.7}$$

are not assumed to be epistemically uncertain. However, as for the other base properties in Eqs. (10.3)-(10.6), the associated aleatory distributions for $\beta_{WL,1}$, $\beta_{WL,2}$, $\beta_{SL,4}$ and $\beta_{SL,5}$ are assumed to be triangular with an epistemically uncertain mode (Table 8).

10.1 Failure Pattern 1: Aleatory and Epistemic Uncertainty

For Failure Pattern 1, LOAS occurs if SL 1, SL 2 or SL 3 fails before WL 1. As indicated in Eqs. (10.4) and (10.6) and illustrated in Fig. 13, the base physical properties $\bar{p}_{SL,i}(t\,|\,\mathbf{e}), i = 1,2,3,$ and base failure properties $\bar{q}_{SL,i}(t\,|\,\mathbf{e}), i = 1,2,3,$ for SLs 1, 2 and 3 are epistemically uncertain.

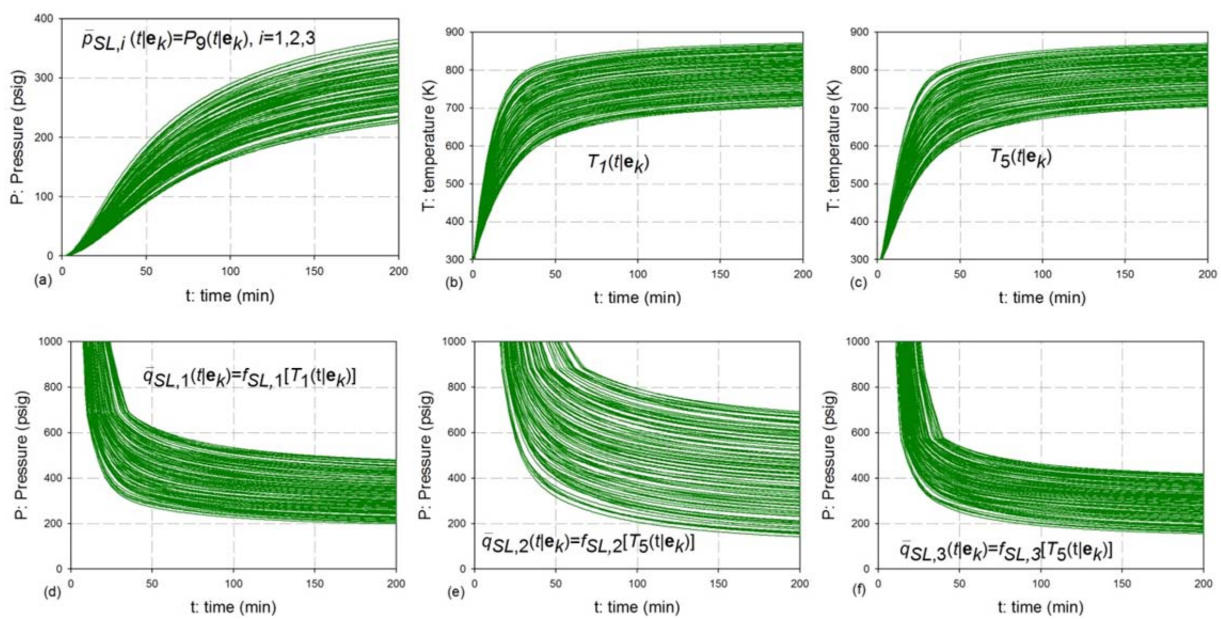

Fig. 13. Values for (a) $\bar{p}_{SL,i}(t\,|\,\mathbf{e}_k) = P_9(t\,|\,\mathbf{e}_k), i = 1,2,3,$ (b) $T_1(t\,|\,\mathbf{e}_k)$, (c) $T_5(t\,|\,\mathbf{e}_k)$, (d) $\bar{q}_{SL,1}(t\,|\,\mathbf{e}_k) = f_{SL,1}[T_1(t\,|\,\mathbf{e}_k)]$, (e) $\bar{q}_{SL,2}(t\,|\,\mathbf{e}_k) = f_{SL,2}[T_5(t\,|\,\mathbf{e}_k)]$, and (f) $\bar{q}_{SL,3}(t\,|\,\mathbf{e}_k) = f_{SL,3}[T_5(t\,|\,\mathbf{e}_k)]$ for the LHS indicated in Eq. (10.2).

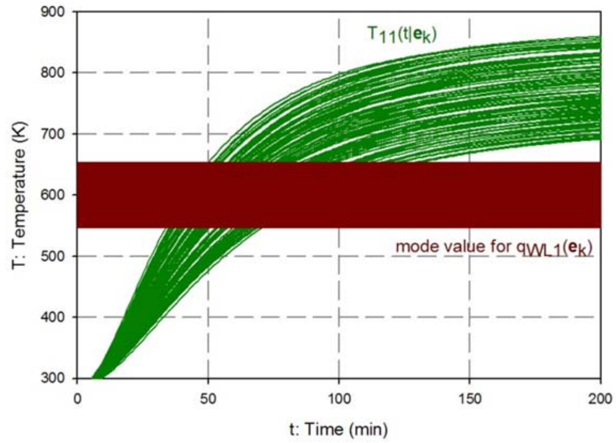

Fig. 14. Values for $\bar{p}_{WL,1}(t\,|\,\mathbf{e}_k) = T_{11}(t\,|\,\mathbf{e}_k)$ and mode for aleatory distribution of $q_{WL,1}(t\,|\,\beta_{WL,1}, MBWL1_k)$ on $[\,0.91\,\bar{q}_{WL,1}(t),\, 1.09\,\bar{q}_{WL,1}(t)\,]$ = [0.91(600 K), 1.09(600 K)] for the LHS indicated in Eq. (10.2).

As indicated in Eq. (10.3) and illustrated in Fig. 14, the base physical property $\bar{p}_{WL,1}(t\,|\,\mathbf{e})$ for WL 1 is epistemically uncertain. As indicated in Eq. (10.7), the base failure value $\bar{q}_{WL,1}(t)$ for WL 1 has a fixed value of 600 K. However, the triangular aleatory distributions for $\beta_{WL,1}$ on [0.91, 1.09] have an epistemically uncertain mode *MBWL1* with a uniform distribution on [0.91, 1.09] (see Table 8). In addition to $\bar{p}_{WL,1}(t\,|\,\mathbf{e})$, the modes

$$MBWL1_k\,\bar{q}_{WL,1}(t) = MBWL1_k\left(600\ K\right) \tag{10.8}$$

for the distributions of $q_{WL,1}(t\,|\,\beta_{WL,1}, MBWL1_k)$ are also shown in Fig. 14.

Each element $\mathbf{e}_k$ of the LHS indicated in Eq. (10.2) produces a set of results of the form shown in Fig. 6 and Fig. 7 for a total of *nLHS* = 100 sets of results. As an example, the failure time CDFs $CDF_{SL,1}(t\,|\,\mathbf{e}_k)$, $CDF_{SL,2}(t\,|\,\mathbf{e}_k)$, $CDF_{SL,3}(t\,|\,\mathbf{e}_k)$ and $CDF_{WL,1}(t\,|\,\mathbf{e}_k)$ for SL 1, SL 2, SL 3 and WL 1 and also the value $pP_1(t|\mathbf{e}_k)$ for PLOAS are shown in Fig. 15. The spread of the results Fig. 15 provides a representation for the epistemic uncertainty present in the estimates for $CDF_{SL,1}(t\,|\,\mathbf{e})$, $CDF_{SL,2}(t\,|\,\mathbf{e})$, $CDF_{SL,3}(t\,|\,\mathbf{e})$, $CDF_{WL,1}(t\,|\,\mathbf{e})$ and $pP_1(t|\mathbf{e})$.

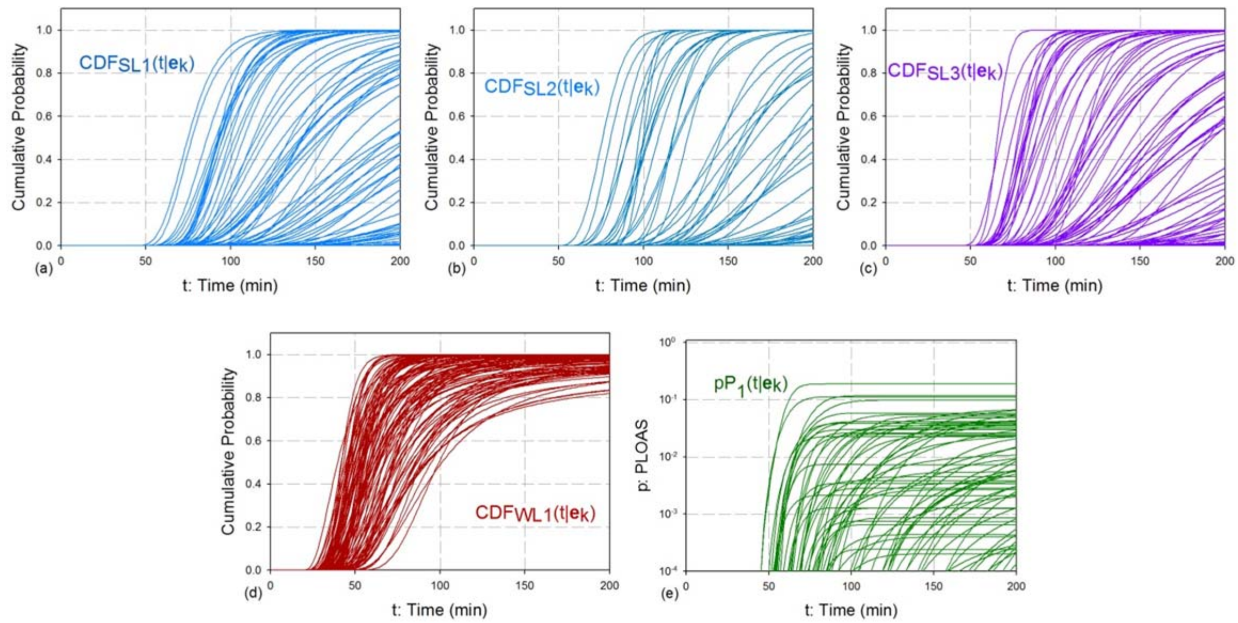

Fig. 15. Failure time CDFs and probability of LOAS for Failure Pattern 1 and elements $\mathbf{e}_k$, $k = 1, 2, \ldots, 100$, of LHS in Eq. (10.2): (a) $CDF_{SL,1}(t\,|\,\mathbf{e}_k)$, (b) $CDF_{SL,2}(t\,|\,\mathbf{e}_k)$, (c) $CDF_{SL,3}(t\,|\,\mathbf{e}_k)$, (d) $CDF_{WL,1}(t\,|\,\mathbf{e}_k)$, and (e) $pP_1(t|\mathbf{e}_k)$.

Some of the curves for $pP_1(t|\mathbf{e}_k)$ in Fig. 15e are level after a specific time $tL(\mathbf{e}_k)$. The time $tL(\mathbf{e}_k)$ corresponds to the earliest time at which (i) WL 1 has failed with probability 1.0 or (ii) one of the three SLs has failed with probability 1.0. Stated more formally, if $pP_1(t|\mathbf{e}_k)$ transitions to a level curve at time $tL(\mathbf{e}_k)$, then $tL(\mathbf{e}_k)$ corresponds to the earliest time at which one of the following four equalities holds: $CDF_{WL,1}(t\,|\,\mathbf{e}_k) = 1.0$, $CDF_{SL,1}(t\,|\,\mathbf{e}_k) = 1.0$, $CDF_{SL,2}(t\,|\,\mathbf{e}_k) = 1.0$ or $CDF_{SL,3}(t\,|\,\mathbf{e}_k) = 1.0$. For most sample elements, the transition to a level curve occurs at the time at which WL 1 has failed with probability 1.0.

10.2 Failure Pattern 2: Aleatory and Epistemic Uncertainty

For Failure Pattern 2, LOAS occurs if SL 4 and SL 5 both fail before WL 2 fails. As indicated in Eqs. (10.3) and (10.5), the base temperatures $T_{13}(t)$, $T_{14}(t)$ and $T_{16}(t)$ associated with the failure of SL 4, SL 5 and WL 2 are functions of epistemically uncertain quantities in the vector $\mathbf{e}$. Specifically,

$$\bar{p}_{SL,4}\left(t\,|\,\mathbf{e}_k\right) = T_{13}\left(t\,|\,\mathbf{e}_k\right), \bar{p}_{SL,5}\left(t\,|\,\mathbf{e}_k\right) = T_{14}\left(t\,|\,\mathbf{e}_k\right) \text{ and } \bar{p}_{WL,2}\left(t\,|\,\mathbf{e}_k\right) = T_{16}\left(t\,|\,\mathbf{e}_k\right). \quad (10.9)$$

The values for $T_{13}(t|\mathbf{e}_k)$, $T_{14}(t|\mathbf{e}_k)$ and $T_{16}(t|\mathbf{e}_k)$ for the LHS indicated in Eq. (10.2) are shown in Fig. 16.

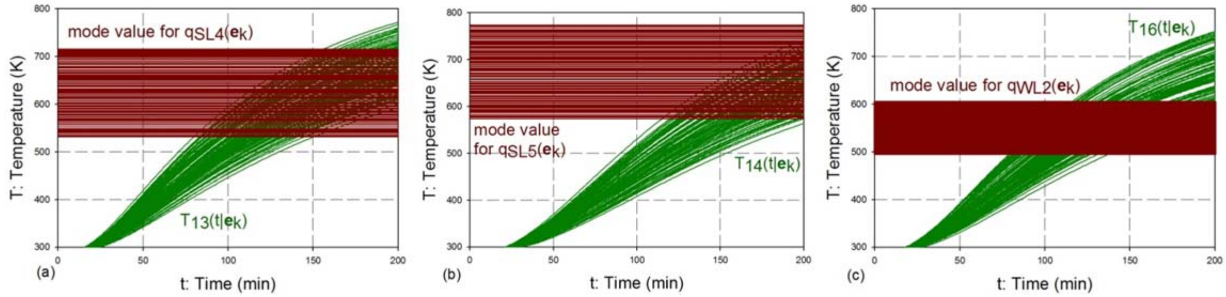

Fig. 16. Values for temperatures $\bar{p}_{SL,4}(t \mid \mathbf{e}_k) = T_{13}(t|\mathbf{e}_k)$, $\bar{p}_{SL,5}(t \mid \mathbf{e}_k) = T_{14}(t|\mathbf{e}_k)$ and $\bar{p}_{WL,2}(t \mid \mathbf{e}_k) = T_{16}(t|\mathbf{e}_k)$ and modes for aleatory distributions of $q_{SL,4}(t \mid \beta_{SL,4}, MBSL4_k)$, $q_{SL,5}(t \mid \beta_{SL,5}, MBSL5_k)$, and $q_{WL,2}(t \mid \beta_{WL,2}, MBWL2_k)$ for elements $\mathbf{e}_k$, $k = 1, 2, \ldots, 100$, of LHS in Eq. (10.2): (a) $\bar{p}_{SL,4}(t \mid \mathbf{e}_k) = T_{13}(t|\mathbf{e}_k)$ and mode for $q_{SL,4}(t \mid \beta_{SL,4}, MBSL4_k)$, (b) $\bar{p}_{SL,5}(t \mid \mathbf{e}_k) = T_{14}(t|\mathbf{e}_k)$ and mode for $q_{SL,5}(t \mid \beta_{SL,5}, MBSL5_k)$, and (c) $\bar{p}_{WL,2}(t \mid \mathbf{e}_k) = T_{16}(t|\mathbf{e}_k)$ and mode for $q_{WL,2}(t \mid \beta_{WL,2}, MBWL2_k)$.

As just described, the base physical properties $\bar{p}_{SL,4}(t \mid \mathbf{e})$, $\bar{p}_{SL,5}(t \mid \mathbf{e})$ and $\bar{p}_{WL,2}(t \mid \mathbf{e})$, for SL 4, SL 5 and WL 2 are epistemically uncertain. As indicated in Eq. (10.7), the base failure values $\bar{q}_{SL,4}(t)$, $\bar{q}_{SL,5}(t)$ and $\bar{q}_{WL,2}(t)$ for SL 4, SL 5 and WL 2 have fixed values of 623 K, 673 K and 550 K, respectively. However, the triangular aleatory distributions for $\beta_{SL,4}$, $\beta_{SL,5}$ and $\beta_{WL,2}$ on [0.85, 1.15], [0.85, 1.15] and [0.9, 1.1], respectively, have epistemically uncertain modes *MBSL4*, *MBSL5* and *MBWL2* with uniform distributions on the corresponding intervals [0.85, 1.15], [0.85, 1.15] and [0.9, 1.1] (see Table 8). In addition to $\bar{p}_{SL,4}(t \mid \mathbf{e})$, $\bar{p}_{SL,5}(t \mid \mathbf{e})$ and $\bar{p}_{WL,2}(t \mid \mathbf{e})$, the modes

$$MBSL4_k \bar{q}_{SL,4}(t) = MBSL4_k\,(623\ K), \tag{10.10}$$

$$MBSL5_k \bar{q}_{SL,5}(t) = MBSL5_k\,(673\ K) \tag{10.11}$$

and

$$MBWL2_k \bar{q}_{WL,2}(t) = MBWL2_k\,(550\ K) \tag{10.12}$$

for the distributions of $q_{SL,4}(t \mid \beta_{SL,4}, MBSL4_k)$, $q_{SL,5}(t \mid \beta_{SL,5}, MBSL5_k)$ and $q_{WL,2}(t \mid \beta_{WL,2}, MBWL2_k)$ are also shown in Fig. 16.

Each element $\mathbf{e}_k$ of the LHS indicated in Eq. (10.2) produces a set of results of the form shown in Fig. 8 and Fig. 9 for a total of $nLHS = 100$ sets of results. As an example, the failure time CDFs $CDF_{SL,4}(t \mid \mathbf{e}_k)$, $CDF_{SL,5}(t \mid \mathbf{e}_k)$ and $CDF_{WL,2}(t \mid \mathbf{e}_k)$ for SL 4, SL 5 and WL 2 and also the value $pF_2(t|\mathbf{e}_k)$ for PLOAS are shown in Fig. 17. The spread of the results in Fig. 17 provides a representation for the epistemic uncertainty present in the estimates for $CDF_{SL,4}(t\,|\,\mathbf{e})$, $CDF_{SL,5}(t\,|\,\mathbf{e})$, $CDF_{WL,2}(t\,|\,\mathbf{e})$ and $pP_2(t|\mathbf{e})$.

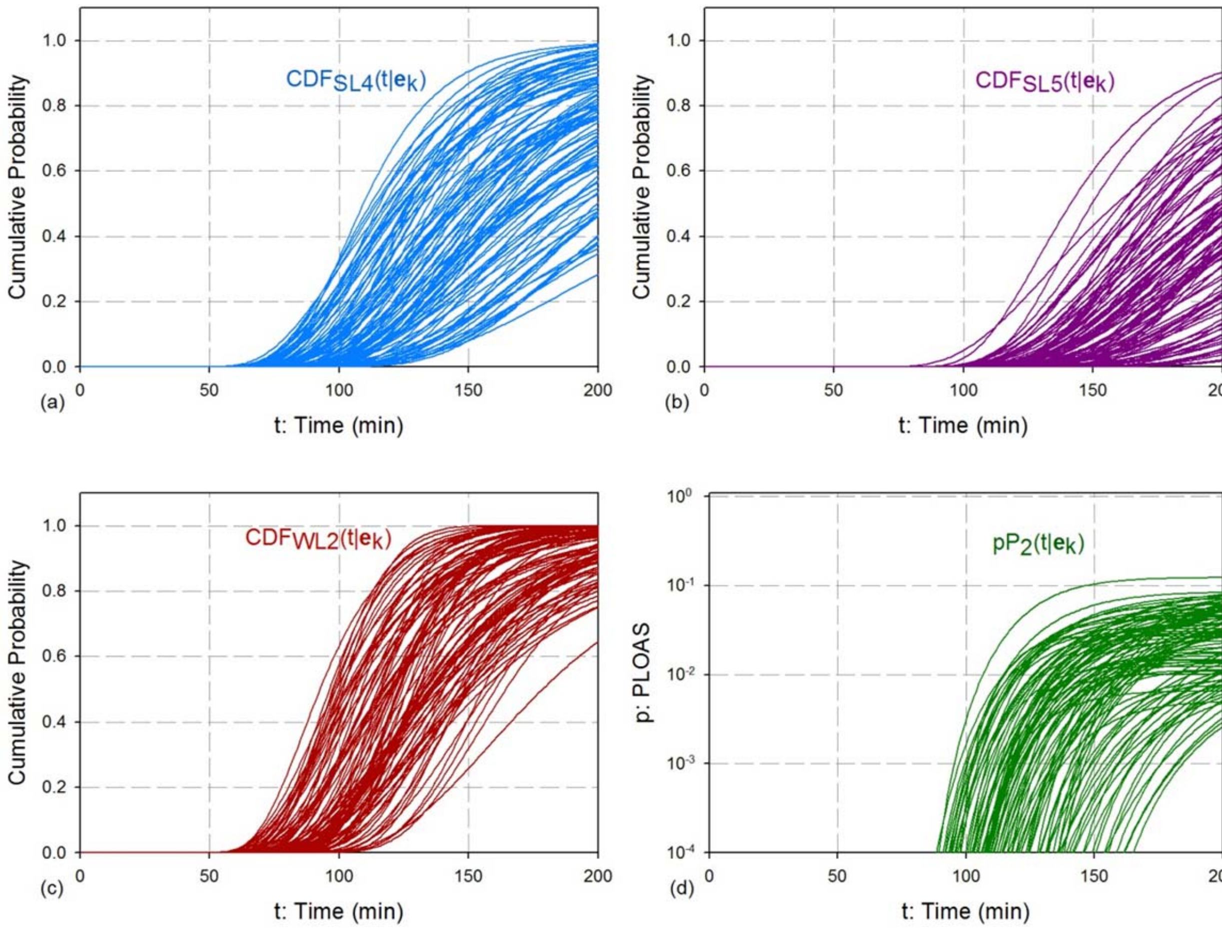

Fig. 17. Failure time CDFs and probability of LOAS for Failure Pattern 2 and elements $\mathbf{e}_k$, $k = 1, 2, \ldots, 100$, of LHS in Eq. (10.2): (a) $CDF_{SL,4}(t\,|\,\mathbf{e}_k)$, (b) $CDF_{SL,5}(t\,|\,\mathbf{e}_k)$, (c) $CDF_{WL,2}(t\,|\,\mathbf{e}_k)$, and (d) $pP_2(t\,|\,\mathbf{e}_k)$.

As discussed in Sect. 7, an alternate approach to determining $pF_1(t)$ for Case 1 in Table 1, and hence for determining $pP_2(t|\mathbf{e}_k)$ for Failure Pattern 2, is to precalculate the CDF $CDF_{SL}(t)$ for the failure of all SLs as indicated in Eq. (7.1) and then calculate $pF_1(t)$ as indicated in Eq. (7.2). For illustration, the resultant values of $CDF_{SL}(t\,|\,\mathbf{e}_k)$ for Failure Pattern 2 are shown in Fig. 18. For Failure Pattern 2, the general representation for $pF_1(t)$ in Eq. (7.2) specializes to the representation for $pP_2(t)$ in Eq. (9.20). Use of the CDFs $CDF_{SL}(t\,|\,\mathbf{e}_k)$ shown in Fig. 18 in conjunction with the representation for $pP_2(t)$ in Eq. (9.20) and use of the representation for $pF_1(t)$ in Table 1 with $nWL = 1$ and $nSL = 2$ produce the same set of values shown in Fig. 17d.

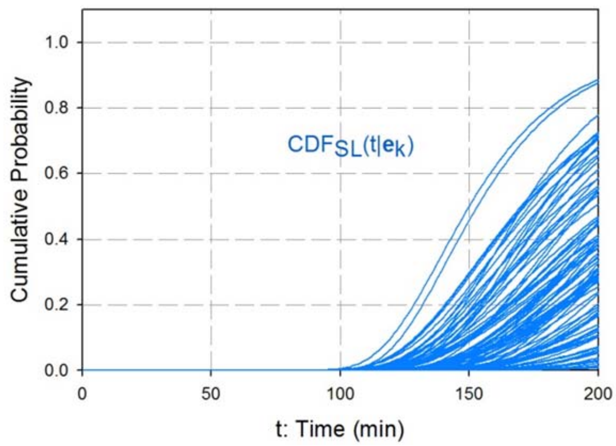

Fig. 18. Failure time CDFs $CDF_{SL}(t\,|\,\mathbf{e}_k)$ for failure of SLs 4 and 5 for Failure Pattern 2 and elements $\mathbf{e}_k$, $k = 1, 2, \ldots, 100$, of LHS in Eq. (10.2).

10.3 Failure Pattern 3: Aleatory and Epistemic Uncertainty

For Failure Pattern 3, LOAS occurs if (i) SL 1, SL 2 or SL 3 fails before WL 1 (i.e., Failure Pattern 1) or (ii) SL 4 and SL 5 both fail before WL 2 (i.e., Failure Pattern 2). As discussed in Sect. 8.3, the probability $pP_3(t\,|\,\mathbf{e}_k)$ of LOAS for Failure Pattern 3 and element $\mathbf{e}_k$ of the LHS in Eq. (10.2) can be obtained from the probabilities $pP_1(t\,|\,\mathbf{e}_k)$ and $pP_2(t\,|\,\mathbf{e}_k)$ for the times at which LOAS occurs for the WL-SL systems indicated in (i) and (ii). The results of this calculation are shown in Fig. 19. The values for $CDF_{SL,i}(t\,|\,\mathbf{e}_k)$, $i = 1, 2, \ldots, 5$, $CDF_{WL,1}(t\,|\,\mathbf{e}_k)$, $CDF_{WL,2}(t\,|\,\mathbf{e}_k)$, $pP_1(t|\mathbf{e}_k)$ and $pP_2(t|\mathbf{e}_k)$ underlying the determination of the values for $pP_3(t\,|\,\mathbf{e}_k)$ in Fig. 19 are shown in Fig. 15 and Fig. 17.

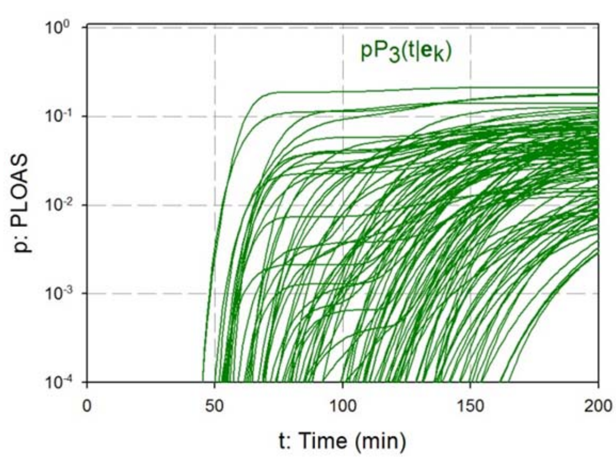

Fig. 19. Probability $pP_3(t|\mathbf{e}_k)$ of LOAS for Failure Pattern 3 for elements $\mathbf{e}_k$, $k = 1, 2, \ldots, 100$, of LHS in Eq. (10.2).

10.4 Failure Pattern 4: Aleatory and Epistemic Uncertainty

For Failure Pattern 4, LOAS occurs if SL 4 and SL 5 both fail before either WL 1 or WL 2 fails. As illustrated in Sect. 9.4, the probability $pP_4(t \mid \mathbf{e}_k)$ of LOAS for Failure Pattern 4 and element $\mathbf{e}_k$ of the LHS in Eq. (10.2) can be calculated with the quadrature procedure indicated in Eq. (4.1). The results of this calculation are shown in Fig. 20. The values for $CDF_{SL,4}(t \mid \mathbf{e}_k)$, $CDF_{SL,5}(t \mid \mathbf{e}_k)$, $CDF_{WL,1}(t \mid \mathbf{e}_k)$ and $CDF_{WL,2}(t \mid \mathbf{e}_k)$ underlying the determination of the values for $pP_4(t \mid \mathbf{e}_k)$ in Fig. 20 are shown in Fig. 15 and Fig. 17.

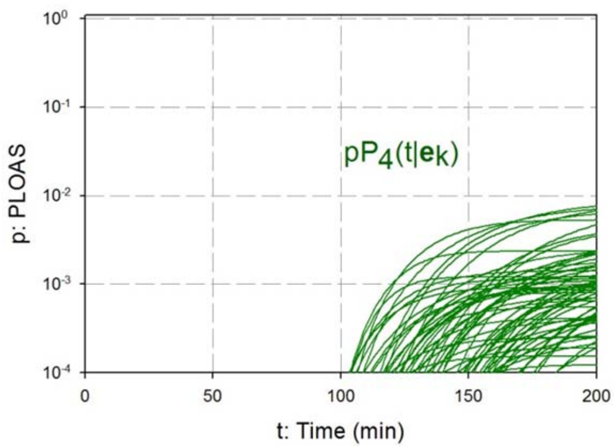

Fig. 20. Probability $pP_4(t|\mathbf{e}_k)$ of LOAS for Failure Pattern 4 for elements $\mathbf{e}_k$, k = 1, 2, …, 100, of LHS in Eq. (10.2).

10.5 Failure Pattern 5: Aleatory and Epistemic Uncertainty

For Failure Pattern 5, LOAS occurs if (i) SL 1, SL 2 or SL 3 fails before WL 1 fails (i.e., Failure Pattern 1) or (ii) SL 4 and SL 5 both fail before WL 1 or WL 2 fails (i.e., Failure Pattern 4). As discussed in Sect. 9.5, it is not possible to obtain the probability $pP_5(t \mid \mathbf{e})$ of LOAS for Failure Pattern 5 from the probabilities $pP_1(t \mid \mathbf{e})$ and $pP_4(t \mid \mathbf{e})$ for LOAS for the failure patterns indicated in (i) and (ii). Instead, $pP_5(t \mid \mathbf{e})$ must be determined as indicated in Eq. (9.34). The results of this calculation are shown in Fig. 21. The values for $CDF_{SL,i}(t \mid \mathbf{e}_k)$, i = 1, 2, …, 5, $CDF_{WL,1}(t \mid \mathbf{e}_k)$ and $CDF_{WL,2}(t \mid \mathbf{e}_k)$ underlying the determination of the values for $pP_5(t \mid \mathbf{e}_k)$ in Fig. 21 are shown in Fig. 15 and Fig. 17.

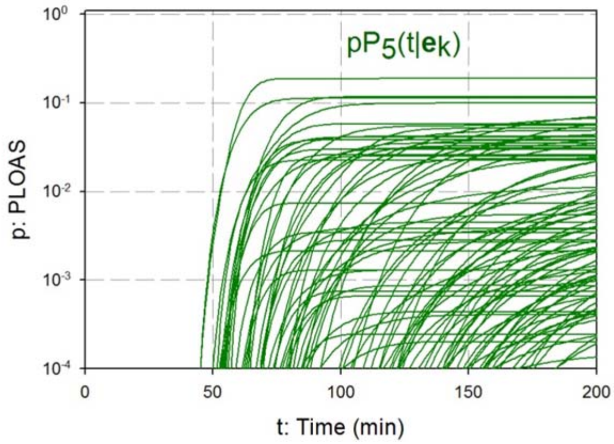

Fig. 21. Probability $pP_5(t|\mathbf{e}_k)$ of LOAS for Failure Pattern 5 for elements $\mathbf{e}_k$, $k = 1, 2, \ldots, 100$, of LHS in Eq. (10.2).

11. Examples Involving Mixtures of Aleatory and Epistemic Uncertainty

The examples in Sect. 9 involve aleatory uncertainty in both link properties and link failure values and no epistemic uncertainty in these quantities, and the examples in Sect. 10 involve aleatory and epistemic uncertainty in both link properties and link failure values. The following additional possibilities are illustrated in this section for the failure pattern involving two SLs and one WL considered in Sects. 9.2 and 10.2 (i.e., Failure Pattern 2): (i) only epistemic uncertainty in link properties and both aleatory and epistemic uncertainty in link failure values, (ii) both aleatory and epistemic uncertainty in link properties and only epistemic uncertainty in link failure values, (iii) only epistemic uncertainty in SL properties and failure values and aleatory and epistemic uncertainty in WL properties and failure values, (iv) aleatory and epistemic uncertainty in SL properties and failure values and only epistemic uncertainty in WL properties and failure values, and (iv) only epistemic uncertainty in link properties and failure values.

11.1 Only Epistemic Uncertainty in Link Properties and Both Aleatory and Epistemic Uncertainty in Link Failure Values

The intermediate analysis results indicated in Fig. 16 are unchanged in this example. Specifically, (i) no aleatory uncertainty is assumed around the temperature curves for each LHS element, and (ii) as in Sect. 10.2, aleatory uncertainty around the failure values is assumed. In turn, the preceding assumptions result in changed values for the link failure time CDFs and the probability of LOAS for Failure Pattern 2 (Fig. 22). Specifically, SL 1 and WL 2 fail earlier than shown in Fig. 17a,c when aleatory uncertainty is included in link properties, and PLOAS values $pP_2(t\,|\,\mathbf{e}_k)$ are smaller than shown in Fig. 17d. The decrease in PLOAS values results primarily from earlier failures for WL 2.

11.2 Both Aleatory and Epistemic Uncertainty in Link Properties and Only Epistemic Uncertainty in Link Failure Values

As for the example in Sect. 11.1, the intermediate analysis results indicated in Fig. 16 are unchanged in this example. Specifically, (i) as in Sect. 10.2, aleatory uncertainty is assumed around the temperature curves for each LHS element, and (ii) no aleatory uncertainty is assumed around the median failure values. For illustration in this example, the 100 median failure values for each link in Fig. 16 are being treated as epistemically uncertain failure values about which there is no aleatory uncertainty (i.e., variability). In turn, the preceding assumptions result in changed values for the link failure time CDFs and the probability of LOAS for Failure Pattern 2 (Fig. 23). Specifically, the failure times for WL 2 in Fig. 23c tend to be later than the failure times for WL 2 in Fig. 22c, with the result that the PLOAS values $pP_2(t\,|\,\mathbf{e}_k)$ in Fig. 23d tend to be significantly larger than the PLOAS values in Fig. 22d.

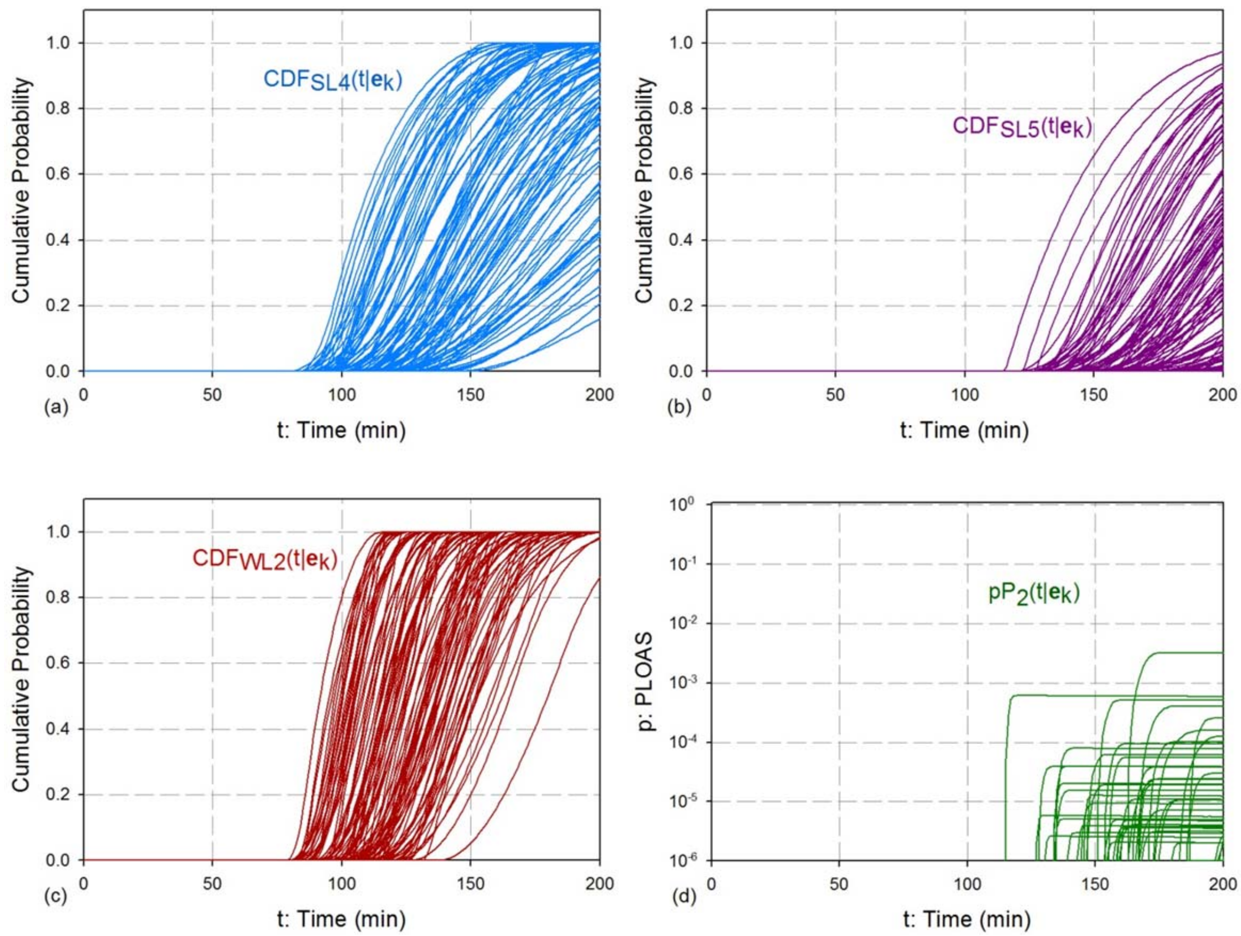

Fig. 22. Failure time CDFs and probability of LOAS for Failure Pattern 2 and elements $\mathbf{e}_k$, $k = 1, 2, \ldots, 100$, of LHS in Eq. (10.2) with only epistemic uncertainty in link properties (i.e., temperatures) and both aleatory and epistemic uncertainty in link failure values (i.e., failure temperatures): (a) $CDF_{SL,4}(t \mid \mathbf{e}_k)$, (b) $CDF_{SL,5}(t \mid \mathbf{e}_k)$, (c) $CDF_{WL,2}(t \mid \mathbf{e}_k)$, and (d) $pP_2(t \mid \mathbf{e}_k)$.

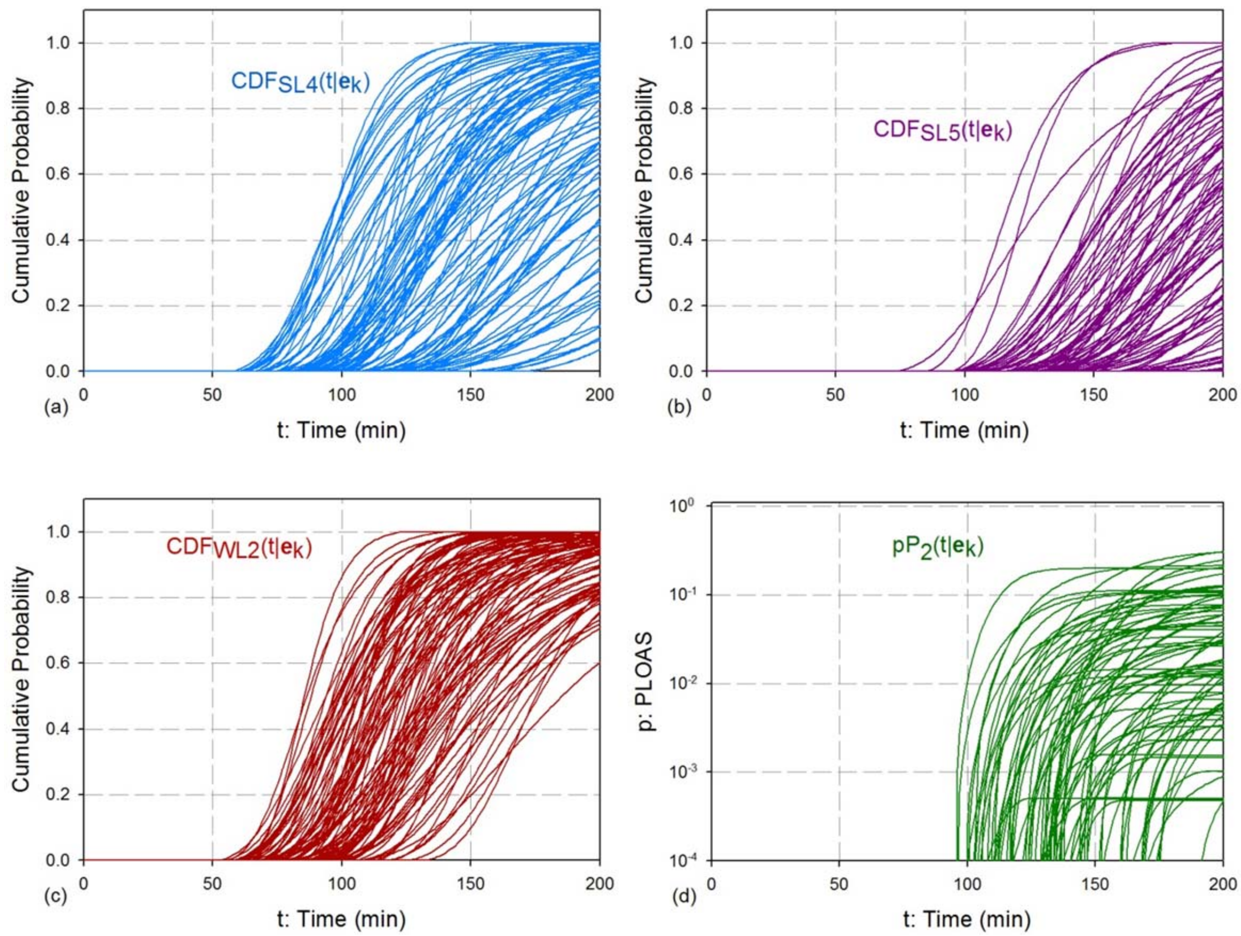

Fig. 23. Failure time CDFs and probability of LOAS for Failure Pattern 2 and elements $\mathbf{e}_k$, $k = 1, 2, \ldots, 100$, of LHS in Eq. (10.2) with aleatory and epistemic uncertainty in link properties (i.e., temperatures) and only epistemic uncertainty in link failure values (i.e., failure temperatures): (a) $CDF_{SL,4}(t \mid \mathbf{e}_k)$, (b) $CDF_{SL,5}(t \mid \mathbf{e}_k)$, (c) $CDF_{WL,2}(t \mid \mathbf{e}_k)$, and (d) $pP_2(t \mid \mathbf{e}_k)$.

11.3 Only Epistemic Uncertainty in SL Properties and Failure Values and Aleatory and Epistemic Uncertainty in WL Properties and Failure Values

As for the examples in Sects. 11.1 and 11.2, the intermediate results in Fig. 16 remain unchanged. However, no aleatory uncertainty is assumed in the temperatures and failure values for SLs 4 and 5. Specifically, the epistemically uncertain temperature curves and failure values are assumed to be as shown in Fig. 16a,b, with the result that there is one temperature curve and one failure value for each SL and LHS element. In turn, this results in (i) a single failure time for each SL and LHS element and (ii) corresponding failure time CDFs that jump from 0 to 1.0 at this single failure time as shown in Fig. 24a,b for SLs 4 and 5. The same aleatory and epistemic uncertainty properties are assumed for WL 2 as for the example in Sect. 10.2 (Fig. 17c, Fig. 24c).

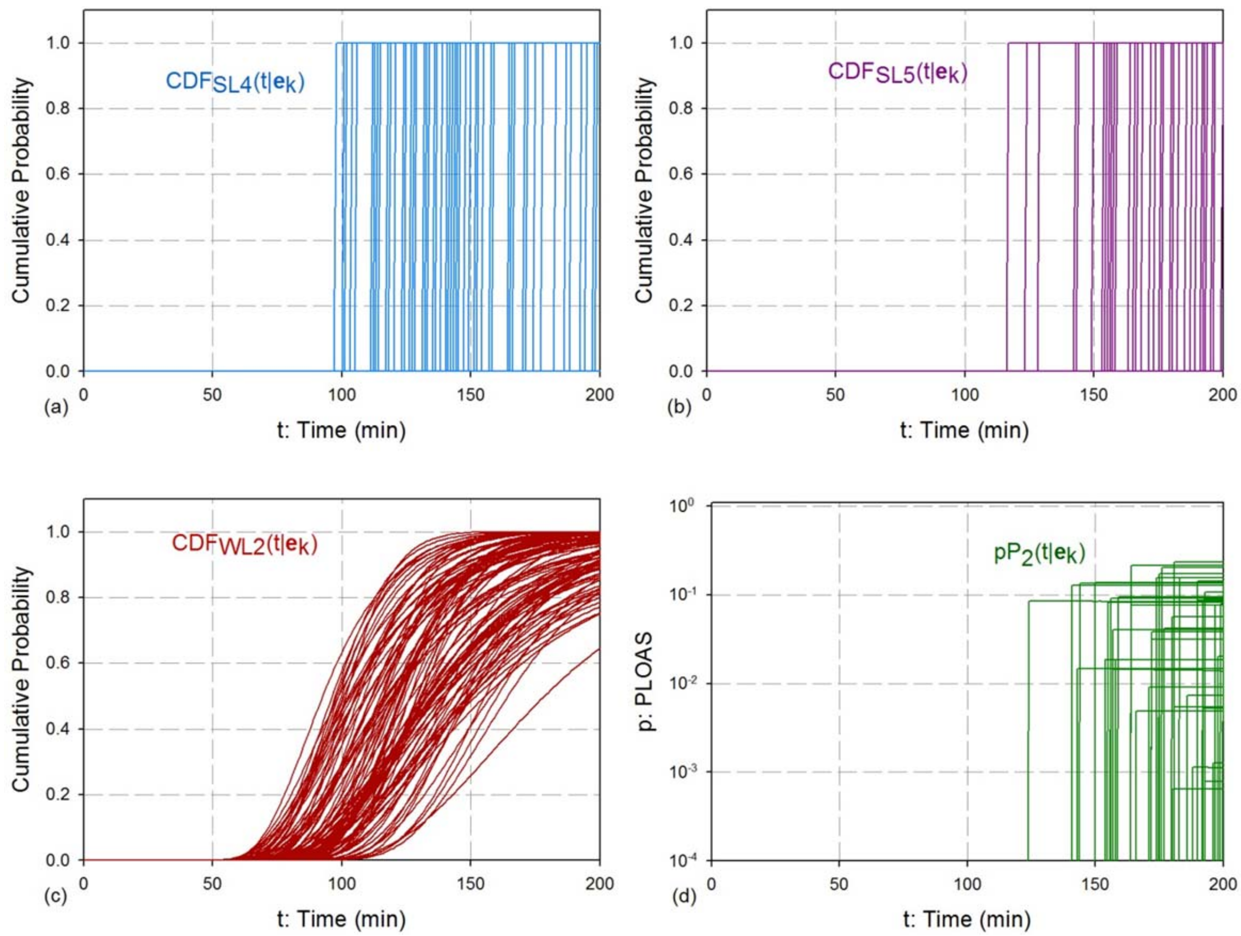

Fig. 24. Failure time CDFs and probability of LOAS for Failure Pattern 2 and elements $\mathbf{e}_k$, $k = 1, 2, \ldots, 100$, of LHS in Eq. (10.2) with only epistemic uncertainty in SL properties (i.e., temperatures) and failure values (i.e., failure temperatures) and aleatory and epistemic uncertainty in WL properties (i.e., temperatures) and failure values (i.e., failure temperatures): (a) $CDF_{SL,4}(t \mid \mathbf{e}_k)$, (b) $CDF_{SL,5}(t \mid \mathbf{e}_k)$, (c) $CDF_{WL,2}(t \mid \mathbf{e}_k)$, and (d) $pP_2(t \mid \mathbf{e}_k)$.

The PLOAS values $pP_2(t \mid \mathbf{e}_k)$ in Fig. 24d jump from 0 to a constant value at the time at which both SLs have failed; the height of this jump corresponds to the probability that WL 2 has failed prior to the failure of both SLs. If WL 2 has failed with probability 1.0 prior to the failure of both SLs, then $pP_2(t \mid \mathbf{e}_k) = 0$ for the time interval under consideration (i.e., $0 \le t \le 200$ min).

11.4 Aleatory and Epistemic Uncertainty in SL Properties and Failure Values and Only Epistemic Uncertainty in WL Properties and Failure Values

This example is the reverse of the example in Sect. 11.3. Specifically, the results shown in Fig. 16c are assumed to characterize the epistemic uncertainty in the temperature curves and failure values for WL 2; in contrast, the results in Fig. 16a,b are assumed to characterize the epistemic uncertainty in the temperature curves and failure values for SLs 4 and 5 in Sect. 11.3. The same aleatory and epistemic uncertainty properties are assumed for SLs 4 and 5 as for the example in Sect. 10.2 (Fig. 17a,b and Fig. 25a,b); in contrast, the results in Fig. 17c were assumed the characterize the aleatory and epistemic uncertainty properties for WL 2 in Sect. 11.3. As for SLs 4 and 5 in Sect. 11.3, the failure time CDFs for WL 2 jump from 0 to 1.0 at single point in time (Fig. 25c). The leveling off of the PLOAS values $pP_2(t \mid \mathbf{e}_k)$ in Fig. 25d occurs when the failure time CDFs for WL 2 jump from 0 to 1.0. Prior to this time,

$$pP_2(t \mid \mathbf{e}_k) = CDF_{SL}(t \mid \mathbf{e}_k), \tag{11.1}$$

where $CDF_{SL}(t \mid \mathbf{e}_k)$ is the failure time CDF for the failure of SLs 4 and 5 (Fig. 18). The preceding equality holds because the probability of WL failure is 0 prior to the leveling off of $pP_2(t \mid \mathbf{e}_k)$.

11.5 Only Epistemic Uncertainty in Link Properties and Link Failure Values

Again, the intermediate analysis results indicated in Fig. 16 are unchanged in this example. However, now only epistemic uncertainty in link properties and failure values is assumed. As a result, the failure time CDFs for SLs 4 and 5 are the same as in Fig. 24a,b, and the failure time CDFs for WL 2 are the same as in Fig. 25c. In turn, these failure time CDFs result in $pP_2(t \mid \mathbf{e}_k)$ = 0 for all sample elements $\mathbf{e}_k$, $k = 1, 2, \ldots, 100$, of LHS in Eq. (10.2). Thus, the probability of LOAS (i.e., PLOAS) for this example is zero. Two important properties are illustrated by this example.

First, the presence of correlations between analysis outcomes can be very important in the determination of PLOAS. A cursory examination of the failure time CDFs in Fig. 24a,b and Fig. 25c shows some of the WL failure times to be greater than some of the SL failure times. This initially suggests that that some of the PLOAS values should be nonzero. However, this is not the case because the link temperatures and associated PLOAS values are calculated conditional on individual LHS sample elements, with the result that there is a strong correlation between the temperatures that SLs 4 and 5 experience and the temperatures that the WL 2 experiences. As a result, the SL and WL CDFs in Fig. 24a,b and Fig. 25c cannot be randomly combined to obtain a distribution of PLOAS values. As illustrated in this example, it is essential that appropriate correlations between WL and SL properties be maintained if meaningful PLOAs results are to be obtained.

Second, the presence of relatively small amounts of aleatory uncertainty has potential to have large effects on PLOAS values (e.g., see Fig. 8 for an illustration of aleatory uncertainty for Failure Pattern 2). In this example, the removal of aleatory uncertainty resulted in all PLOAS values being zero. In contrast, several different mixtures of aleatory and epistemic always resulted in at least some LHS elements having nonzero PLOAS values and also in wide ranges of nonzero PLOAS values (Fig. 26). Given the wide range of possible conditions for an accident involving a high consequence system in a fire, careful thought must be given to the manner in which aleatory uncertainty is to be defined and quantified in an analysis intended to determine meaningful PLOAS values. As suggested by the results in Fig. 26, the definition and quantification of aleatory uncertainty can have large effects on the outcome of an analysis. As illustrated in Sect. 10, the same is also true of the definition and quantification of epistemic uncertainty.

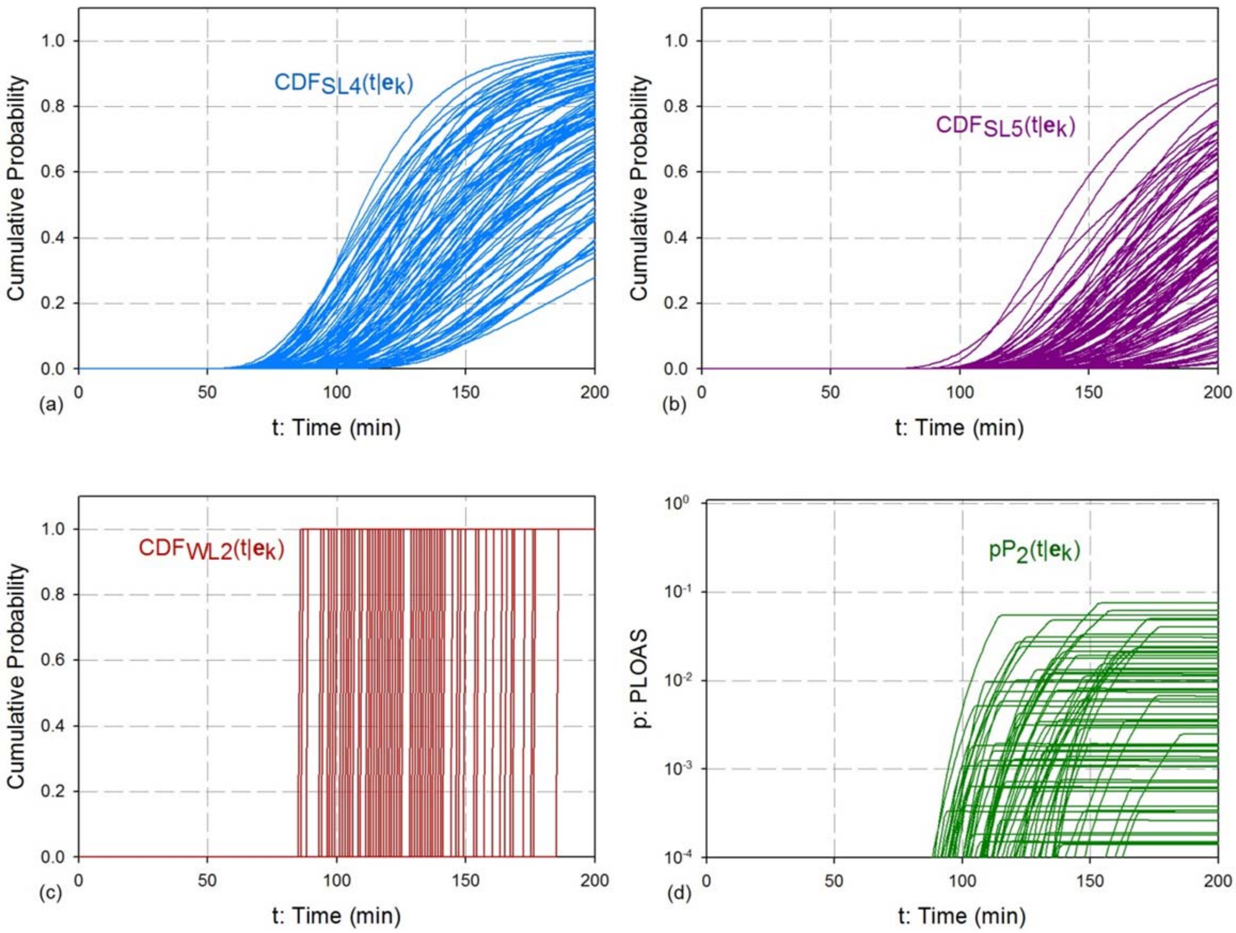

Fig. 25. Failure time CDFs and probability of LOAS for Failure Pattern 2 and elements $\mathbf{e}_k$, $k = 1, 2, \ldots, 100$, of LHS in Eq. (10.2) with aleatory and epistemic uncertainty in SL properties (i.e., temperatures) and failure values (i.e., failure temperatures) only epistemic uncertainty in WL properties (i.e., temperatures) and failure values (i.e., failure temperatures): (a) $CDF_{SL,4}(t \mid \mathbf{e}_k)$, (b) $CDF_{SL,5}(t \mid \mathbf{e}_k)$, (c) $CDF_{WL,2}(t \mid \mathbf{e}_k)$, and (d) $pP_2(t \mid \mathbf{e}_k)$.

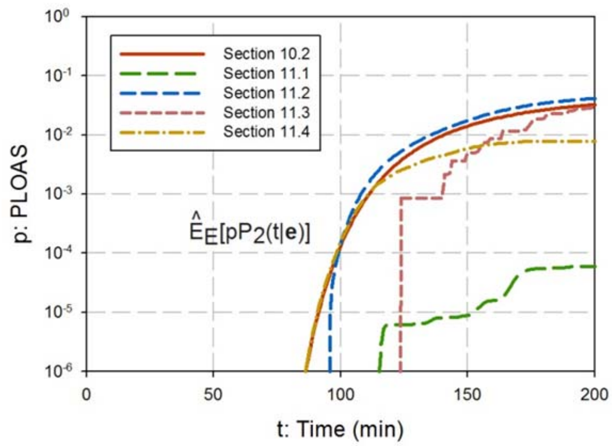

Fig. 26. Estimated expected values $\hat{E}_E[pP_2(t \mid \mathbf{e})]$ over epistemic uncertainty for probabilities of LOAS for Failure Pattern 2 for the treatments of aleatory and epistemic uncertainty in Sects. 10.2 and 11.1-11.4.

12. Summary Discussion

Representations for PLOAS for four general configurations of WL/SL systems are developed: (i) Failure of all SLs before failure of any WL, (ii) Failure of any SL before failure of any WL, (iii) Failure of all SLs before failure of all WLs, and (iv) Failure of any SL before failure of all WLs (Table 1). For these general representations, the failure times for the WLs and SLs are assumed to be independent. In addition, one example is included for two WLs and five SLs where a dependency exists due to the presence of the same WL in two different subsystems.

The presented representations for PLOAS are developed for analysis contexts in which both link physical properties (e.g., temperature, pressure, …) and link failure properties (e.g., failure temperature, failure pressure, …) are (i) time dependent and (ii) exhibit random (i.e., aleatory) behavior. Here, aleatory uncertainty is being used in the designation of random behavior in the evolution of accident conditions that is known to exist but is outside the details of the physical modeling of the accident under considerations (e.g., wind speed and wind direction at the time of an accident involving a fire).

The presented PLOAS representations are developed under the assumption that external calculations with what will generally be complex and computationally demanding models will supply the time-dependent link properties used in the determination of PLOAS. In turn, the presented PLOAS representations take these link properties and the distributions characterizing aleatory uncertainty as input to (i) a formal structure that defines PLOAS and (ii) an associated computational procedure that determines time-dependent values for PLOAS. The formal structure that defines PLOAS is based on the assumptions that (i) time-dependent link physical properties are nondecreasing, (ii) time-dependent link failure properties are nonincreasing, and (iii) aleatory uncertainty in link properties can be defined by a multiplier on the original precalculated link properties.

Both quadrature procedures (Sect. 4) and sampling-based (i.e., Monte Carlo) procedures (Sect. 5) for the numerical evaluation of PLOAS are presented. The quadrature procedures are more numerically efficient than the presented sampling-based procedures. Thus, it is anticipated that the quadrature procedures will usually be used in the numerical evaluation of PLOAS.

Appropriate verification procedures are an important part of any analysis that supports important decisions [25-32]. It is anticipated that the primary use of the indicated sampling-based procedures for the numerical evaluation of PLOAS will be in the verification of the conceptual definition and computational implementation of the quadrature procedures for the numerical evaluation of PLOAS. The sampling-based procedures provide effective verification tests because their implementation is, to a significant extent, independent of the implementation of the quadrature procedures. More specifically, two different sampling-based procedures are presented that differ in the extent to which their implementation overlaps with the implementation of the quadrature procedures for the numerical evaluation of PLOAS. Presented comparisons of PLOAS results for quadrature and sampling-based procedures are in agreement, which helps provide confidence that the calculations are correctly implemented.

In addition to verification tests based on comparing PLOAS results obtained with quadrature and sampling-based procedures, an effective verification test based on known PLOAS values is also available and illustrated. In this procedure, each link is assigned the same properties and hence the same CDF for failure time, with the result that PLOAS has a known value that is a function of the number of WLs and SLs involved and the particular failure pattern under consideration (see Table 1; also, Refs. [9; 10]). Although this assignment of WL and SL properties is not physically realistic, its value as a verification test lies in the fact that it entails exercising all the numerics involved in the determination of PLOAS for situations where the correct value for PLOAS is known (e.g., see Table 3).

Realistic analyses for PLOAS will involve both aleatory uncertainty and epistemic uncertainty. The procedures described in this presentation involve a direct incorporation of aleatory uncertainty into PLOAS results based on a scaling of precalculated link physical properties and link failure properties. Epistemic uncertainty can be present in both (i) the precalculated link physical properties and link failure properties and (ii) the parameters that define the distributions that characterize aleatory uncertainty. It is anticipated that epistemic uncertainty will be incorporated into analyses for PLOAS with sampling-based procedures (e.g., Latin hypercube sampling [21; 22]), where the associated sample includes variables affecting link physical properties and link failure properties and also variables affecting the characterization of aleatory uncertainty. In this situation, the model or models that determine link physical properties and link failure properties will be initially run for each sample element. Then, the results of these calculations will be supplied to the program that uses these results and the sampled values for variables affecting the characterization of aleatory uncertainty to determine PLOAS values for each sample element. The result of this sequence of calculations is a mapping between epistemically uncertain analysis inputs and PLOAS values that provides both (i) a representation of the epistemic uncertainty present in the estimation of PLOAS and (ii) a basis for performing sensitivity analyses to determine the effects individual epistemically uncertain input variables on the epistemic uncertainty present in estimates for PLOAS.

A number of examples are presented to illustrate PLOAS calculations with (i) only aleatory uncertainty (Sect. 9), (ii) aleatory and epistemic uncertainty (Sect. 10), and (iii) various mixtures of aleatory and epistemic uncertainty (Sect. 11). These examples involve a notional system in a fire defined by a system of ordinary differential equations (Sect. 8) and five different WL-SL failure patterns, where LOAS occurs if (i) SL 1, SL 2 or SL 3 fails before WL 1 fails, (ii) SL 4 and SL 5 both fail before WL 2 fails, (iii) SL 1, SL 2 or SL 3 fails before WL 1 fails or SL 4 and SL 5 both fail before WL 2 fails, (iv) SL 4 and SL 5 both fail before WL 1 or WL 2 fails, and (v) SL 1, SL 2 or SL 3 fails before WL 1 fails or SL 4 and SL 5 both fail before WL 1 or WL 2 fails. Examination of these examples helps provide perspective on what the results in a real PLOAS might look like and how such results might be displayed.

Sensitivity analyses based on stepwise rank regression were tried on the PLOAS results in Sect. 9 obtained with aleatory uncertainty and epistemic uncertainty. Although this is a common and often successfully used technique for sensitivity analysis [33], it did not perform very well on these results due to the strong correlations between variables affecting the properties of individual links and the interaction of variables affecting PLOAS values. Successful sensitivity analyses for PLOAS results in this study and in similar, but more complex, studies will require more sophisticated sensitivity analysis procedures. An approach to sensitivity analysis for PLOAS results that is likely to be successful is to (i) initially fit a metamodel to the PLOAS results using a nonparametric construction procedure [34-36] and (ii) then perform a stepwise variance decomposition of the constructed metamodel as illustrated in Table 11 of Ref. [36]. This procedure is more effective in appropriately assessing the effects of variable interactions than traditional parametric regression procedures. Specifically, this procedure allows a stepwise identification of variable importance that incorporates both individual variable effects and interaction effects of multiple variables. In the stepwise procedure, the most important variable is selected first; then the next most important variable is selected; and so on until some appropriate stopping criterion is met.

A program (i.e., CPLOAS_2) that implements the PLOAS calculations described in this presentation and an associated user's manual [20] are available.

This page intentionally left blank.

13. References

1. Plummer DW, Greenwood WH. The History of Nuclear Weapon Safety Devices. In. *Paper no. AIAA-1998-3464. AIAA/ASME/SAE/ASEE 34th Joint Propulsion Conference and Exhibit, Cleveland, OH, July 13-15, 1998*. Reston, VA: American Institute of Aeronautics and Astronautics, 1998.
2. Caldwell M, D'Antonio PE. A Study of Using Electronics for Nuclear Weapon Detonation Safety. In. *Paper no. AIAA-1998-3465. AIAA/ASME/SAE/ASEE 34th Joint Propulsion Conference and Exhibit, Cleveland, OH, July 13-15, 1998*. Reston, VA: American Institute of Aeronautics and Astronautics, 1998.
3. Winter WL, Covan JM, Dalton LJ. Passive Safety in High-Consequence Systems. *Computer* 1998; 31(4):35-37.
4. D'Antonio PE. Surety Principles Development and Integration for Nuclear Weapons. In: D Isbell, ed. *High Consequence Operations Safety Symposium II, SAND98-1557*. Albuquerque, NM: Sandia National Laboratories, 1998:141-149.
5. Demmie PN. A First-Principle Based Approach to Quantitative Assessment of Nuclear-Detonation Safety. In: D Isbell, ed. *High Consequence Operations Safety Symposium II, SAND98-1557*. Albuquerque, NM: Sandia National Laboratories, 1998:325-341.
6. Jones M. The Role of Microelectronics and Software in a Very High Consequence System. In: D Isbell, ed. *High Consequence Operations Safety Symposium II, SAND98-1557*. Albuquerque, NM: Sandia National Laboratories, 1998:411-429.
7. Helton JC, Johnson JD, Oberkampf WL. Probability of Loss of Assured Safety in Temperature Dependent Systems with Multiple Weak and Strong Links. *Reliability Engineering and System Safety* 2006; 91(3):320-348.
8. Helton JC, Johnson JD, Oberkampf WL. Effect of Delayed Link Failure on Probability of Loss of Assured Safety in Temperature-Dependent Systems with Multiple Weak and Strong Links. *Reliability Engineering & System Safety* 2009; 94(2):294-310.
9. Helton JC, Johnson JD, Oberkampf WL. Verification of the Calculation of Probability of Loss of Assured Safety in Temperature Dependent Systems with Multiple Weak and Strong Links. *Reliability Engineering and System Safety* 2007; 92:1363-1373.
10. Helton JC, Johnson JD, Oberkampf WL. Verification Test Problems for the Calculation of Probability of Loss of Assured Safety in Temperature Dependent Systems with Multiple Weak and Strong Links. *Reliability Engineering and System Safety* 2007; 92:1374-1387.
11. Parry GW. The Characterization of Uncertainty in Probabilistic Risk Assessments of Complex Systems. *Reliability Engineering and System Safety* 1996; 54(2-3):119-126.
12. Parry GW, Winter PW. Characterization and Evaluation of Uncertainty in Probabilistic Risk Analysis. *Nuclear Safety* 1981; 22(1):28-42.
13. Apostolakis G. The Concept of Probability in Safety Assessments of Technological Systems. *Science* 1990; 250(4986):1359-1364.
14. Helton JC. Treatment of Uncertainty in Performance Assessments for Complex Systems. *Risk Analysis* 1994; 14(4):483-511.
15. Helton JC, Burmaster DE. Guest Editorial: Treatment of Aleatory and Epistemic Uncertainty in Performance Assessments for Complex Systems. *Reliability Engineering and System Safety* 1996; 54(2-3):91-94.

16. Helton JC. Uncertainty and Sensitivity Analysis in the Presence of Stochastic and Subjective Uncertainty. *Journal of Statistical Computation and Simulation* 1997; 57(1-4):3-76.
17. Paté-Cornell ME. Uncertainties in Risk Analysis: Six Levels of Treatment. *Reliability Engineering and System Safety* 1996; 54(2-3):95-111.
18. Parzen E. *Modern Probability Theory and Its Applications*. New York, NY: John Wiley & Sons; 1960.
19. Press WH, Teukolsky SA, Vetterling WT, Flannery BP. *Numerical Recipes in FORTRAN: The Art of Scientific Computing*, 2nd edn. Cambridge: Cambridge University Press; 1992.
20. Sallaberry CJ, Helton JC. *CPLOAS_2 User Manual*. SAND2012-9305. Albuquerque, NM: Sandia National Laboratories; 2013.
21. McKay MD, Beckman RJ, Conover WJ. A Comparison of Three Methods for Selecting Values of Input Variables in the Analysis of Output from a Computer Code. *Technometrics* 1979; 21(2):239-245.
22. Helton JC, Davis FJ. Latin Hypercube Sampling and the Propagation of Uncertainty in Analyses of Complex Systems. *Reliability Engineering and System Safety* 2003; 81(1):23-69.
23. Iman RL, Conover WJ. A Distribution-Free Approach to Inducing Rank Correlation Among Input Variables. *Communications in Statistics: Simulation and Computation* 1982; B11(3):311-334.
24. Iman RL, Davenport JM. Rank Correlation Plots for Use with Correlated Input Variables. *Communications in Statistics: Simulation and Computation* 1982; B11(3):335-360.
25. American Institute of Aeronautics and Astronautics. *AIAA Guide for the Verification and Validation of Computational Fluid Dynamics Simulations*. AIAA G-077- 1998. Reston, VA: American Institute of Aeronautics and Astronautics; 1998.
26. Roache PJ. *Verification and Validation in Computational Science and Engineering*. Albuquerque, NM: Hermosa Publishers; 1998.
27. Oberkampf WL, Trucano TG. Verification and Validation in Computational Fluid Dynamics. *Progress in Aerospace Sciences* 2002; 38(3):209-272.
28. Oberkampf WL, Trucano TG, Hirsch C. Verification, Validation, and Predictive Capability in Computational Engineering and Physics. *Applied Mechanics Review* 2004; 57(5):345-384.
29. Roache PJ. Building PDE Codes to be Verifiable and Validatable. *Computing in Science & Engineering* 2004; 6(5):30-38.
30. Babuska I, Oden JT. Verification and Validation in Computational Engineering and Science: Basic Concepts. *Computer Methods in Applied Mechanics and Engineering* 2004; 193(36-38):4057-4066.
31. Trucano TG, Swiler LP, Igusa T, Oberkampf WL, Pilch M. Calibration, Validation, and Sensitivity Analysis: What's What. *Reliability Engineering and System Safety* 2006; 91(10-11):1331-1357.
32. Oberkampf WL, Roy CJ. *Verification and Validation in Scientific Computing*. New York, NY: Cambridge University Press; 2010.
33. Helton JC, Johnson JD, Sallaberry CJ, Storlie CB. Survey of Sampling-Based Methods for Uncertainty and Sensitivity Analysis. *Reliability Engineering and System Safety* 2006; 91(10-11):1175-1209.

34. Storlie CB, Helton JC. Multiple Predictor Smoothing Methods for Sensitivity Analysis: Description of Techniques. *Reliability Engineering and System Safety* 2008; 93(1):28-54.
35. Storlie CB, Helton JC. Multiple Predictor Smoothing Methods for Sensitivity Analysis: Example Results. *Reliability Engineering and System Safety* 2008; 93(1):55-77.
36. Storlie CB, Swiler LP, Helton JC, Sallaberry CJ. Implementation and Evaluation of Nonparametric Regression Procedures for Sensitivity Analysis of Computationally Demanding Models. *Reliability Engineering and System Safety* 2009; 94(11):1735-1763.

This page intentionally left blank.

Distribution

1	MS0346	D. Dobranich	1514
1	MS0386	K.J. Dowding	1544
1	MS0405	N.N. Brown	0432
1	MS0405	J.L. Darby	0433
1	MS0405	L.C. Sanchez	0432
1	MS0457	R.A. Paulsen	2210
1	MS0492	T.D. Brown	0411
5	MS0747	C.J. Sallaberry	6224
5	MS0748	J.C. Helton	1514
1	MS0748	K.M. Groth	6231
1	MS0812	V.J. Romero	1544
1	MS0828	R.G. Hills	1544
5	MS0828	M. Pilch	1514
1	MS0828	T.L. Durbin	1513
1	MS0836	R.E Hogan	1514
1	MS0836	N.D. Francis	1514
1	MS0836	J.W. Shelton	1514
1	MS0828	H. Silva	1514
1	MS1318	M.S. Eldred	1441
1	MS1318	J.R. Stewart	1441
1	MS1318	L.P. Swiler	1441
1	MS1318	T.G. Trucano	1440
1	MS9042	R.D. Teeter	8259
1	MS9409	J.A. Templeton	8365
1	MS0899	Technical Library	9536 (electronic copy)